Biologie

Generation and molecular analysis of *in vitro* germ cells from mouse and human pluripotent stem cells

Inaugural-Dissertation
zur Erlangung des Doktorgrades
der Naturwissenschaften im Fachbereich Biologie
der Westfälischen Wilhelms-Universität Münster

vorgelegt von
Fumihiro Sugawa
aus Tokyo, Japan
2014

Dekan:	Prof. Dr. Dirk Prüfer
Erster Gutachter:	Prof. Dr. Hans R. Schöler
Zweiter Gutachter:	Prof. Dr. Erez Raz

Tag der mündlichen Prüfung:	23.05.2014
Tag der Promotion:	

List of Publications

Human PGC commitment shares gene expression dynamics to mouse, but owns a unique PRDM14 expression pattern

Fumihiro Sugawa, Marcos J Araúzo-Bravo, Kee-Pyo Kim, Guangming Wu, Martin Stehling, Karin Hübner, Hans R. Schöler (under revision)

Ultrastructural characterization of mouse embryonic stem cell-derived oocytes and granulosa cells.

Psathaki OE, Hübner K, Sabour D, Sebastiano V, Wu G, **Sugawa F**, Wieacker P, Pennekamp P, Schöler HR. ***Stem Cells Dev***. 2011 Dec; 20(12):2205-15.

Book Chapter

In vitro differentiation of germ cells from stem cells

Fumihiro Sugawa, Karin Hübner, Hans R. Schöler. **Biology and Pathology of the Oocyte 2nd Edition**, 2013 Dec; Chapter 20: 236-49.

Table of contents

Acknowledgement

I would like to give many thanks to Prof. Dr. Hans Schöler for giving me the opportunity to work on these exciting projects and for his supervision, research guidance and support. Furthermore, I would like to give a special thanks to Karin Hübner for her help, guidance and mentoring in the lab as well as outside.

Furthermore, I would like to thank all the members of the Schöler department for the pleasant and fruitful working environment. In particular, I would like to give a special thanks to all the lab members who contributed to the experiments and the writing of the manuscripts I prepared during the PhD program.

.

Last but not least, I would like to thank my family and friends for all their supports, especially my girlfriend Miori. Without their patience and support, I could not have completed my PhD thesis.

Table of figures and tables

Abbreviations

APC	allophycocyanin
bFGF	basic fibroblast growth factor
BMP	bone morphogenetic protein
BSA	bovine serum albumin
DMEM	Dulbecco's Modified Eagle Medium
DMR	differentially methylated regions
DMSO	dimethyl sulfoxide
DNA	deoxyribonucleic acid
dpc	days post coitum
dpp	days post partum
EB	embryoid body
ECM	extracellular matrix
EDTA	ethylenediaminetetraacetic acid
EM	electron microscopy
EpiLC	epiblast-like cell
EpiSC	epiblast stem cell
ESC	embryonic stem cell
ExE	extra-embryonic ectoderm
FACS	fluorescence-activated cell sorting
FBS	fetal bovine serum
FSH	follicle-stimulating hormone
GFP	green fluorescent protein
GLC	germ-like cell line
GMEM	Glasgow Minimum Essential Medium
GSEA	gene set enrichment analysis
HCl	hydrogen chloride
hFGSC	human fetal gonadal stromal cell
ICM	inner cell mass
ICSI	intracytoplasmic sperm injection
iPSC	induced pluripotent stem cell
LB	Lennox Broth
LH	luteinizing hormone

LIF	Leukemia inhibitory factor
MEF	mouse embryonic fibroblasts
PBS	phosphate buffered saline
PCR	polymerase chain reaction
PE	phycoerythrin
PGC	primordial germ cell
RA	retinoic acid
RAR	retinoic acid receptors
RNA	ribonucleic acid
SCF	stem cell factor
SCID	severe combined immunodeficiency
SEM	scanning electron microscope
SSC	spermatogonial stem cell
TEM	transmission electron microscopy
TF	transcription factor
TZPs	transzonal projections
VE	visceral endoderm

Zusammenfassung

Nur Keimzellen können die genetische Information von einer Generation zur nächsten übertragen. Trotz großen Interesses sind aber die grundsätzlichen Abläufe, die der Keimzellentwicklung unterliegen, bis heute kaum verstanden. Ein Grund dafür ist sicherlich, dass uns nur ungenügende Mengen an Zellmaterial für experimentelle Untersuchungen zur Verfügung stehen. Eine Lösung dafür könnte die Etablierung von *in vitro* Differenzierungsmethoden zur Gewinnung Primordialer Keimzellen (PGC) aus pluripotenten Stammzellen der Maus und des Menschen sein. Wenn die Differenzierungen in der Kulturschale die Keimzellentwicklung *in vivo* rekapitulierten, hätte man eines wichtigen Verfahren, um die Keimzellentwicklung besser zu verstehen.

Ziel der hier vorgelegten Dissertation war es, ein effizientes und reproduzierbares Differenzierungsprotokoll zur Generierung Primordialer Keimzellen aus pluripotenten, humanen Stammzellen zu etablieren und molekulare Mechanismen, die den Ablauf bestimmen, aufzuklären. Da ein Großteil unseres Wissens über die Keimzellentwicklung mit Mäusen entwickelt wurde, enthält diese Dissertation auch Studien zweier Keimzellprojekte die modellhaft mit Mäusen durchgeführt wurden: "Differenzierung von primordialen Keimzellen aus normalen Epiblast Stammzellen (EpiSC) und stabilisierten Epiblast Stammzellen (Δ PE-Oct4-GFP+)" und "Ultrastrukturelle Charakterisierung von Oozyten und Granulosazellen aus embryonalen Stammzellen".

In meiner Arbeit habe ich ein definiertes und effizientes Differenzierungssystem zur Induktion prämigratorischer PGC aus humanen ESC und iPSC entwickelt. Durch eine stufenweise Differenzierung konnte ich eine *OCT4*+/*T*+/*BLIMP1*+ PGC-Vorläuferpopulation ableiten. Diese Vorläuferpopulation wurden dann in *STELLA*-positive (auch bekannt als *DPPA3*) Zellen differenziert, die wesentliche Merkmale von PGCs der Maus besaßen, u.a. die Expression von Schlüsselgenen und eine globale epigenetische Reprogrammierung. Obwohl in diesen Zellen *PRDM14* nur schwach exprimiert wird, werden ähnlich wie in der Maus Pluripotenz/PGC Gene aktiviert und die neurale Induktion sowie die *de novo* DNA Methylierung unterdrückt. Diese Studie zeigt, dass die PGC Spezifizierung im Menschen und in der Maus recht

ähnlich aber nicht identisch ist, , was auf bislang unbekannte Regulationsabläufe hinweist.

Mittels Zellen der Maus haben wir PGCs aus EpiSCs und ΔPE-Oct4-GFP+ EpiSCs induziert. Wir konnten PGC-ähnliche Zellen aus EpiSC generieren, die charakteristische, prä-meiotische Gene wie *Stella*, *Dazl* und *Vasa* stark induzierten und zudem SYCP3 Protein im Kern aufwiesen. Allerdings war die Induktion von PGC-ähnlichen Zellen ausgesprochen variabel, was meines Erachtens an Unterschieden der verwendeten konditionierten Medienchargen liegt. Um PGCs reproduzierbar von EpiSC abzuleiten, müssen aus meiner Sicht chemisch definierte Differenzierungsbedingungen entwickelt werden.

Im zweiten Mausprojekt wurden ESC-abgeleitete Oozyten und Granulosazellen via Elektronenmikroskopie charakterisiert. Wir konnten außergewöhnliche ultrastrukturelle Ähnlichkeiten zwischen den in vitro-generierten Oozyten und Granulosazellen und den entsprechenden Komponenten natürlicher Keimbahnfollikel der Maus aufzeigen, wie z.B. die charakteristische Struktur der Organellen in Granulosa Zellen, die Formation von Transzonalen Projektionen (TZPs) und die Bildung von kortikalem Granulat im Kortex der Eizelle. Unsere Studie belegt, dass *in vitro* Differenzierungssysteme die essentiellen Komponenten, welche für die Oozytenentwicklung erforderlich sind, generieren können: Oozyten, eine ECM-basierte Interphase und Granulosazellen.

Zusammengefasst zeigen unsere Daten, dass ESC-abgeleitete humane PGCs und *in vitro* generierte Oozyten der Maus ihren natürlichen Gegenstücken stark ähneln. Zusätzlich weisen unsere Studien auf bisher unbekannte Mechanismen während der humanen Keimzellspezifikation hin. Weitere Untersuchungen werden zeigen wie vorteilhaft solche *in vitro* Differenzierungsmodelle als alternative Ansätze für Untersuchungen in der reproduktiven Entwicklung tatsächlich sind.

Abstract

Germ cells are the only cell type that can transmit genetic information from one generation to the next. The key mechanisms underlying germ cell development remain poorly understood due to the insufficient availability of cell materials for experimental investigations. The establishment of *in vitro* PGC differentiation models from mouse and human pluripotent stem cells that recapitulate the development of *in vivo* germ cells provides an alternative approach for studying reproductive development.

The aim of this dissertation was to establish an efficient and reproducible differentiation protocol of PGCs from human pluripotent stem cells, and the investigation of molecular mechanisms involved in their development. Since most of our common knowledge of germ cell development is based on the mouse system, this dissertation also contains work performed on two mouse germ cell differentiation projects, namely "Differentiations of PGC-like cells from normal EpiSCs and so called stabilized EpiSCs" and "Ultrastructural characterization of mouse ESC-derived oocytes and granulosa cells".

I developed a defined and efficient differentiation system for the induction of pre-migratory PGC-like cells from human ESCs and iPSCs. By step-wise differentiation, we generated an *OCT4*+/*T*+/*BLIMP1*+ PGC-precursor-like cell population that transitioned into *STELLA* (also known as *DPPA3*) expressing PGC-like cells that exhibited a similar key gene expression as mouse PGCs as well as global epigenetic reprogramming. Interestingly, even though these PGC-like cells expressed *PRDM14* only at very low levels, they underwent activation of pluripotency/PGC genes, suppression of neural induction and suppression of *de novo* DNA methylation, events that are regulated by *Prdm14* during mouse PGC specification. This study demonstrates that human PGC commitment shares many key features with mouse PGC specification, but harbors unique and so far unknown mechanisms that point to a novel human transcriptional regulation.

In another project, we attempted to induce PGCs from mouse EpiSCs and from mouse stabilized EpiSCs (ΔPE-Oct4-GFP+). We generated PGC-like cells from normal

EpiSCs that exhibited upregulation of PGC genes, such as *Stella*, *Dazl* and *Vasa*, and nuclear expression of SYCP3, which are characteristics of pre-meiotic PGCs. Unfortunately, we could not achieve reproducible induction of PGCs from these cells, nor from ΔPE-Oct4-GFP+ EpiSCs, most probably due to batch-dependent differences in the condition medium we used during the course of the experiments. Our results strongly suggest the requirement of chemically defined media compositions for the reproducible induction of PGCs from EpiSCs *in vitro*.

In the second mouse project, characteristics of mouse ESC-derived oocytes and granulosa cells were determined at the electron microscopy level. We found a striking ultrastructural similarity of *in vitro*-generated oocytes and granulosa cells to cells comprising the natural follicle, such as the characteristic appearance of organelles in granulosa cells, the formation of transzonal projections (TZPs) and the formation of cortical granules in the oocyte cortex. This study demonstrated that *in vitro* differentiation systems can generate the essential components required for oocyte development: oocytes, an ECM-based interface, and granulosa-like cells.

In summary, our data demonstrate that ESC-derived human PGC and *in vitro* generated mouse oocytes exhibit similar characteristics to their natural counterparts. In addition, our study proposes novel molecular mechanisms during human PGC specification. Those results clearly demonstrate the benefit of *in vitro* germ cell differentiation models as alternative approach for studying reproductive development.

1. Introduction

The aim of this dissertation was to investigate the molecular mechanisms of mouse and human germ cell development. In order to achieve this, we aimed at the establishment and utilization of *in vitro* differentiation of mouse or human PGCs from PSCs. Prior to presenting the obtained results, it is important to provide an overview of our current understanding of germ cell development per se and the development of *in vitro* differentiation systems in both mouse and human. The introduction will lay a solid foundation and place the presented data in the relevant context of the current knowledge.

1.1. Germ cells

Germ cells are the only cell type in the body that can carry genetic information onto the next generation, whereas the somatic cell lineages give rise to the soma, or body (Weismann, 1893). The development of germ cells from PGCs to mature gametes (sperm and oocyte) involves a series of complicated biological processes that occur over a given period of time, which can be subdivided into several steps: specification, migration, epigenetic reprogramming, sex differentiation and meiosis, and oogenesis or spermatogenesis. A complex temporal and spatial activation of genetic programs rigorously regulates the sequence of developmental events. Despite recognizing the importance of germ cells, the scientific community has not yet elucidated the molecular mechanisms underlying the individual steps of germ cell development—these remain poorly understood, owing in part to the lack of sufficient cell materials for conclusive studies.

Current understanding of the mechanisms underlying germ cell determination and differentiation is based largely on studies performed in mice. As the series of sequential events during germ cell development is conserved among mammalian species, this section mainly provides an overview of germ cell development in the mouse, followed by a fragmentary but essential knowledge of human germ cell development. Despite large numbers of essential sets of genes involved in gametogenesis, only a small subset of genes that are known to play pivotal roles during germ cell development will be outlined in this introduction.

1.1.1. Primordial gem cell specification

MOUSE The germ cell lineage is not allocated in the embryo proper of mammals before implantation—unlike the case of lower-order eukaryotes, as early epiblast cells injected into blastocysts have an equipotent ability to enter the mouse germline (Gardner & Rossant, 1979; Rossant *et al*, 1978). Cells within the proximal epiblast begin their commitment to become PGCs at the onset of gastrulation, between 5.5 to 6 dpc (Yoshimizu *et al*, 2001), with the entire epiblast retaining this germline plasticity as late as 7 dpc (Tam & Zhou, 1996) in response to paracrine signaling from the extra-embryonic ectoderm (ExE) and visceral endoderm (VE) (Ginsburg *et al*, 1990). BMP2, BMP4, and BMP8, members of the bone morphogenetic protein family, induce Smad1, Smad5, and Smad8 signaling in the *Oct4*, TNAP, *fragilis* triple-positive founding cell population of the proximal epiblast, which subsequently comprises approximately 45 committed PGCs by 7.25 dpc (Fujiwara *et al*, 2001; Lawson *et al*, 1999; Ying *et al*, 2000; Ying & Zhao, 2001). Studies on this process at a single cell level have revealed that PGCs initially share similar properties with their somatic mesodermal neighbors, as indicated by the expression of *T* and *Hoxb1*. Subsequent repression of the somatic program and activation of the PGC program enable the emergence of PGCs with TNAP activity and *Stella* expression (Figure 1) (Kurimoto *et al*, 2008; Saitou *et al*, 2002; Yabuta *et al*, 2006). Importantly, Sox2 appeared to be repressed at the initiation of specification and re-acquired upon establishment of committed PGCs, while Nanog is constantly expressed. *Blimp1* (also known as *Prdm1*) and *Prdm14* are key factors for mouse PGC specification. They play an essential role in the repression of the somatic mesodermal program, activation of the PGC program, and global epigenetic reprogramming (Saitou et al, 2002; Seki *et al*, 2007; Yabuta et al, 2006). Interestingly, a recent study has demonstrated that ectopic expression of *Blimp1* and *Prdm14* together with *Tfap2c* is sufficient to induce mouse PGC-like cells from Epiblast-like cells *in vitro*, supporting the idea that these two factors play a dominant role in mouse PGC specification (Nakaki *et al*, 2013).

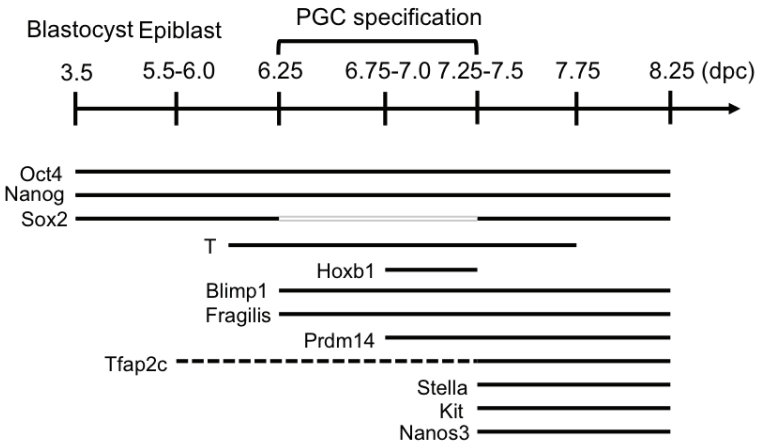

Figure 1 Scheme of gene expression dynamics during mouse PGC specification.

HUMAN The founders of germ cells are recognized in the embryo at the wall of the yolk sac at the angle with the allantois at around the end of the third week (Felix, 1911; Fuss, 1911; Fuss, 1912). These cells are distinguishable by their large size, spherical shape, the presence of abundant glycogen granules in the cytoplasm and their TNAP activity (Mc *et al*, 1953). BMP4 signaling seems to play a role in human PGC specification, as *in vitro* differentiation of PGCs from human ESCs has been shown to be enhanced by BMP4 (Kee *et al*, 2006). Those observations indicated that human germ cells have similar properties to mouse germ cells. However, there are only a few reports in the literature that detail gene expression dynamics during human PGC specification, which occurs before the 4th week of embryonic development. Nevertheless, immunochemical studies of carcinomas, germ cell tumors, and early-mid stage germ cells have revealed that human germ cells exhibit a similar expression pattern of a number of key genes. BLIMP1 was observed to be expressed in germ cells within 12 week gonads and 19 week testis (Eckert *et al*, 2008). TFAP2C was also found in germ cells from both testis and ovary from the 10th to the 22nd week. The expression of these genes at late stage implies their conserved roles during human PGC specification. In contrast, the expression pattern of PRDM14 and STELLA in human germ cells has not been investigated so far. Among the genes associated with pluripotency, OCT4 and NANOG are expressed in human germ cells (Kerr *et al*, 2008a; Kerr *et al*, 2008b). OCT4 expression was observed in 5.5 week and 7 week gonads in female and male, respectively. These OCT4+ PGCs co-expressed NANOG. On the other hand, SOX2 has been shown to be absent in human germ cells (de Jong

et al, 2008; Perrett *et al*, 2008), but cooperates with OCT4 and NANOG to regulate pluriotency in both mouse and human ESCs (Boyer *et al*, 2005; Fong *et al*, 2008; Wang *et al*, 2006). It is expressed in cells of the inner cell mass (ICM) and PGCs in mouse (Avilion *et al*, 2003), as well as in the human ICM (Cauffman *et al*, 2009). Those studies support the notion that the pluripotency network in human germ cells is differentially regulated compared to other cell types. Interestingly, a study in sheep revealed that Sox2 was apparently downregulated during PGC development, despite the maintenance of Oct4 and Nanog (Ledda *et al*, 2010), which further implies the difference of Sox2/SOX2 expression in different species.

1.1.2. Germ cell migration

MOUSE After their commitment, PGCs migrate through amoeboid-like movements toward the dorsal region of the fetus and reach the genital ridges at around 10.5 dpc. Genes that are expressed in the germ cells and in the soma ensure not only PGC survival, but also proper gonad formation. Signaling cascades emanating from gonadal somatic cells as well as cell-to-cell interactions ensure PGC proliferation, survival, and colonization of the gonads. For example, expression of β1 integrin and E-cadherin (Anderson *et al*, 1999; Bendel-Stenzel *et al*, 2000) in PGCs facilitates their interaction with the extracellular matrix (ECM) and cell-to-cell adhesion via cellular processes. Receptor-ligand interactions, such as c-Kit signaling by KITL (also known as SCF) or chemokine responsiveness of PGCs to SDF1 signaling from the genital ridge, are crucial (Hutt *et al*, 2006; Molyneaux *et al*, 2003) for germ cell development and subsequent maturation of PGCs into gametes. Upon reaching the genital ridges, PGCs upregulate Dazl (Cooke *et al*, 1996) and Vasa (also known as *Ddx4*) (Noce *et al*, 2001; Toyooka *et al*, 2000). Interestingly, these genes are primarily regulated by promoter DNA methylation (Maatouk *et al*, 2006), suggesting that their expression possibly reflects the global epigenetic reprogramming during migration (described later). Indeed, recent studies suggest that many genes implicated in later stages of germ-cell development, such as gametogenesis and meiosis, are regulated by promoter DNA methylation (Borgel *et al*, 2010; Guibert *et al*, 2012).

HUMAN During the fourth week, when the embryonic disc undergoes a process of folding, PGCs are passively incorporated into the embryo together with the yolk sac

wall. The gonadal ridges are visible as a distinct structure at the beginning of the fifth week. At this time, PGCs start migrating and reach the gonadal ridges at week 6 (Falin, 1969; Fujimoto *et al*, 1977; Mc et al, 1953; Mollgard *et al*, 2010). Human PGCs show several features of motile cells and are able to move actively both on cellular and ECM substrates (Freeman, 2003; Kuwana & Fujimoto, 1983). Similar to mice, KITLG (human homolog of mouse KITL) and SDF1 are also implicated in directing the migration of human PGCs, as the KITLG receptor c-KIT is expressed in human PGCs (Hoyer *et al*, 2005) and putative PGCs derived from human ESCs express the SDF1 receptor CXCR4 (Bucay *et al*, 2009). DAZL and VASA are also expressed in human gonadal germ cells from week 6 on (Anderson *et al*, 2007; Castrillon *et al*, 2000; Gkountela *et al*, 2013). Interestingly, the CpG islands of Dazl and Vasa in the mouse appear to be conserved in humans, and they remain hypomethylated in sperm but not other somatic tissues (Chai *et al*, 1997; Sugimoto *et al*, 2009). Whether regulation of germline-specific genes by promoter methylation is a general feature in humans is still unclear.

1.1.3. Epigenetic reprogramming

MOUSE The full commitment of cells toward the germ cell lineage is contingent upon the fine-tuned molecular mechanisms regulating the maintenance of genomic imprinting. DNA methylation, a key mechanism of this stage of development, regulates the imprinted allele-specific gene expression. Once established, the methylation status of the DNA is typically stable through generations. However, the dynamic changes in the DNA methylation of germ cells take place at specific time points in germ cell development—namely in fertilized embryos and in PGCs. There are two phases of DNA demethylation during PGC development. The first phase occurs immediately during migration at around 8.0–8.5 dpc and involves global depletion of cytosine methylation and histone modification. There is a marked reduction in H3K9me2, starting at around 7.5 dpc until and continuing until 8.75 dpc, followed by an increase in H3K27me3 between 8.25 and 9.5 dpc (Seki et al, 2007). There is also a decrease in Dnmt3a and 3b transcripts and protein at 7.25 and 8 dpc, respectively (Seki *et al*, 2005; Yabuta et al, 2006). This is accompanied by a reported decrease in 5-methylcytosine (5mC) at 8 dpc (Seki et al, 2005). Prmt5, an arginine-specific histone methyltransferase that mediates H2AR3me2s and/or H4R3me2s, is

enriched in PGCs from 8.5 dpc on, and the H2A/H4R3me2s shows higher accumulation in PGCs than somatic cells at 10.5 dpc (Ancelin *et al*, 2006). The second phase takes place at 11 dpc and involves locus-specific demethylation at DMRs in a Tet-dependent manner (Hajkova *et al*, 2008; Hajkova *et al*, 2002; Hajkova *et al*, 2010; Vincent *et al*, 2013). This reprogramming results in demethylation of many repetitive elements but critically includes the erasure of imprints, allowing the establishment of sex-specific imprints during gametogenesis.

HUMAN The early stage of reprogramming has not been well studied in humans at this early stage of development. Nevertheless, some studies have revealed similarities to mice after colonization of the gonad (Gkountela et al, 2013; Wermann *et al*, 2010). The level of 5mC in human PGCs seemed to be reduced during development, as 5mC was undetectable in PGCs from the 7th-17th week in testes and the 6th-19th week in ovaries, while it was detected in surrounding somatic cells. H3K27me3 was enriched in the nuclei of PGCs in testes between the 7th to 10.5th week. However, at 11 weeks, H3K27me3 was undetectable in most of the OCT4+ PGCs. Interestingly, at 17 weeks in testes, H3K27me3 was again observed in the nuclei of 38% OCT4A+ PGCs. In ovaries, H3K27me3 was absent in 50–60% of PGCs at 6–8.5 weeks, after which all PGCs were negative for H3K27me3. Furthermore, H2A.Z was enriched in the nuclei of PGCs at 7–9 weeks in the testis and 7.5 weeks in the ovary. The high level of H2A.Z, a variant of histone H2A, was observed at 16–20 weeks in testis. Another study also reported the low levels of H3K9me2, H3K27me3, and H3K9me3, but high levels of H3K9ac and H2A.Z in male germ cells at around week 16–20 (Almstrup *et al*, 2010). PRMT5 was expressed in BLIMP1+ germ cells (Eckert et al, 2008). These data demonstrate the change of histone modification in human PGCs. Demethylation of imprinted genes seems to start between week 9 and 16. The paternally methylated H19 and MEG3 DMRs were methylated between the 9th-20th week in male c-KIT+ PGCs, whereas maternally methylated DMRs in the testis exhibited a sharp reduction of methylation between the 16th and 17th week. In the ovary, a significant reduction of CpG methylation was observed by 16.5 weeks at all loci (H19, MEG3, PEG3 and KCNQ1) (Gkountela et al, 2013).

1.1.4. Sex differentiation and Meiosis

MOUSE After colonizing the genital ridges, the PGCs (now called gonia) are exposed to retinoic acid (RA) and interact with sex-specific somatic Sertoli or granulosa cells. The signals from these gonadal somatic cells precipitate the onset of sexual differentiation of the gonia at around 13.5 dpc (Koubova *et al*, 2006). Consequently, in the male genital ridge, PGCs undergo mitotic arrest and become irreversibly committed to a spermatogenic cell fate by 14.5 dpc (Ohta *et al*, 2004). These spermatogonia resume cell proliferation at around 10 dpp to continue spermatogenesis. In the female gonads, gonia reside in clusters, the so-called germ cell cysts, enter meiosis at around 13.5 dpc, and transiently arrest at the diplotene stage of meiosis 1 as oocytes by 18.5 dpc. Meiosis is a unique type of cell division that generates gametes with a haploid parental chromosome set. Specialized interactions between chromosomes and modification of the cell cycle machinery facilitate chromosome segregation—a precisely timed process involving complex pathways. Errors in meiosis are the leading cause of birth defects and infertility, and unraveling the mechanisms involved in the meiotic process represents one of the biggest challenges in developmental biology. In female mice, RA induces the expression of pre-meiosis gene Stra8 and oocytes initiate meiosis in the fetal ovary between 13.5 and 16.5 dpc and arrest in the diplotene stage of the meiotic prophase 1 by 18.5 dpc. At the onset of meiosis, germ cells express meiosis-specific proteins, such as SYCP1, SYCP2, and SYCP3, and form γH2AX, which play a role in axial core compaction, synapsis, and recombination. Downregulation of *Sycp1* in occytes coincides with the arrest of oocytes in the diplotene stage of prophase 1 and is thought to signal somatic cells to begin organizing the primordial follicles (Paredes *et al*, 2005). Oocytes resume meiosis 1 by entering into metaphase 1 during folliculogenesis a few weeks after birth to arrest again in the second meiotic division prior to ovulation.

HUMAN Whether in human during sex differentiation is also induced by RA has not yet been determined. However, the expression of RA synthesizing enzymes (RALDH1, 2 and 3), along with retinoic acid receptor (RAR) expression was detected in human fetal ovaries (Childs *et al*, 2011; Le Bouffant *et al*, 2010), indicating that the induction of meiosis by RA is not limited to mice. In a human fetal organ culture system, RALDH1 was expressed at highest levels during meiosis initiation (11th–12th

week) and its inhibition by citral reduced numbers of meiotic germ cells. Conversely, addition of exogenous RA to this system increased the numbers of meiotic germ cells compared to controls (Childs et al, 2011). Importantly, STRA8 expression is reported to start from the 12th week on in the gonad (Houmard *et al*, 2009) and SYCP3 expression was observed in human gonadal germ cells at least in the ovary at week 16 (Liu *et al*, 2007), indicative of meiotic progression.

1.1.5. Folliculogenesis and oocyte maturation

MOUSE Shortly after birth, germ cell cysts degenerate and about one third of the oocytes become enclosed by granulosa cells and form primordial follicles, while the remaining oocytes undergo programmed cell death (Pepling & Spradling, 2001). Upon activation of the primordial follicle, the complex process of folliculogenesis ensues, with a bidirectional communication between the oocyte and the companion granulosa cells directing follicle development (Eppig, 2001; Eppig *et al*, 2002). The oocyte and surrounding granulosa cells are structurally and functionally associated via specialized cytoplasmic processes called transzonal projections (TZPs) and zona pellucida (ZP), representing a highly dynamic interaction regulating folliculogenesis in vivo and thereby ensuring appropriate oocyte maturation and ovulation (Albertini *et al*, 2001). Primordial follicles transition to become primary follicles when the granulosa cells surrounding the oocyte turn into cuboidal granulosa cells. SCF, LIF and bFGF secreted by the somatic compartment, and *c-kit*, *Figla*, *Sohlh1*, *Sohlh2*, *Nobox* and *Lhx8* expressed by the oocyte promote this transition and rapid growth of the oocyte. During the secondary follicle stage, proliferation of granulosa and theca cells is mediated by expression of *Gdf9* and *Bmp15* in the oocyte (Jagarlamudi *et al*, 2010). Subsequently, in response to follicle-stimulating hormone (FSH) and luteinizing hormone (LH), follicles form an antrum, initiating the process of steroidogenesis. Once the oocyte reaches maturity within the antral follicle, ovulation proceeds and meiosis resumes.

HUMAN A detailed expression pattern of genes during development has not been reported yet. Nevertheless, the expression of a variety of genes expressed in mouse oocytes has also been observed in human oocytes. *FIGLA* expression was observed in ovaries between week 14 to at least week 19 (Bayne *et al*, 2004) and in all follicle

stages of the adult ovary (Huntriss *et al*, 2006). *NOBOX* is expressed in all follicle stages of the adult ovary (Huntriss et al, 2006) and *LHX8*, *GDF9*, *ZP1*, *ZP2* and *ZP3* are expressed in oocytes (Moriguchi *et al*, 2012). These studies support the notion that oocyte-related genes are well conserved between humans and mice. Importantly, mutations of *LHX8*, *FIGLA* and *BMP15* have been detected in premature ovarian failure patients, suggesting that these genes are likely key mediators of fertility in humans (Suzumori *et al*, 2007).

Table 1 Comparison of gene expression profiles of PGCs between different mammals.

		Mouse	**Human**
Early PGC genes	Blimp1	+	+
	Prdm14	+	ND
	Tfap2c	+	+
	Stella	+	ND
Pluripotency genes	Oct4	+	+
	Nanog	+	+
	Sox2	+	-
	SSEA-1	+	+
	c-KIT	+	+
Late PGC genes	Dazl	+	+
	Vasa	+	+
Meiosis genes	Stra8	+	+
	Sycp1-3	+	+
Oocyte genes	Figla	+	+
	Nobox	+	+
	Lhx8	+	+
	Gdf9	+	+
	Zp1-3	+	+

1.2. Germ cell differentiation from mouse and human embryonic stem cells

ESCs are cells derived from the ICM of preimplantation blastocysts (Evans & Kaufman, 1981; Martin, 1981; Thomson *et al*, 1998). These cells have the ability to self-renew indefinitely while maintaining the feature of pluripotency, defined as the potential to differentiate into cell types of all three germ layers (ectoderm, endoderm, and mesoderm) and germ cells. The establishment of mouse and human ESCs brought great excitement not only to the scientific community, but also to the clinical setting, raising high expectations on the potential use of these cells to broaden our understanding of the mechanisms involved in development and disease. However, the

controversy surrounding the derivation of ESCs from "human embryos" has limited the number of cell lines that were derived.

A breakthrough from 2006 in the field of stem cell research has the potential to overcome this limitation. Mouse somatic cells were reprogrammed into so-called iPSCs by the ectopic co-expression of the four transcription factors *Oct4*, *Sox2*, *Klf4*, and *c-Myc* (Takahashi & Yamanaka, 2006). Mouse iPSCs are able to generate functional germ cells (Okita *et al*, 2007; Wernig *et al*, 2007) and, most importantly, are competent to form a full embryo by tetraploid embryo complementation (Kang *et al*, 2009; Zhao *et al*, 2009). Only one year after the first mouse iPSCs report, reprogramming of human cells was achieved by the same combination of transcription factors (*OCT4*, *SOX2*, *KLF4* and *C-MYC*) and by a different combination of factors (*OCT4*, *SOX2*, *LIN28* and *NANOG*) (Takahashi *et al*, 2007; Yu *et al*, 2007). Although further investigations are required to unravel how the reprogramming machinery works, this new technique enables the derivation of patient-specific iPSCs for disease modeling, drug screening, and investigations into the causative mechanisms underlying disease.

Over the past few years, several studies reported the differentiation of PGCs *in vitro* from pluripotent stem cells, including iPSCs, from a variety of organisms. Amazingly, some reports even demonstrated further maturation of these germ cells into presumptive gametes, suggesting that *in vitro* differentiation models are powerful tools for the studying gametogenesis. Prior to examining *in vitro* germ cell development and gametogenesis, a brief review of mouse germline development will be provided. This will be followed by an overview of the advances in germ cell differentiation using mouse and human stem cells to date, with a focus on the generation of oocytes. The chapter will end with a presentation of the challenges encountered in the successful generation of mature gametes.

1.2.1. *In vitro* differentiation of mouse germ cells

1.2.1.1. *In vitro* differentiation of post-migratory PGCs

Between 2003 and 2004, three independent groups showed that mouse ESCs are capable of spontaneously differentiating into both male and female germ cells

(Geijsen *et al*, 2004; Hubner *et al*, 2003; Toyooka *et al*, 2003). During the following 10 years, this research field experienced a steady increase of attention, and gradually shifted from spontaneous differentiation strategies to inductive strategies.

In 2003, Hübner et al. reported the generation of PGCs *in vitro* from XY-mouse ESCs that followed the oogenesis pathway upon extended culture (Hubner et al, 2003). The authors differentiated ESCs as a feeder-free monolayer in the absence of LIF and observed *Oct4*+/*Vasa*+ post-migratory PGC-like cells after about 8 days of culture. Aggregates of Oct4-/Vasa+ cells were subsequently found to detach from the cell layer and produce large SYCP3 positive oocyte-like cells. After 30 days of culture, rare blastocyst-like structures were detected, indicative of parthenogenetic activation. However, the functionality of the presumptive oocytes was not shown. Shortly afterwards, Toyooka et al. published a study describing the differentiation of ESCs into male germ cells *in vitro* (Toyooka et al, 2003). In this study, mouse ESCs were co-aggregated with BMP4-producing transgenic cells to form EBs and, interestingly, *Vasa*+ post-migratory PGC-like cells were detected within 1 day. These *Vasa*+ cells developed into sperm-like cells upon transplantation into mouse testis; however, fertilization was not reported. Similarly, Geijsen et al. described the *in vitro* generation of male haploid cells from spontaneously differentiating EBs under serum-containing condition (Geijsen et al, 2004). Upon injection into oocytes by intracytoplasmic sperm injection (ICSI), the haploid cells developed into blastocysts, but offspring were not produced. Taken together, these initial reports clearly demonstrated the differentiation capacity of mouse ESCs into both male and female germ cells in culture, and spurred further efforts in the development of robust *in vitro* differentiation systems.

It is worthwhile to mention that none of the early studies provided proof of competence and functionality of the ESC-derived germ cells. In this context, Novak et al. reported that ESC-derived germ cells exhibit abnormal progression through meiosis (Novak *et al*, 2006). Even though the PGC-like cells generated by those researchers exhibited SYCP3 protein expression, additional meiotic markers or homologous chromosome synapses specific for meiotic progression could not be detected, such as SYCP1 and SYCP2. This data imply that the majority of *in vitro*–generated germ cells fail to undergo normal meiosis, which may explain their failure

to further differentiate into functional gametes. Nevertheless, a recent ultrastructural comparison between natural and ESC-derived oocytes and follicles by Psathaki et al. revealed that oocytes exhibited remarkable similarities, as did, interestingly, the *in vitro* produced granulosa-like cells. The aggregates analyzed in this study exhibited characteristics typical of natural follicles, i.e. one or multiple oocyte-like cells, an ECM-based interphase, and granulose-like cells exhibiting TZPs. This data suggest the presence of ongoing folliculogenesis with active interactions between germ cells and granulosa cells generated *in vitro* (Psathaki *et al*, 2011).

In 2006, one report described the *in vitro* differentiation of fully-grown sperm, as ascertained by morphology and immunocytochemical staining for known sperm markers (Nayernia *et al*, 2006). According to this report, stable PGC-like cell lines were derived from mouse ESCs carrying a Stra8 reporter construct. Upon differentiation on inactivated MEFs and induction with RA, about 60% of the cells expressed *Stra8*, a RA-responsive gene involved in meiosis in the male mouse. The Stra8+ cell population was further cultivated under non-inducing conditions, giving rise to stabile cell lines with conserved Stra8 and PGC marker expression, including *Oct4*, *Stella*, and *Vasa*, indicative of spermatogonial stem cells (SSCs). After another course of RA treatment, Acrosin+ and haploid cells were detected in the culture, indicative of post-meiotic spermatids. However, analysis of these differentiated cells revealed incomplete epigenetic resetting. ESC-derived SSC-like cells gave rise to sperm after implantation into testis. After ICSI of the sperm into oocytes, live offspring were produced, but the progeny had obvious growth abnormalities and died within 5 months. This report has provided evidence for the potential derivation of male gametes *in vitro*, but the generation of healthy offspring still has to be demonstrated.

1.2.1.2. Differentiation by co-culture with animal-origin somatic cells

Other approaches for the *in vitro* generation of germ cells from ESCs utilize co-cultures with gonadal somatic cells or cultures in conditioned medium. Lacham-Kaplan et al. reported the formation of ovary-like structures containing oocyte-like cells from differentiating EBs in testis-conditioned medium that were collected from testicular cell cultures of male newborn mice (Lacham-Kaplan *et al*, 2006). After 2–5

days of differentiation, *Oct4*+/*c-Kit*+/*Vasa*+ PGC-like cells were observed, which further developed to 15–30 μm large oocyte-like cells within follicle-like structures. Even though expression of the oocyte markers *Figla* and *Zp3* was shown, neither meiotic progression nor functionality had been confirmed. A similar report came from Qing et al., demonstrating that co-culturing EBs with granulosa cells from female newborn mice enhances female germ cell marker expression and oocyte-like cell formation (Qing *et al*, 2007). Different from other publications is the reported expression of *Sycp1*, *Sycp2,* and *Sycp3* at the mRNA level in oocyte-like cells. However, SYCP3 proteins were detected in the cytoplasm in these cells, while SYCP proteins co-localize with DNA during meiosis in natural germ cells. Taken together, these data suggested that factors secreted by the somatic component of the gonads and the direct interaction of gonadal somatic cells with *in vitro*–generated germ cells appear to have a positive effect on the outcome of *in vitro* germ cell differentiation. However, these effects could not give rise to mature and functional gametes. Nevertheless, the identification of factors that enhance germ cell differentiation in these culture systems would greatly enhance our understanding of germ cell development both *in vivo* and *in vitro*.

The lack of markers that can distinguish germ cells from ESCs likely constitutes the biggest limitation in the field of *in vitro* germ cell differentiation. PGCs and ESCs share most of the known markers of the germ cell lineage, hampering the ability to efficiently separate PGCs from ESCs or pluripotent cell populations. For example, SSEA-1 is not only commonly used for the identification of undifferentiated mouse ESCs, but it also serves as surface marker for the isolation of early PGCs from somatic cell populations. Nicholas et al. utilized ΔPE-Oct4-GFP ESCs and reported a combination of common markers can be used to distinguish early PGCs and late female germ cells, respectively, from differentiating ESCs, by considering the signal intensity during purification (Nicholas *et al*, 2009). An isolated Oct4+/SSEA1+ (high signal) population was enriched within differentiation cultures with early PGC markers, such as *Oct4*, *Stella*, *Nanos3,* and *Vasa*, while the corresponding Oct4+/SSEA1- population expressed the meiotic marker *Stra8* and the oocyte-specific gene *Gdf9*, suggesting an oocyte identity. In addition, the expression of the meiotic markers was enhanced by addition of BMP4, RA, and CYP26 inhibitor—factors

known to stimulate meiosis. However, these *in vitro* ESC-derived oocyte-like cells showed blockage of meiotic progression, as indicated by only a partial SYCP3 chromosomal alignment and the absence of SYCP1 elongation. To further assess the developmental capacity of the generated meiotic oocytes, co-aggregates with dissociated wild-type newborn ovarian tissues were transplanted into recipient female mice. The ESC-derived GFP+ oocytes were found to recruit somatic granulosa cells and develop up to the primary follicle stage. However, whether these follicles can progress further in development remains to be elucidated.

1.2.1.3. *In vitro* differentiation of pre-migratory PGCs

While the difficulty of meiotic progression *in vitro* impedes the robust establishment of post-migratory PGCs, one group successfully recapitulated PGC specification in vitro and generated pre-migratory PGCs. In 2009, Ohinata et al. established an *ex vivo* system for the generation of early PGCs from embryonic day (E)6.0 epiblast under serum-free defined culture conditions in the presence of BMP4, BMP8B, LIF, and SCF. After 6 days of culture, a small cell population expressing exclusively early PGC markers (including *Blimp1*, *Stella*, *Oct4,* and *Vasa*) had formed, representative of migratory PGCs. Furthermore, upon injection of PGC-like cells into neonatal mouse testis, they were found to develop into sperm, which subsequently produced live offspring after ICSI into oocytes (Ohinata *et al*, 2009). This study suggested that if epiblast-like cells can be obtained from other pluripotent cell types *in vitro*, the same protocol could be used to facilitate further differentiation into PGCs. Based on this report, Hayashi et al. introduced a 2-step differentiation protocol for ESCs—an approach that closely recapitulates germ cell commitment *in vivo*. ESCs were first converted into epiblast-like cell (EpiLCs) by induction with Activin A and bFGF, followed by differentiation into PGCs according to Ohinata et al. Global gene expression profiling of EpiLCs and PGC-like cells revealed a high similarity to their *in vivo* counterparts. Interestingly, EpiLCs were similar to E5.75 epiblast, but different from EpiSCs. Consistent with this observation, EpiSCs did not give rise to PGCs under the same differentiation regime. *In vitro*–derived PGCs also exhibited epigenetic properties and cellular dynamics similar those of *in vivo* PGCs. ESC-derived PGCs were injected into neonatal mouse testis to produce sperm, which subsequently produced live offspring after ICSI into oocytes (Hayashi *et al*, 2011).

The authors later reported that these PGC-like cells are able to differentiate into oocyte upon transplantation into ovary (Hayashi *et al*, 2012). The authors reported that BLIMP1+/STELLA- PGCs were able to generate oocytes, demonstrating that PGC precursors have already acquired distinct PGC properties. The same group reported the induction of PGC-like cells by overexpression of three germ cell-related transcription factors (TFs), Blimp1, Prdm14 and Tfap2c (Nakaki et al, 2013). Overexpression of these TFs in EpiLCs successfully induced PGC-like cells under the same culture conditioned as described before but in the absence of cytokines. These TF-induced PGC-like cells exhibited similar global gene profiles and epigenetic profiles as wild type PGCs, and gave rise to functional sperm. Interestingly, even though the combination of the three factors induced PGC-like cells most efficiently, Prdm14 alone also induced the cells, indicating that Prdm14 plays a core function in PGC specification. This study revealed the core gene regulation of PGC specification in mouse.

1.2.2. *In vitro* germ cell derivation from human pluripotent stem cells

A great deal of our knowledge on PGC specification and development has been borne out of studies in the mouse embryo and over the last decade in particular in mouse ESC differentiation models. Due to the limited accessibility of cell materials, investigations into human gem cell development have only recently gained headway with the increasing use of human ESCs and iPSCs as an experimental model. Human pluripotent stem cells differ significantly from mouse pluripotent stem cells, and the same is thought true for germ cells. Direct extrapolation of data obtained from animal models to the human system is obviously not possible and several studies have already identified a variety of fundamental differences.

1.2.2.1. The generation of post-migratory PGC-like cells

One year after the first report of mouse in vitro germ cells, Clark et al. demonstrated that human ESCs are also capable of differentiating into PGCs (Clark *et al*, 2004). The authors compared the gene expression of human homologs of known mouse PGC markers in several human ESC lines, the ICM from human blastocysts, and human testis and observed that ESCs expressed early PGC markers such as *STELLA* and *DAZL* but not the late PGC markers such as *VASA, SYCP1, SYCP3, BOULE, and*

TEKT1. After the spontaneous differentiation of ESCs in EBs, the down-regulation of early PGC markers and up-regulation of later PGC markers confirmed the commitment of cells within the cultures to the germ cell lineage. In addition, a small number of VASA+ cells, representative of post-migratory PGCs, were detected at the border of the EBs. These encouraging findings spurred fervent interest toward the discovery of more efficient differentiation protocols.

The same group later reported the inductive effect of BMP proteins on PGC marker expression during the differentiation of human ESCs into PGCs *in vitro* and addressed the conserved role of BMP proteins on PGC induction between human and mouse (Kee et al, 2006). BMP4 was found to induce *VASA* expression, whereas BMP7 and BMP8B did not show any individual effect, but rather enhanced the action of BMP4. Based on these data, the authors concluded that the combination of BMP4, BMP7, and BMP8B most strongly induces germ cell formation *in vitro*. This data indicated conserved molecular mechanisms on PGC specification between two species.

Another report described the generation of human transgenic VASA-GFP ESC lines based on the observation that *VASA* is not expressed in ESCs (Kee *et al*, 2009). Those authors differentiated trangenic ESCs in medium supplemented with BMP4, BMP7, and BMP8b, based on their previous study (Kee et al, 2006). After 2 weeks, GFP+ cells were observed within cultures, which expressed also *BLIMP1, STELLA,* and *DAZL* and showed initiation of imprinting erasure of the H19 locus. However, the potential of meiotic progression and sexual bipotentiality of VASA+ cells remained unclear, as most of the analyzed cells did not express SYCP3 protein nor γH2AX, which are required for meiotic recombination and binding to double-stranded DNA breaks. The authors then investigated the role of DAZ, DAZL, and BOULE during the differentiation of human PGCs by utilizing the same differentiation protocol but omitting BMPs. Knockdown of the genes by short hairpin RNA (shRNA) led to a decrease in GFP+ cells, whereas overexpression of the genes led to progression of meiosis, indicated by a punctuate or elongated SYCP3 signal at higher frequency than that observed in wild type cells. These cells differentiated further into ACROSIN+, male haploid cells., The same group reported later that iPSCs could be differentiated into PGCs similarly to hESCs, suggesting that iPSCs might depict a promising

alternative to ESCs (Panula *et al*, 2011). Surprisingly, iPSC cultures contained more SYCP3-expressing cells than ESC lines under non-differentiating culture conditions, and one of the iPSC lines even contained a subpopulation of cells with elongated SYCP3 distribution. The authors suggested that iPSCs preferentially differentiate into the germ line, which might be linked to the enhanced expression of pluripotency markers during the reprogramming process. Medrano et al. utilized overexpression of *VASA* to enhance meiotic progression, and reported that even though VASA is not as effective as DAZL overexpression, VASA exhibits a synergistic effect with DAZL in ESCs and iPSCs (Medrano *et al*, 2011). These studies together suggest that DAZL and VASA play an important role in human germ cell development like in the mouse.

In the context of meiotic competence of *in vitro* human germ cells, Chuang et al. reported the generation of SYCP3+ PGC-like cells without genetic modification. The authors differentiated OCT4-GFP transgenic ESCs in a serum-based medium containing BMP4 and WNT3A for up to 30 days and purified OCT4+ putative germ cells. Some of these OCT4+ cells expressed STELLA, DAZL and VASA at the protein level and importantly, 30% of the OCT4+ cells expressed SYCP3 in the nuclei. These PGC-like cells were then co-aggregated with dissociated newborn mouse ovaries and transplanted into the kidney capsule of NOD/SCID mice for 2 months. Even though some VASA+ or GDF9+ cells were detected in the reconstituted ovaries, further development into mature oocytes had not been shown.

1.2.2.2. The generation of putative gametes

There are some reports describing the generation of putative sperm-like cells without genetic manipulation. Bucay et al. reported the co-differentiation of *in vitro* PGCs and Sertoli cells from ESCs (Bucay et al, 2009). ESCs were first differentiated into VASA and AP double-positive PGC-like cells that revealed morphological characteristics of natural PGCs at the electron microscopy (EM) level. Upon further differentiation, these cultures showed increased expression of the late male GC markers *VASA* and *ACROSIN* and of the Sertoli cell markers *MIS*, *FSHR,* and *SOX9*, indicating the induction of late PGCs and Sertoli cell in the culture. In fact, these Sertoli-like cells exhibited morphological features characteristic of their *in vivo* counterparts, as analyzed by EM. However, although 45% of cells within the differentiation cultures expressed VASA and 35% expressed FSHR at the protein level, haploid cells were

not detected. Interestingly, this report mirrors the main findings of Psathaki et al., who performed an ultrastructural analysis of co-differentiated presumptive oocytes and granulosa cells generated from mouse ESCs.

Eguizabal et al. reported the spontaneous generation of haploid cells from iPSCs (Eguizabal *et al*, 2011). iPSCs were cultured on MEF feeder cells without bFGF for 3 weeks, followed by treatment with RA for additional 3 weeks. Early spermatogonia and spermatid marker-expressing cells were isolated and further cultivated in the presence of bFGF, LIF, Forskolin, and CYP26 inhibitor for another 3–4 weeks. By this time, VASA-expressing cells surrounded by somatic cells with marker expression typical of Sertoli and Leydig cells (VIMENTIN, NESTIN and 3β-HSD) were observed. Upon differentiation for an additional 4 weeks in the presence of factors supporting meiosis, a subpopulation of cells showed expression of the meiotic markers SYCP3 and γH2AX and the post-meiotic marker ACROSIN, indicating the formation of meiotic, i.e., haploid, cells. Analysis of the methylation status revealed a male-specific hypermethylation pattern of the H19 locus. Of importance is that the differentiation protocol did not work the same way for ESCs—as ESCs produced only VASA and SYCP3 double-positive and γH2AX-negative cells, similar to the report by Kee et al. (Kee et al, 2009). These findings and the report by Panula et al. (Panula et al, 2011) suggest that certain iPSC lines differentiated preferentially toward the germ line.

1.2.2.3. Differentiation by co-culture with animal-origin somatic cells

There are few studies employing co-cultures with animal-origin somatic cells that obtained putative matured gametes. West et al. reported the emergence of VASA+ PGC-like cells when ESCs were differentiated on MEF cells in the presence of bFGF without being passaged for 10 days (West *et al*, 2008). Amazingly, about 60% of the cells expressed OCT4 and VASA proteins. However, VASA localized to the nucleus—a phenomenon that needs to be explained and clarified, as it is typically expressed in the cytoplasm. The same group subsequently reported the establishment of a stable germ-like cell line (GLC) from those ESC-derived VASA+ cells (West *et al*, 2011). Extended culture of GLCs without passaging purportedly produced more than 70% of cells positive for the meiotic marker SYCP3 and the meiotic

recombination protein MLH1. Upon further differentiation, cells showed increased expression of the male germ cell marker ACROSIN, with more than 6% of cells being haploid. Interestingly, this group and Nayernia et al., who also generated haploid cells, reported similar data (Nayernia et al, 2006). For instance, both groups established ESC-derived stable germ-like cell lines that expressed late PGC markers (*VASA* and *Stra8*) and upon further differentiation produced SYCP3-expressing meiotic subpopulations. As the cell lines established by Nayernia et al. showed imprinting abnormality, it would be interesting to know the imprinting status of these GLCs.

Park et al. reported that co-culturing of ESCs and iPSCs with human fetal gonadal stromal cells (hFGSCs) enhances the generation of PGCs (Park *et al*, 2009). When differentiated on hFGSCs in the absence of bFGF, both ESCs and iPSCs produced c-KIT, SSEA-1, and VASA triple-positive cells that additionally co-expressed *BLIMP1, STELLA,* and *DAZL* by day 7. PGCs generated from ESCs initiated imprinting erasure, whereas iPSC-derived PGCs did not, indicating that iPSC-derived PGCs may have a compromised ability to undergo erasure of CpG methylation at imprinted genes. Of importance is that the induced differentiation of hFGSCs into PGCs was more efficient than that of placenta or liver stromal cells, suggesting that PGC induction is affected by not only the topology of the feeder cells, but also the specific cell type of the starting cell population.

Table 2. Overview of germ cell differentiation procedures cited in the introduction (modified Sugawa *et al.* 2013). mESC: mouse embryonic stem cell, miPSC: mouse induced pluripotent stem cell, hESC: human embryonic stem cell, hiPSC: human induced pluripotent stem cell, MN: monolayer, EB: embryoid body, MEF: mosue embryonic fibroblast, hFGSC: human fetal gonad stromal cell, R115866: CYP26 inhibitor, postPGC: post-migratory PGC, prePGC: pre-migratory PGC, PGC: primordial germ cell, 1: Upon transplantation into mouse, 2:Upon overexpression of germ cell-related genes(s)

Reference	Origin	Approach / Factors supplemented	Cells observed / Offspring
Hübner et al. 2003	mESC	ML / -	postPGC, oocyte, blastcyst
Toyooka et al. 2003	mESC	EB / co-aggregate with TM4 secreting BMP4	postPGC, sperm
Geijsen et al. 2004	mESC	ML / -	sperm, blastcyst (by ICSI)
Lacham-Kaplan et al. 2006	mESC	EB / mouse testis-conditioned medium	oocyte
Nayernia et al.2006	mESC	ML / RA	postPGC, sperm, offspring[1] (abnormal)
Novak et al. 2006	mESC	ML / -	oocyte
Qing et al. 2007	mESC	EB / co-culture with mouse granulosa cells	oocyte
Nicholas et al. 2009	mESC	EB / BMP4, CYP26 inhibitor, SDF1, SCF, bFGF, n-acetyl-cysteine, forskolin	postPGC, oocyte
Hayashi et al. 2011, 2013	mESC, miPSC	ML+EB / Activin A, bFGF, BMP4, BMP8b, LIF, SCF, EGF	prePGC, offspring[1]
Vincent et al. 2011	mESC	EB / -	prePGC
Psathaki et al. 2011	mESC	ML+EB / ITS, EGF, SCF, BMP4, LIF, FSH	oocyte
Nakaki e al. 2013	mESC	ML+EB / Activin A, bFGF	postPGC[2] (Blimp1, Prdm14, Tfap2c), offspring[1]
Clark et al. 2004	hESC	EB / -	postPGC
Kee et al.2006	hESC	EB / BMP4, BMP7, BMP8b	
West et al.2008	hESC	ML / co-culture with MEF, bFGF	postPGC
Tilgner et al. 2008	hESC	ML / -	postPGC
Bucay et al. 2009	hESC	ML / co-culture with MEF	postPGC
Park et al. 2009	hESC, hiPSC	ML / co-culte with hFGSCs	postPGC
Kee et al. 2009	hESC	ML / BMP4, BMP7, BMP8b	postPGC, sperm[2] (DAZ family)
Panula et al. 2011	hESC, hiPSC	ML / BMP4, BMP7, BMP8b	postPGC, sperm[2] (DAZ family)
West et al. 2011	hESC	ML / co-culture with MEF, bFGF	postPGC, sperm
Eguizabal et al. 2011	hESC, hiPSC	ML / co-culture with MEF, RA, bFGF, LIF, Forskolin, R115866	sperm
Medrano et al. 2011	hESC, hiPSC	ML / -	postPGC, sperm[2] (VASA)
Chuang et al.2012	hESC	EB / BMP4, WNT3A	postPGC

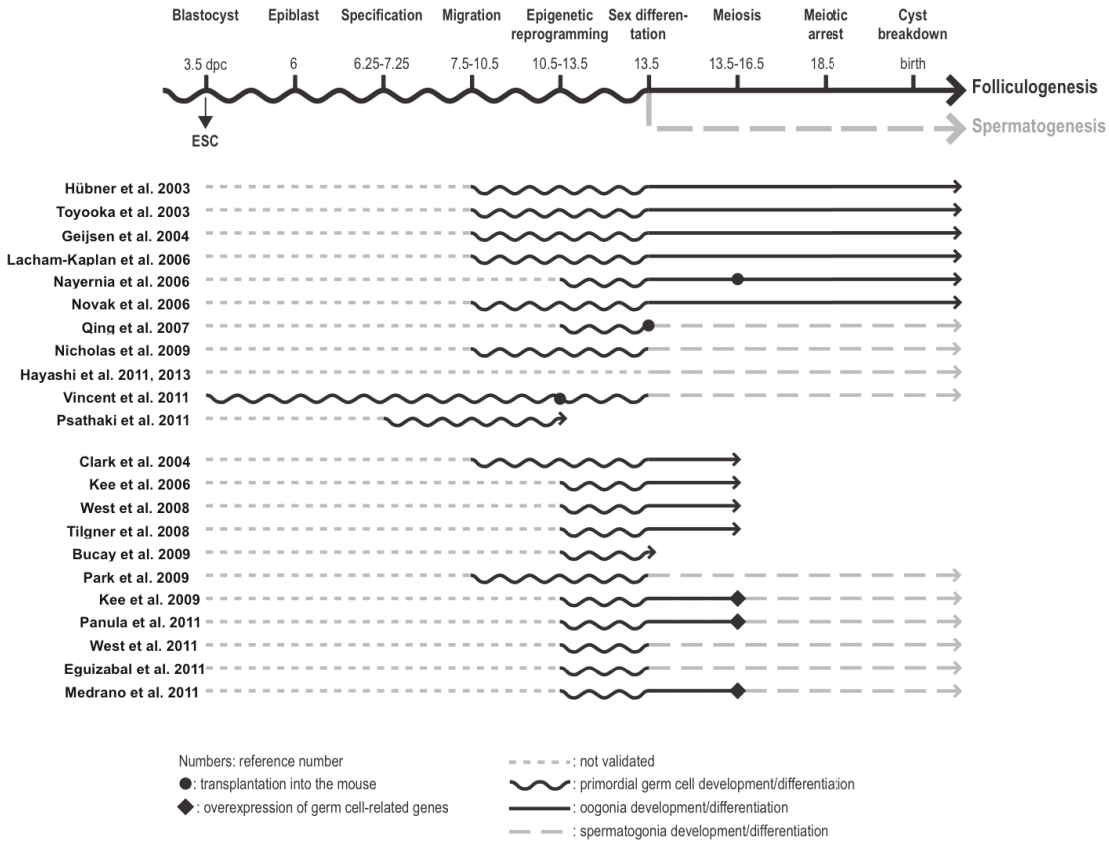

Figure 2 Chronology of mouse germ cell development and correlation of cited in vitro germ cell protocols (modified Sugawa *et al.* 2013).

2. Materials and methods

2.1. Materials

2.1.1. Reagents

Name	Manufacturer	Catalogue number
Accutase	PAA	L11-007
Activin A, recombinant human/mouse/rat	R&D systems	338-AC-010
Anti-BLIMP1 antibody	Cell Signaling	9115
Anti-BRACHYURY (T) antibody	Santa Cruz	sc-17745
Anti-OCT4A antibody	Santa Cruz	sc-8628
Anti-SSEA-1 (CD15) MicroBeads, human and mouse	Miltenyi Biotec	130-094-530
Anti-STELLA Antibody	Millipore	MAB4388
Anti-5-Methylcytosine (Methyl-CpG) Antibody	Aviva	Amm99021
α -MEM	Sigma-Aldrich	M4526
BLIMP1 shRNA lentiviral knockdown constructs	Thermo Fisher	RHS4533-EG639
BMP4, CF, recombinant Human	R&D systems	314-BP-050/CF
B27 supplement minus vitamin A	Invitrogen	12587-010
Chicken serum	Invitrogen	16110-082
CHIR99021	Biovision	1667-5
DMEM/F-12	Invitrogen	21041-025
DMEM high glucose	PAA	E15-009
DMEM low glucose	PAA	E15-005
DMSO	Sigma-Aldrich	D2650
DNase I	Sigma-Aldrich	DN25
Epidermal growth factor, recombinant human	Invitrogen	PHG0315
EpiTect Bisulfite Kit	QIAGEN	59104
FastDigest Green Buffer	Fermentas	B72
Fetal bovine serum	Hyclone	SH30070.03
Fetal bovine serum gold	PAA	A15-151
FGF-basic, recombinant human	Peprotech	100-18B
Fibronectin	Sigma-Aldrich	F2006
Follicle stimulating hormone, recombinant human	Sigma-Aldrich	F4021
Gelatin solution, 2%	Sigma-Aldrich	G1393
GMEM	Invitrogen	11710-035
G418 sulfate	Invitrogen	10131-035
HindIII	Fermentas	FD0504
HumanHT-12 v4 expression BeadChip kit	Illumina	BD-103-0204

Human Stem Cell Nucleofector Kit	Lonza	VPH-5012
Illumina TotalPrep RNA Amplification Kit	Ambion	AMIL1791
Insulin-Transferrin-Selenium-Sodium	Invitrogen	51300-044
Insulin-Transferrin-Selenium-Sodium	Sigma-Aldrich	
iTaq Universal SYBR Green Supermix	BioRad	172-5125
Knockout DMEM	Invitrogen	10829-018
Knockout serum replacement	Invitrogen	10828-028
Leukemia inhibitory factor, mouse	Millipore	ESG1107
Leukemia inhibitory factor, recombinant human	Millipore	LIF1010
L-glutamine	Invitrogen	25030-081
Lipofectamine 2000	Invitrogen	11668-019
MACS MS column	Miltenyi Biotec	130-042-201
MACS MultiStand	Miltenyi Biotec	130-042-303
Matrigel Matrix High Concentration, Growth Factor Reduced *LDEV-Free	BD Biosciences	354263
MiniMACS Separator	Miltenyi Biotec	130-042-102
M-MLV Reverse Transcriptase	Affymetrix	78306
Neurobasal medium	Invitrogen	12348-017
Nonessential amino acids	PAA	M11-003
NucleoBond Xtra Maxi	MACHEREY-NAGEL	740416.5
Nucleofector II device	Lonza	
N2 supplement	Invitrogen	17502-048
Opti-MEM	Invitrogen	31985062
Penicillin /streptomycin	PAA	P11-010
Penicillin /streptomycin /glutamine	PAA	P11-013
PD0325901	Stemgent	04-0006
pCRII TOPO vector	Invitrogen	K4650-40
pEGFP-1 vector	Clontech	6086-1
pMD2.G	Addgene	12259
psPAX2	Addgene	12260
Phusion High-Fidelity DNA Polymerase	Thermo Fisher	F530
QIAquick PCR Purification Kit	QIAGEN	28106
QIAquick Gel Extraction Kit	QIAGEN	28704
PRDM14 shRNA lentiviral knockdown constructs	Thermo Fisher	RHS4533-EG63978
RPMI 1640	PAA	E15-039
RNeasy Micro Kit	QIAGEN	74004
Sodium pyruvate	PAA	S11-003
Stem cell factor, recombinant mouse	Millipore	GF141

Stem cell factor, recombinant human	Invitrogen	PHC2116
Streptavidin-Cy3	GE Healthcare	PA43001
TOP10 Chemically Competent *E. coli*	Invitrogen	C4040-10
TrypLE express enzyme, no phenol red	Invitrogen	12604-021
Trypsin-EDTA 0.25%, phenol red	Invitrogen	25200-056
T4 ligase	Roche	10799009001
WNT3A, recombinant human	R&D systems	5036-WN-010
XhoI	Fermentas	FD0694
Y-27632 dihydrochloride	Abcam Biochemicals	ab120129
ZR Plasmid Miniprep	ZYMO research	D4015
2-mercaptoethanol	Invitrogen	31350-010

2.1.2. Equipment

Name	**Manufacture**	**Catalogue number**
Conical tube, 15 ml	SARSTEDT	62.554.002
Conical tube, 50 ml	SARSTEDT	62.547.004
Culture plate, 10 cm	SARSTEDT	83.1802
Culture plate, 12 well	Nunc	150628
Culture plate, 15 cm	SARSTEDT	83.1803
Culture plate, 6 cm	SARSTEDT	83.1801
Culture plate, 6 cm suspension	Corning	430589
Culture plate, 6 well	SARSTEDT	83.§839
Culture plate, 96 well U-Bottom Ultra Low Attachment	Corning	7007
CryoTube vial	Nunc	377244
Cell strainer, 40 μ m	BD Biosciences	352340
Cell strainer, 70 μ m	BD Biosciences	351350
Vacuum Filter, 0.22 µm	Corning	431153

2.2. Methods

2.2.1. Animals

The SCID mice used in this study were raised in a temperature and humidity controlled animal facility with a 12 hr light- dark cycle controlled environment at a

temperature of 22 ± 1 °C and 35 ± 5 % humidity. All the animal experiments were performed under the ethical guidelines of the Max Planck Institute.

2.2.2. Cell culture medium

MEF medium

- DMEM Low Glucose
- 15% Fetal bovine serum Gold
- 1x Penicillin /streptomycin /glutamine

Mouse ESC medium

- Knockout DMEM
- 15% Knockout serum replacement
- 1x Penicillin /streptomycin /glutamine
- 1x Nonessential amino acids
- 0.1 mM β-Mercaptoethanol
- 1,000 units/ml Leukemia inhibitory factor, mouse

Mouse PGC medium (serum-containing)

- DMEM high Glucose
- 15% Fetal bovine serum
- 1x Penicillin /streptomycin /glutamine
- 1x Nonessential amino acids
- 0.1 mM β-Mercaptoethanol

Mouse PGC medium (serum-free)

- modified αMEM
- 3 mg/mL Bovine serum albumin
- 1x Penicillin /streptomycin
- 2 mM L-glutamine
- 0.23 mM Sodium pyruvate (Invitrogen)
- 1x Insulin-Transferrin-Selenium-Sodium (Invitrogen)
- 1 ng/ml Epidermal growth factor, recombinant human

- 50 ng/ml Stem cell factor, recombinant mouse

Mouse oocyte growth media

- modifiedαMEM
- 3 mg/mL Bovine serum albumin
- 1x Penicillin /streptomycin
- 0.23 mM Sodium pyruvate (Invitrogen)
- 5mg/mL Insulin, 5mg/mL Transferrin, 5ng/mL Selenium (Sigma-Aldrich)
- 1 ng/ml Epidermal growth factor, recombinant human
- 5 ng/mL Follicle stimulating hormone, recombinant human

Mouse oocyte maturation medium

- modified αMEM
- 3 mg/mL Bovine serum albumin
- 1x Penicillin /streptomycin
- 0.23 mM Sodium pyruvate (Invitrogen)
- 5mg/mL Insulin, 5mg/mL Transferrin, 5ng/mL Selenium (Sigma-Aldrich)
- 1 ng/ml Epidermal growth factor, recombinant human
- 100 ng/mL Follicle stimulating hormone, recombinant human

Human ESC medium

- Knockout DMEM
- 20% Knockout serum replacement
- 1x Penicillin /streptomycin /glutamine
- 1x Nonessential amino acids
- 0.1 mM β-Mercaptoethanol
- 5 ng/ml FGF-basic, recombinant human

Human PGC precursor medium (unless stated otherwise)

- DMEM/F-12
- 1x N2 supplement
- 1x B27 supplement minus vitamin A
- 1x Penicillin /streptomycin /glutamine

- 1x Nonessential amino acids
- 0.1 mM β-Mercaptoethanol
- 0.5% (wt/vol) bovine serum albumin
- 50 ng/ml Activin A, recombinant human/mouse/rat
- 5 ng/ml BMP4, career-free, recombinant human
- 20 ng/ml FGF-basic, recombinant human
- 10 ng/ml FGF-basic, recombinan

In some experiments, the following cytokine was added to the medium

- 100 ng/ml WNT3A, recombinant human

GK20 medium (Human PGC medium) (unless stated otherwise)

- GMEM
- 20% Knockout serum replacement
- 10 mM Sodium pyruvate (PAA)
- 1x Penicillin /streptomycin /glutamine
- 1x Nonessential amino acids
- 0.1 mM β-Mercaptoethanol
- 20 µM Y-27632 dihydrochloride

For the PGC differentiation, the following cytokines were added to the medium

- 100 ng/ml BMP4, career-free, recombinant human
- 20 ng/ml Leukemia inhibitory factor, recombinant human

In some experiments, the following cytokine was added to the medium

- 0.5-100 ng/ml Stem cell factor, recombinant human

RPMI medium

- RPMI 1640
- 15% Fetal bovine serum Gold
- 1x Penicillin /streptomycin /glutamine

Cell freezing medium

- The corresponding medium for cell lines without cytokines or chemicals
- 20% DMSO
- 10 μM Y-27632 dihydrochloride (only for human ESCs and iPSCs)

2.2.3. Cell culture

2.2.3.1. Derivation of MEF

MEFs were generated from E12.5 dpc embryos of C57BL/6, C3H, or CF1 mice. The pregnant female mice were sacrificed by cervical dislocation and extraembryonic membranes and placentas were removed and placed in PBS. The uteri were isolated and the embryos were removed and immersed in PBS. After decapitation of the embryos, heart and liver as well as the extremities were removed and the remaining embryos were placed in MEF medium. The embryos were cut into small pieces with scissors and digested with 0.05% Trypsin/EDTA for 4 min at 37 °C. The tissue was further digested with a 4 to 1 dilution of 0.05% Trypsin/EDTA with MEF medium. Subsequently, the digests were filtered through a 100 μm cell strainer and the cell suspension was centrifuged at 1,000 rpm for 5 min and then plated onto gelatinized plates at a density of 2-3 embryos per 15 cm tissue culture dish and cultivated at 37 °C with 5% CO2 in a humidified incubator.

2.2.3.2. MEF culture

MEFs were cultured in MEF medium on 0.1 % gelatin-coated 15-cm plates (2.0×10^6 cell/dish) at 37 °C with 8.5 % CO_2. The cells were passaged every other day by 0.25% Trypsin/EDTA dissociation of the culture into single cells until passage number 3. The cells were then mitotically inactivated by irradiation at 1 gy/min for 45 min and stored in freezing medium in liquid nitrogen.

2.2.3.3. Preparation of MEF-conditioned medium (MEF-CM)

Irradiated MEFs (CF1) were plated at 56,000 cells/cm^2 in MEF medium. To condition medium, MEF medium was replaced with human ESC medium (0.5 ml/cm^2). MEF-CM was collected and replaced with fresh human ES medium every day for 1 week.

The collected MEF-CM was then filtered (0.22 number 3), aliquoted and frozen at -20^{o}C.

2.2.3.4. Preparation of coated-plates

Gelatin-coated plates

Tissue culture dishes of the required size were coated with a layer of 0.1% gelatin in sterile PBS and incubated at 37 °C for 1 hr in a humidified incubator.

FBS-coated plates

Tissue culture dishes of the required size were coated with a layer of FBS and incubated at room temperature for 1 hr.

Matrigel-coated plates

Matrigel was thawed on ice overnight and then diluted 1:3 with ice-cold knockout DMEM. 1-ml aliquotes were then frozen at -20^{o}C as stocks. For coating of plates, each 1-ml stock was diluted with 24 ml of knockout DMEM on ice (1:75 total dilution). Precooled 6- or 12-well plates were covered with 1ml or 0.4ml of diluted matrigel, respectively. Plates were then wrapped in parafilm and kept at room temperature overnight. The next day, plates were transferred to 4 °C for at least 1 day.

2.2.3.5. Mouse ESC culture

Mouse ESCs were cultured either in mouse ESC medium on irradiated MEF (C57BL/6 or C3H)-coated plates or in mouse N2B27+2i medium on poly-L-ornithine/laminin-coated plates. The cells were passaged every other day by accutase dissociation of the culture into single cells.

2.2.3.6. Mouse EpiScs and Δouse EpiScs+ EpiSCs culture

Mouse EpiSCs and Δ and EpiSCs+ EpiSCs were cultured in MEF-CM supplemented with 5 ng/ml human bFGF at 37 °C with 5% CO_2 on FBS-coated plates. The medium was changed every day and the cells were passaged every 4–6 days by accutase dissociation of the culture into single cells.

2.2.3.7. Mouse PGC differentiation

Mouse ESC lines (gcOct4-GFP (XY) and OG2 (ΔPE-Oct4-GFP, XY; XX)) were differentiated into oocytes according to 3 protocols: a serum-containing protocol, a serum-containing/serum-free differentiation combination protocol, and a serum-free differentiation protocol. Briefly, for the serum-containing differentiation procedure, cells were grown in tissue culture plates in mouse PGC medium (serum-containing) in the absence of MEF feeder cells and LIF for up to 30 days. The medium was changed every 3 days for 9 days and every other day thereafter. Floating cell aggregates after day 12 of differentiation were collected and processed as published (Hubner et al, 2003).

For the serum-containing/serum-free differentiation combination technique, ESCs were differentiated under serum-containing conditions for 7–12 days. The adherent cell layer was digested with accutase and the single-cell suspension was then plated as a suspension culture at a 1:1 ratio in serum-free PGC medium in a humidified incubator at 37 °C in 5% O2 and 5% CO2. Cells were cultured for 7–15 days, and putative oocytes were then individually picked with a drawn-out glass capillary.

For the serum-free differentiation protocol, feeder-free ESCs were plated on gelatin-coated tissue culture plates in mouse N2B27 medium supplemented with 10 ng/ml Bmp4 and 1,000 units/ml LIF and cultured for 48 h. The adherent cell layer was then digested with accutase and the single-cell suspension was replated at a 1:2 ratio in IVG media supplemented with SCF (100 ng/ml) and LIF (1,000 units/ml) in suspension plates. After 3 days of culture, cell aggregates were transferred to gelatinized 24-well tissue culture plates at a density of 5–6 aggregates per well and further cultivated for 5 days in medium lacking LIF. Cultures were then partially digested in 0.05% trypsin/ EDTA supplemented with 0.02% DNase I, replated in oocyte growth media and cultured in a humidified incubator at 37°C in 5% O2 and 5% CO2 for additional 12–15 days. Putative oocytes were cultivated in maturation medium.

2.2.3.8. Human ESC and iPSC culture

Human ESCs and iPSCs were cultured in MEF-CM supplemented with 5 ng/ml human bFGF at 37 °C and 5% CO_2 on Matrigel-coated plates and used at a passage number below 50. The medium was changed every day and the cells were passaged every 4–6 days by collagenase IV (1 mg/ml) dissociation of the culture into cell clumps.

2.2.3.9. Human PGC precursor and PGC differentiation

To induce differentiation, human ESCs and iPSCs were dissociated into single cells by TrypLE and plated on a matrigel-coated well of a 12-well plate (2.0×10^5 cells/well) in PGC precursor medium. After 48 hours, cells were dissociated by TrypLE and plated in a well of an ultra-low-attachment U-bottom 96-well plate in human PGC medium (9,000 cells/well).

2.2.4. Amplification of STELLA promoter sequence

5 kbps of human STELLA promoter was amplified by PCR from genomic DNA of human ESCs (H9 human ESCs) using Phusion High-Fidelity DNA Polymerase. The condition and primers used for amplification are described below. The PCR products were analyzed by electrophoresis. Bands with expected product size were cut out of the gel and purified using the QIAquick Gel Extraction Kit according to the manufacture's protocol.

98 °C	30 sec	
98 °C	10 sec	40 cycles
60 °C	30 sec	
72 °C	2 min	
72 °C	10 min	
4 °C	∞	

	Primer sequence (5'-3')	**Product size (bp)**
STELLA promoter	Fw: TAGTTAGAGCTCATTCTCGAGAACAGCAGGTGCTGAAGG	4739
	Rv: TATTGAATTCAATTAAGCTTGATCGCCTAGGGGCTTAAC	
TEX13B promoter	Fw: TAGTTAGAGCTCATTCTCGAGGCTGCATGTTGGTAGGGTTT	4659
	Rv: TATTGAATTCAATTAAGCTTCGGCGTCTTGACACAACACT	

2.2.5. Ligation of the STELLA promoter sequence into pEGFP-1 vector

The PCR fragments and the pEGFP-1 plasmid were digested with HindIII and XhoI in FastDigest Green Buffer at 37 °C for 4 hr. The digested samples were purified using the QIAquick PCR Purification Kit according to the manufacture's protocol. The STELLA promoter fragment was then ligated into the pEGFP-1 vector using T4 ligase overnight at 16 °C.

2.2.6. Transformation of competent bacterial cells

50 µl of TOP10 Chemically Competent *E. coli* cells were thawed on ice for 10 min, mixed with 6-25 µl of the ligation reaction mix and placed on ice for 30 min and occasionally mixed. The transformation reaction mixture was heat shocked at 42 °C for 30 sec and immediately placed on ice for 5 min. 180 e tranLB medium was added to the reaction mixture and incubated at 37 °C with shaking for 1 hr. Cells were then plated on LB-agar plates containing kanamycin and incubated overnight at 37 °C in an upside-down position.

2.2.7. Plasmid DNA preparation

Individual transformed *E. coli* colonies were picked up and cultivated in 2 ml LB medium containing kanamycin at 37 °C for 16 hr. Plasmid DNA was isolated from 1 ml bacterial cultures using the ZR Plasmid Miniprep kit according to the manufacturer's protocol. For selection of clones containing the appropriate plasmid, the purified plasmids were digested with HindIII and analyzed by agarose gel electrophoresis. Samples that showed expected band size were further cultivated in 200 ml LB medium containing kanamycin at 37°C for 16 hr and purified using NucleoBond Xtra Maxi kit according to the manufacturer's protocol. Purified plasmids were stored at -20 °C until use.

2.2.8. Generation of STELLA-GFP human ESCs and iPSCs

For the generation of stable GFP reporter lines, the STELLA-GFP transgene was transfected using the Human Stem Cell Nucleofector Kit and Nucleofector II device according to the manufacturer's protocol. Briefly, human ESCs or iPSCs were pretreated with 10 µM Y-27632 dihydrochloride for 1 hour and dissociated into single

cells by TrypLE. 2 x 10^6 cells were resuspended in 100 µl nucleofection solution and incubated at 37 °C for 5 min. Then, 4 µg plasmid DNA were added to the cell suspension and transferred to the provided cuvette avoiding air bubbles. Nucleofection was performed with the A-23 program. After nucleofection, 500 µl pre-warmed RPMI medium was added to the cuvette, transferred to Eppendorf tubes and incubated at 37 °C for 5 min. The cell suspension was plated onto 1 well of a 6-well plate in hESC medium with 10 µM Y-27632 dihydrochloride. Transgene selection was done under standard human ESC/iPSC condition supplemented with G418 (200 µg/ml) from day 3 for 2 weeks. After the selection, individual colonies were clonally expanded for further experiments.

2.2.9. Lentivirus Production

Lentivirus were produced by transfecting the lentivirus constructs psPAX2 and pMD2.G using Lipofectamine 2000. Briefly, 12 mg of the lentivirus construct, 9 mg psPAX2 and 3 mg pMD2.G were mixed into 1.5 ml Opti-MEM. In parallel, 45 µl Lipofectamine 2000 was gently mixed with 1.5 ml fresh Opti-MEM and incubated at room temperature for 5 min. DNAs and Lipofectamine were then gently mixed and incubated at room temperature for 20 min to allow DNA and lipid to form complexes. The DNA-Lipofectamine complexes (3 ml) were dropped onto a 10 cm dish of 2.2 x 10^6 293T HEK cells in 6 ml Opti-MEM (total 9 ml) and incubated at 37 °C for 5 hr. The medium was replaced with MEF medium lacking antibiotics and incubated at 37 °C and 5 % CO_2. The supernatant was collected every day for 2 days and the virus was concentrated by ultracentrifugation at 26,000 rpm for 2 hours at 4 °C. Viral pellets were resuspended in 1ml knockout DMEM and stored at -80 °C.

2.2.10. Knock-down of BLIMP1 and PRDM14

BLIMP1 and PRDM14 shRNA lentiviral knockdown constructs were purchased from Thermo Fisher. The Lentivirus were produced as described in section 3.2.3.15. For infection of cells, iPSCs pretreated with 10 μM Y-27632 dihydrochloride for 1hr were dissociated into single cells by TrypLE. 1 x10^5 cells in 1 ml of human ESC medium were infected with 60 µl of concentrated virus in 15 ml tubes and incubated at 37°C and 5% CO_2 for 5 hr with occasional mixing. Thereafter, cells were washed with PBS three times and used for experiments.

2.2.11. Fluorescence-Activated Cell Sorting Analysis

Aggregates were dissociated with 0.25% Trypsin/EDTA supplemented with 2% chicken serum (37°C, 30 min). Dissociated cells were incubated with anti-TRA-1-81 antibody (eBioscience, cat. no. 14-8883) and anti-c-KIT antibody (eBioscience, cat. no. 550412) conjugated with PE and APC, respectively, on ice for 30 min. The cells were then washed three times with PBS supplemented with 5% FBS and analyzed on a flow cytometer.

2.2.12. Immunocytochemistry

Cells were fixed with 4% paraformaldehyde for 15 min, permeabilized with 0.2–1% Triton X-100 for 10 min, and blocked with a solution comprising 2% BSA, 5% FBS, and 0.1% Tween 20 in PBS for 45 min. For 5mC, cells were treated with 4N HCl for 30 min at room temperature before blocking. Primary and secondary antibodies were applied overnight at 4°C and for 1 h at room temperature, respectively, in 0.5% BSA in PBS-T. Hoechst stain was applied to the second-to-last washing step at 1 µg/ml. The primary antibodies used in this study were as follows: OCT4 (1:100), BLIMP1 (1:100), T (1:100), STELLA (1:100), and 5mC (1:100).

2.2.13. Real-Time PCR (qPCR)

Total RNA from cells was extracted and purified using the RNeasy Micro Kit. For qPCR, total RNA was reverse transcribed by M-MLV Reverse Transcriptase and the resultant cDNA was used for qPCR analysis. qPCR was performed with iTaq Universal SYBR Green Supermix and 0.375 µg total RNA.

	Primer sequence (5'-3')	**Product size (bps)**
OCT4	F: GGAAGGAATTGGGAACACAAAGG	71
	R: AACTTCACCTTCCCTCCAACCA	
NANOG	F: CCTGTGATTTGTGGGCCTG	78
	R: GACAGTCTCCGTGTGAGGCAT	
SOX2	F: TGGCGAACCATCTCTGTGGT	111
	R: CCAACGGTGTCAACCTGCAT	
T	F: CCTTGCTCACACCTGCAGTAGC	79
	R: GGCCAACTGCATCATCTCCA	
BLIMP1	F: AGGAAAGGACCTCTACCGTTC	118

	R: GATGGGGTAAACGACCCGAG	
STELLA	F: CATGTTACTCGGCGGAGT	63
	R: ACTCCCTTAGGCTCCTTG	
c-KIT	F: ACTTGAGGTTTATTCCTGACCCC	78
	R: GCAGACAGAGCCGATGGTAG	
HAND1	F: TCCCTTTTCCGCTTGCTCTC	114
	R: CATCGCCTACCTGATGGACG	
CDX2	F: TCACTACAGTCGCTACATCACCATC	78
	R: TTAACCTGCCTCTCAGAGAGCC	
PAX6	F: CCAGGGCAATCGGTGGTAGT	84
	R: ACGGGCACTCCCGCTTATAC	
MIXL1	F: CAGAACAGGCGTGCCAAGTC	94
	R: TTCCAGGAGCACAGTGGTTGA	
MESP1	F: CAACTGACGCCGTCTCTGTGA	71
	R: GTCTGCCAAGGAACCACTTCG	
GSC	F: ACCTCCGCGAGGAGAAAGTG	101
	R: CTTCTCCGCGTTCTCCGACT	
EOMES	F: CGGCCTCTGTGGCTCAAA	76
	R: AAGGAAACATGCGCCTGC	
GATA4	F: AATGACTCCAGAACAACAACTGGG	111
	R: CTCCCTCCAGTCCCATCAGC	
GATA6	F: TGTGCGTTCATGGAGAAGATCA	83
	R: TTTGATAAGAGACCTCATGAACCGACT	
NPNT	F: GTAAGCACAGGTGCATGAACA	79
	R: GAACCATCCGGCATGAGCATA	
SOX17	F: TTCGTGTGCAAGCCTGAGATG	99
	R: GTCGGACACCACCGAGGAA	
GAPDH	F: CTGGTAAAGTGGATATTGTTGCCAT	81
	R: TGGAATCATATTGGAACATGTAAACC	
ACTB	F: TCAAGATCATTGCTCCTCCTGAG	87
	R: ACATCTGCTGGAAGGTGGACA	

2.2.14. Microarray analysis

For microarray, total RNA was used as input into a linear amplification protocol (Illumina TotalPrep RNA Amplification Kit), which involved synthesis of T7-linked double-stranded cDNA and 12 h of *in vitro* transcription incorporating biotin-labeled nucleotides. Purified and labeled cRNA was then hybridized for 18 h onto HumanHT-12 v4 expression BeadChips (Illumina) following the manufacturer's instructions. After washing as recommended, chips were stained with streptavidin-Cy3 (GE Healthcare) and scanned using the iScan reader (Illumina) and accompanying software. Samples were exclusively hybridized as biological replicates.

2.2.15. Microarray data processing (performed by Araúzo-Bravo, Marcos J)

The bead intensities were mapped to gene information using BeadStudio 3.2 (Illumina). Background correction was performed using the Affymetrix Robust Multi-array Analysis (RMA) background correction model (Irizarry *et al*, 2003). Variance stabilization was performed using the $\log_2$ scaling and gene expression normalization was calculated with the method implemented in the lumi package of R-Bioconductor. Data post-processing and graphics was performed with in-house developed functions in Matlab. Hierarchical clustering of genes and samples was performed with one minus correlation metric and the unweighted average distance (UPGMA) (also known as group average) linkage method.

The gene ontology terms were taken from the AMIGO gene ontology database (Ashburner *et al*, 2000). The significance of the gene ontology terms of the different expressed genes was analyzed using an enrichment approach based on the hypergeometric distribution. All the sets of gene ontology terms were back propagated from the final term appearing in the gene annotation to the root term of each ontology. The significance (*p*-value) of the gene ontology terms enrichment was calculated using the hypergeometric distribution. The multitest effect influence was corrected through controlling the false discovery rate using the Benjamini-Hochberg correction at a significance level.

The data discussed in this publication have been deposited in NCBI's Gene Expression Omnibus and are accessible through GEO Series accession number GSE53498.

2.2.16. Bisulfite Sequencing

PCR products were purified using either QIAquick gel extraction kit or PCR purification kit (Qiagen), cloned into TOPO vector (Invitrogen), and then subsequently transformed into TOP10 *E. Coli* . Individual colonies were inoculated into LB medium containing Kanamycin (50 μ g/ml) and cultured overnight in a 37°C shaking incubator. Plasmids were extracted using the ZR Plasmid Miniprep kit. Ten insert-containing colonies (determined by the EcoRI digestion) were sequenced with the M13 forward primer.

To determine the DNA methylation status at regulatory regions of imprinted genes, bisulfite conversion was carried out on 2 μg of isolated genomic DNA with the EpiTect Bisulfite Kit according to the manufacturer's protocol. The bisulfite-converted DNA was amplified by PCR using the condition and primers according to a previous study (Kim *et al*, 2007). Briefly, PCR was performed in a 25 μl reaction volume, with 0.625 units of Hotstar Taq polymerase (Qiagen), 1× supplied reaction buffer, 0.5 μM of each primer, 1.5–2.5 mM of $MgCl_2$, 0.25 mM of dNTP (Invitrogen), and 50 ng of each DNA template. The PCR cycling conditions were as described below.

95 °C	15 min	
95 °C	1 min	40 cycle
58 °C	30 sec	
72 °C	1 min	
72 °C	9 min	
4 °C	∞	

Thereafter, the PCR products were cloned into the pCRII TOPO vector according to the manufacturer's protocol. Individual clones were sequenced with the M13 forward primer by GATC-biotech (http://www.gatc-biotech.com/en/index.html). Sequences

were analyzed using the Quantification Tool for Methylation Analysis (QUMA, http://quma.cdb.riken.jp).

	Primer sequence (5'-3')	**Product size (bps)**
PEG1 DMR	F: TYGTTGTTGGTTAGTTTTGTAYGGTT	290
	R: AAAAATAACACCCCCTCCTCAAAT	
KvDMR1	F: TGATGTGTTTATTATTTYGGGG	304
	R: CCCTAAAATCCCAAATCCTC	
PEG10 DMR	F: GGTGTAATTTATATAAGGTTTATAGTTTG	234
	R: AACAAAAAAAATAAAATCCCACAC	
NESP55 DMR	F: TTTTTGTAGAGTTAGAGGGTAGGT	344
	R: AAAAAAAACAACTCAAAATCTACC	
M13	F: GTAAAACGACGGCCAGT	

2.2.17. Transplantation of reconstituted ovaries under the ovarian bursa

Generation of reconstituted ovaries and transplantation under the ovarian bursa of mice was carried out according to a published protocol with slight modifications (Hayashi & Saitou, 2013). Briefly, fluorescence-activated cell sorting (FACS)-sorted d4 TRA-1-81+/c-KIT+ cells were re-aggregated with embryonic day (E) 12.5 gonadal somatic cells at a ratio of 5,000:50,000. For this, female gonads were collected from embryos at E12.5. The mesonephri were surgically separated from the gonads using tungsten needles. The gonads were dissociated with 0.05% Trypsin/EDTA supplemented with 0.02% DNase I (10–15 min, 37°C) and endogenous PGCs were removed by magnetic cell sorting using anti-SSEA1 antibody conjugated with magnetic beads and MACS MS column according to the manufacturer's protocol. The resulting gonadal somatic cells and FACS-sorted PGCLCs were plated in the wells of a low-cell–binding U-bottom 96-well lipid-coated plate in GK20. After 2 days of culture in GK20, the reconstituted ovaries were transplanted under the ovarian bursa. Briefly, two reconstituted ovaries were inserted with a glass capillary through a slit under the ovarian bursa of 4-week-old SCID female mice that had been anesthetized.

Transplanted ovaries were then collected from the recipient female mice 3 months after transplantation.

2.2.18. Electron microscopy (performed by Psathaki, O. E.)

For transmission electron microscopy (TEM), cells were fixed with 2.5% glutaraldehyde (Merck) in 0.1 M sodium cacodylate buffer (pH 7.4), postfixed in 1% aqueous osmium tetroxide, dehydrated stepwise in a graded ethanol series, and embedded in Epon 812 (Fluka, Buchs, Switzerland). Ultrathin (50 nm) sections were prepared with an ultramicrotome (EM UC6; Leica), stained first with 1% uranyl acetate and then with 3% lead citrate, and subsequently examined using a Zeiss EM 109 electron microscope (Zeiss). Images were taken on 70 mm films (Maco ORT 25c orthochromatic; Hans O. Mahn & Co., Photo Division).

For scanning electron microscopy (SEM), cells were fixed with 2.5% glutaraldehyde in 0.1 M phosphate buffered saline (pH 7.4) and dehydrated stepwise in a graded ethanol series. Samples were dried with 100% ethanol via CO_2 in a critical- point apparatus (Balzers). Dried samples were mounted onto aluminum stubs with leit-tabs and coated with gold film to a thickness of 40–50 nm in a sputter coater (Leitz). Cells were viewed under a Hitachi S-530 scanning electron microscope operated in a secondary mode at 20 kV.

3. Results

3.1. PGC differentiation from human ESCs and iPSCs

3.1.1. Examination of in-house protocol and published protocol for PGC differentiation from human ESCs

A study on human PGC differentiation was reported demonstrating that serum-based medium supplemented with BMP4 sufficiently induces VASA-GFP+ putative PGCs (up to 5%) (Kee et al, 2009). I therefore assessed if the protocol works similarly in our laboratory. To this end, I differentiated human ESCs according to the study and analyzed expression levels of *OCT4*, *BLIMP1*, *PRDM14*, *STELLA*, *SYCP3*, *LHX8* and *NOBOX* on day 2, 5, 10 and 15. As shown in Figure 3A, the serum-based differentiation procedure generated very similar expression changes as the mouse protocol, with the exception that *STELLA* expression was significantly downregulated. To further substantiate PGC identity, I analyzed SSEA1 and c-KIT expression in my cultures, since a previous study had demonstrated that post-migratory human PGCs could be distinguished from other cell types by those two surface antigens (Park et al, 2009). Although the publication reported induction of up to 5% PGC-like cells after 14 days of differentiation, I barely found SSEA-1+/c-KIT+ cells, independent of cell lines used (Figure 3B). This outcome is most probably due to common serum lot differences indicate that serum-based conditions are uncontrollable and therefore difficult to reproduce between different laboratories.

I then assessed the protocol, which we had developed to differentiate PGCs from mouse ESCs (Psathaki et al, 2011). I differentiated human ESCs following the mouse protocol and again analyzed expression levels of *OCT4*, *BLIMP1*, *PRDM14*, *STELLA*, *SYCP3*, *LHX8* and *NOBOX* on day 2, 5, 10 and 15. As shown in Figure 4A, *OCT4* and *PRDM14* were strongly downregulated upon differentiation, indicating the loss of pluripotency in the culture, as these genes are known to be involved in pluripotency. The early PGC genes *BLIMP1* got upregulated on day 2 (4-fold) and then downregulatd on later days. *STELLA* was slightly upregulated on day 2 (1.5-fold), but downregulated on later days (0.7-fold). *NOBOX* did not show significant expression change. On the other hand, the meiotic gene *SYCP3* was upregulated on day 2, however, became undetectable on day 10 and 15. Interestingly, the late PGC gene

LHX8 was upregulated on day2 (25-fold) and its expression level further increased until day 15 (81-fold). I interpreted this observation as an indication for the presence of putative PGCs. I then assessed if this condition could induce SSEA-1+/c-KIT+ putative PGCs. However, this condition proved insufficient to induce putative PGCs, as I did not observe a significant induction of SSEA-1+/c-KIT+ cell population from three independent human ESCs and iPSC lines (Figure 4B). These data demonstrated that the mouse protocol works insufficiently to induce putative PGCs from human ESCs.

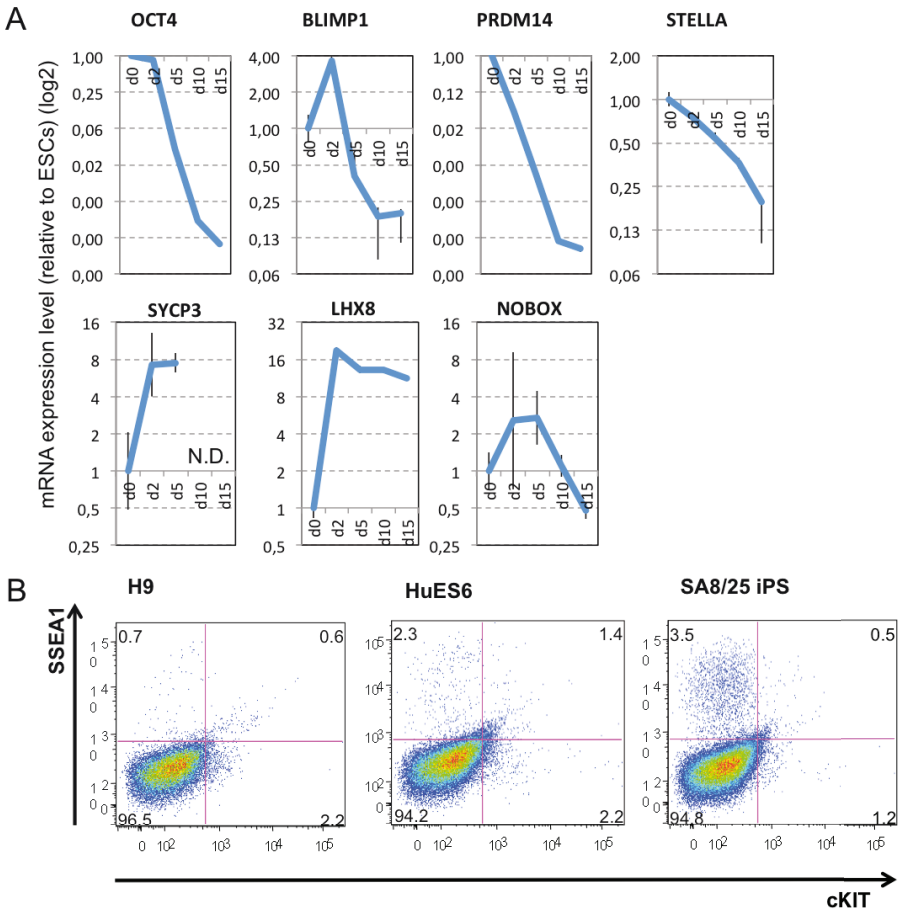

Figure 3 Differentiation of human pluripotent stem cells by a published protocol. (**A**) Gene expression dynamics in bulk cultures during differentiation. The value for ESCs is set as 1, and values are on log2 scale. N.D.: not detectable (**B**) FACS analysis of SSEA-1+/c-KIT+ cells from three independent ESC and iPSC lines.

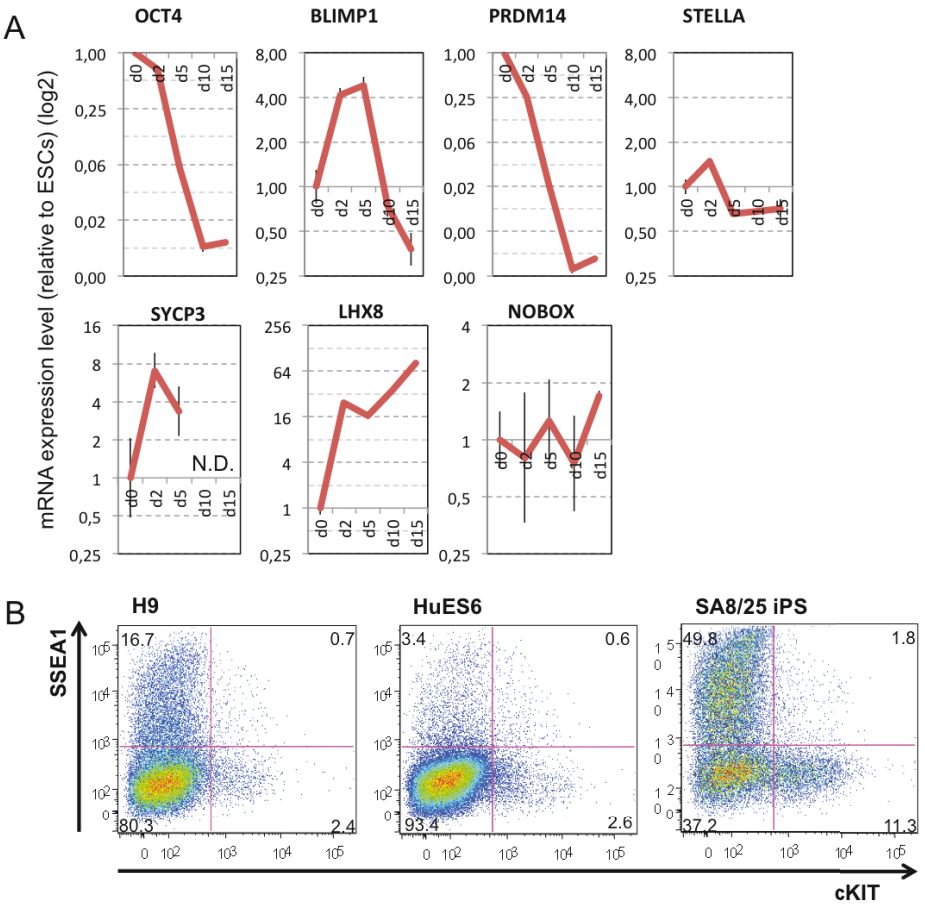

Figure 4 Differentiation of human pluripotent stem cells by the mouse PGC induction protocol. **(A)** Gene expression dynamics in bulk cultures during differentiation. The value for ESCs is set as 1, and values are on log2 scale. N.D.: not detectable **(B)** FACS analysis of SSEA-1+/c-KIT+ cells from three independent ESC and iPSC lines.

Next, I asked whether human ESCs contain a subpopulation of BLIMP+ PGC precursor, similar to mouse ESCs. In mouse, it is known that mouse EpiSCs contain a subpopulation of Bimp1+ (10-50 %) cells and Stella+ cells (0-1.5 %) (Hayashi & Surani, 2009). I performed immunofluorescent analysis for OCT4 and BLIMP1 in undifferentiated human ESCs. As shown in Figure 5, I could not detect any BLIMP1+ cells in OCT4+ human ESCs. I therefore concluded that human ESCs do not contain a sub-population of PGC and, thus, demonstrate a different character from mouse EpiSCs.

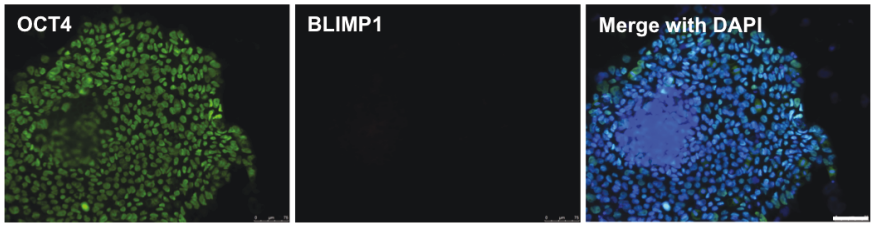

Figure 5 Immunofluorescence analysis of undifferentiated human ESCs. Scale bar: 75 dif

3.1.2. Search for a candidate gene for PGC identification

Based on the results of the initial experiments, I set out to develop a new serum-free, directed differentiation protocol for the reproducible and efficient induction of germ cells from human pluripotent stem cells. To monitor early PGC induction in the complex cell mixture within differentiation cultures, I decided to engineer a GFP reporter construct and generate stably transfected ESC and iPSC cell lines. One of the known earliest human PGC genes is *BLIMP1* (see introduction). However, *BLIMP1* is known to be expressed in other somatic cell types, such as B cells (Turner *et al*, 1994), differentiating macrophages (Chang *et al*, 2000) and a subset of T-cells (Kallies *et al*, 2006; Martins *et al*, 2006). Therefore, I sought genes that exhibit a similar expression pattern as *BLIMP1* but would not be expressed in other cell types. To this end, I differentiated human ESCs in directed conditions by promoting or inhibiting BMP, TGF β and FGF signaling (table 3), and assessed the expression pattern and level of the pluripotency genes *OCT4*, *NANOG* and *SOX2*, and the PGC genes *BLIMP1* and *STELLA*, on day 7. In addition, I included 9 genes that were previously found to be specifically upregulated in 11.5-16.5 dpc mouse germ cells as compared to ESCs, namely *PLCL2*, *TDRKH*, *FKBP6*, *MOV10L1*, *C4ORF48*, *PIK3R3*, *AKT3*, *TEX13B* and *C19ORF57* (Sabour *et al*, 2011). As shown figure 6A, *OCT4* and *NANOG* were strongly downregulated in all conditioned. In contrast, *SOX2* was slightly upregulated when BMP signaling was inhibited. Interestingly, *BLIMP1* and *STELLA* were upregulated coincidently when BMP signaling was inhibited and WNT signaling was activated. Furthermore, among the genes that had been identified in the mouse study, *FKBP6* and *TEX13B* were upregulated in the condition that upregulated *BLIMP1* and *STELLA*. Interestingly, I did not observe any STELLA+ cells in our cultures, indicating that those cultures activate genes associated with germ cells, but not sufficient enough to induce bona fide PGCs. Nevertheless, *STELLA*, *FKBP6* and

TEX13B exhibited a similar expression pattern to *BLIMP1* and thus could potentially be used as germ cell specific reporters. In fact, qPCR analysis revealed that *STELLA* and *TEX13B* were distinctly expressed in the *in vitro* generated SSEA1+/c-KIT+ cells, together with *OCT4* and *NANOG*, again suggesting that these genes could be used as specific maker for identifying putative germ cells in humans (Figure 6B).

Table 3 List of additives used for differentiation. Concentration of each additive; BMP4: 10 ng/ml, Dorsomorphin: 1 eachCHIR99021: 3 μM, SB431542: 10 μM, PD325901: 1 μM.

Additive	**Function**	**Condition**										
		1	**2**	**3**	**4**	**5**	**6**	**7**	**8**	**9**	**10**	**11**
BMP4	BMP activator	+	+	+	-	+	-	-	-	+	+	-
Dorsomorphin	BMP inhibitor	-	-	-	+	-	+	+	+	-	-	+
CHIR99021	WNT activator	-	-	+	-	+	-	+	+	+	+	+
SB431542	Activin inhibitor	-	+	-	-	+	+	-	+	-	+	-
PD325901	FGF inhibitor	-	-	-	-	-	-	-	-	+	+	+

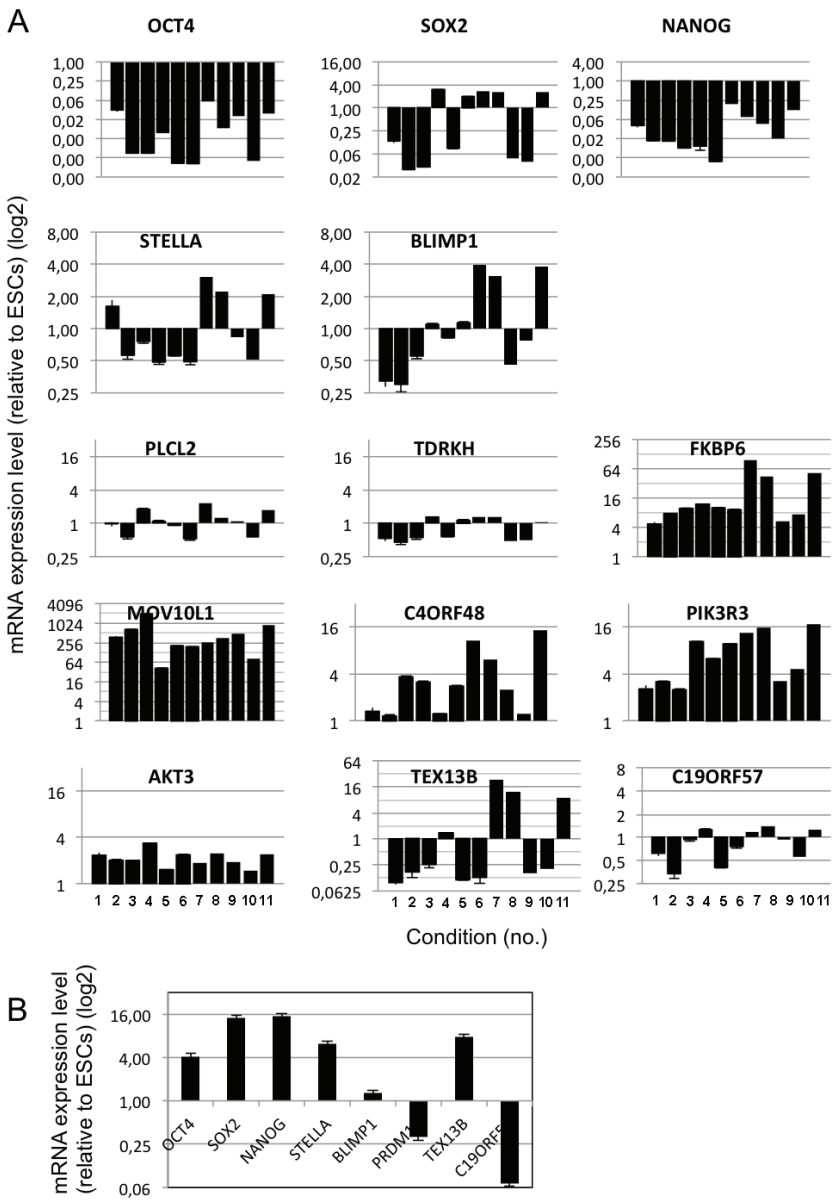

Figure 6 Expression of germ cell-relate genes in differentiated human ESCs (**A**) Gene expression analysis of human ESCs differentiated by modulating TGFen BMP and FGF signaling pathway. The value for ESCs is set as 1, and values are on log2 scale. (**B**) Gene expression analysis of SSEA-1+/c-KIT+ putative PGCs. The value for ESCs is set as 1, and values are on log2 scale.

3.1.3. Establishment of GFP reporter human pluripotent stem cells

Next I constructed a GFP-conjugated STELLA and a TEX13B reporter. The promoter of these genes was amplified from genomic DNA extracted from human ESCs (H9) by PCR. I tested several conditions, for example the presence or absence of DMSO, which is known to bind to the DNA at the cytosine residue and thus changes its conformation. This makes the DNA more labile for heat denaturation and thus enhances amplification. As shown Figure 7A, an enhanced amplification in the presence of DMSO is observed, although both approaches efficiently amplified the target fragment from gDNA (4739 bps and 4659 bps). Those PCR products were ligated into the pEGFP-1 vector (Fig. 7B). The sequence of the obtained construct was confirmed by enzymatic digestion and those showing appropriate band size were introduced in undifferentiated hESCs and human induced pluripotent stem cells (hiPSCs) (Fig. 7C, left two lanes) via transfection.

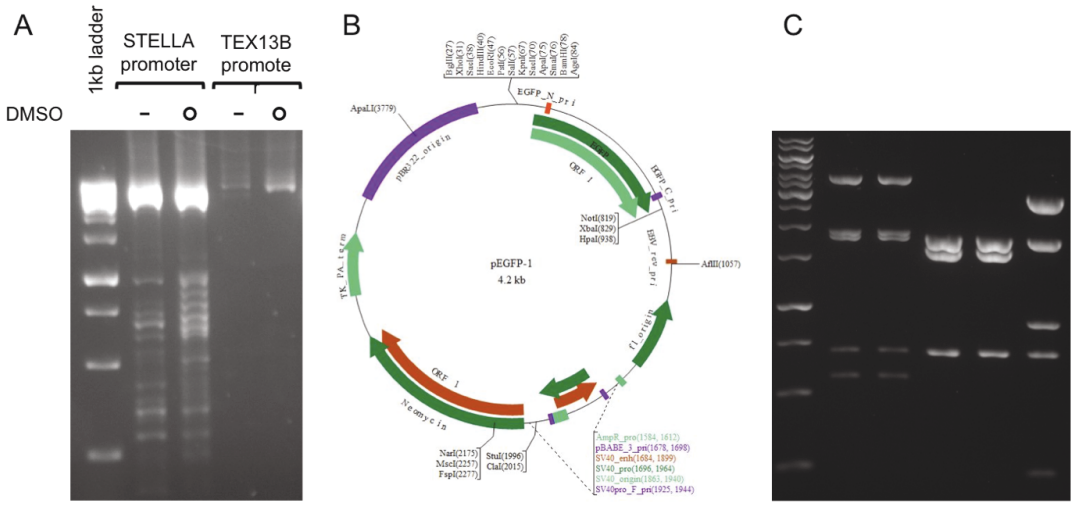

Figure 7 Construction of the STELLA and TEX13B reporters. (**A**) Amplified promoter region of STELLA and TEX13B by PCR (**B**) Schematic map of the pEGFP-1 vector (**C**) Enzymatic digestion of the STELLA-GFP plasmid.

3.1.4. Differentiation of STELLA-GFP human pluripotent stem cells

STELLA is known as definitive marker for PGCs in mouse, I therefore utilized STELLA-GFP cell lines for further experiments. I first differentiated these cells in serum-containing GMEM medium conditions. I did not observe GFP expression in

undifferentiated ESCs nor iPSCs, but detected it in some cells within embryoid bodies (EBs) (Fig. 8). However, only small numbers of GFP-positive cells were generated. I therefore switched to a defined serum-free differentiation conditions containing knockout serum replacement (KSR) (GMEM + 20% KSR, hereafter referred to as GK20), in which the amount and effect of cytokines can be strictly controlled. GK20 alone failed to produce any GFP+ cells (Fig. 8). Previous studies have demonstrated that BMP4 plays an important role in germ cell induction in both mice and humans (Kee et al, 2006; Ohinata et al, 2009). The addition of BMP4 to GK20 led to the induction of GFP+ cells, albeit still inefficiently (Fig. 8), demonstrating that the culture conditions still needed to be optimized.

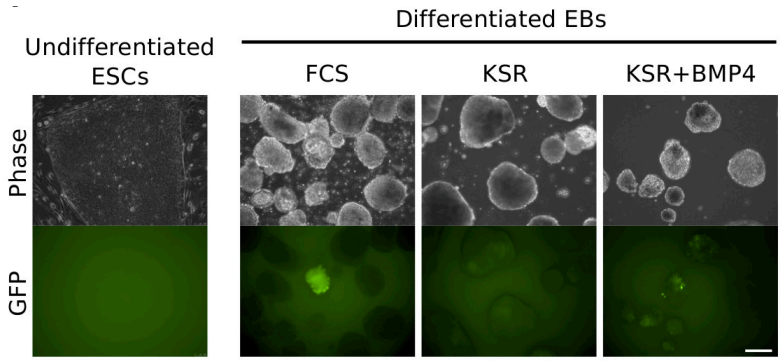

Figure 8 Morphology and GFP signal of undifferentiated STELLA-GFP ESCs and differentiated EBs. Scale bar: 100 FP signal of undifferentiated STELLA-GFP ESCs and different

Therefore, I attempted to improve the differentiation efficiency using two different approaches: 1) the formation of homogeneous EBs from dissociated single cells, and 2) the pre-differentiation of hPSCs toward early mesoderm–committed PGC precursors with the help of known cytokines (Activin A, BMP4, and bFGF).

Spontaneous EB formation of a defined number of single cells resulted in the more homogeneous size of EBs compared to the previous approach (Fig. 9A). On the other hand, EBs generated by this approach often uncontrollably stuck to each other and formed large sized aggregates. In addition, although GFP+ cells were observed in a higher number of EBs, a still considerable number of EBs lacked GFP+ cells, indicating that formed EBs were still inhomogeneous. To solve this problem, I used

ultra-low attachment U-bottom 96-well plates. The ultra-low attachment surface is a covalently bound hydrogel layer that is hydrophilic and neutrally charged. Since proteins and other biomolecules passively adsorb to polystyrene surfaces through either hydrophobic or ionic interactions, this hydrogel surface naturally inhibits nonspecific immobilization via these forces, thus inhibiting subsequent cell attachment (Fig. 9B). As shown figure 9C, this approach successfully generated homogeneous sized EBs from single cells and more importantly, also resulted in a homogeneous GFP signal with all EBs containing GFP+ cells. While this approach successfully resolved two problems, the formation of equally sized EBs and the homogenous distribution of GFP+ cells within each EB, the yield of GFP+ cells in each EB was still unsatisfactory and needed to be improved.

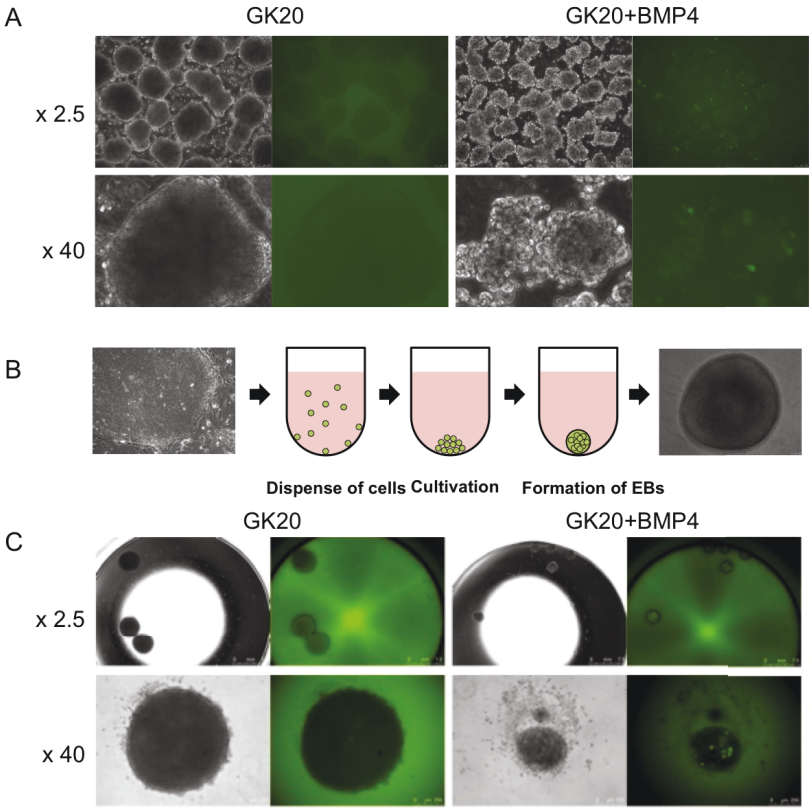

Figure 9 PGC differentiation from single-cell dissociated human ESCs. **(A)** Spontaneous EB formation of single-cell human ESCs **(B)** The scheme of EB formation by ultra-low attachment U-bottom 96-well plates **(C)** Forced EB formation of single-cell human ESCs by ultra-low attachment U-bottom 96-well plates

Next, I used a second approach. In mice, PGC specification involves activation of the mesodermal program, indicated by the expression of *T* followed by activation of the PGC program (Saitou et al, 2002). Thus, the efficient generation of mesoderm-committed PGC precursors should support the differentiation of lineage-restricted PGCs at a higher efficiency. To proof this idea, I treated the cells with various concentrations of Activin A and BMP4 in the presence of bFGF for two days to induce mesoderm differentiation, followed by germ cell induction with BMP4 for additional 6 days, followed by evaluation of GFP expression (Fig. 10A). As shown in Figure 10B, this approach efficiently induced STELLA-GFP+ cells. In addition, based on STELLA-GFP expression on day 8, the addition of BMP4 played a crucial role in the GFP+ cell induction. This experiment clearly demonstrated that pre-differentiation of human iPSCs enables the induction of STELLA-GFP signal at high efficiency.

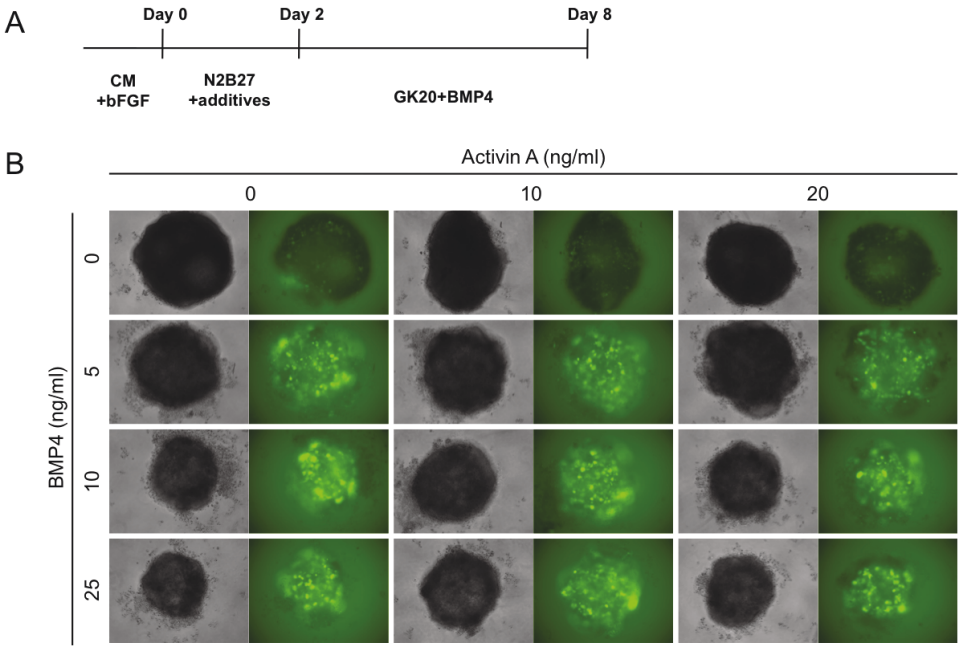

Figure 10 Two-step differentiation of human PSCs towards the germ cell lineage. (**A**) Schematic presentation of the differentiation strategy. (**B**) STELLA-GFP expression on day 8 of differentiation.

3.1.5. Differentiation toward mesoderm-committed germ cell precursors

To dissect the effect of Activin A and BMP4 during the pre-differentiation, I again treated the cells with various concentrations of Activin A (ActA) and BMP4 in the presence of bFGF for two days to induce differentiation and then analyzed the gene

expression profiles of representative pluripotency-associated genes (*OCT4*, *NANOG*, and *SOX2*), PGC genes (*BLIMP1* and *STELLA*), and mesodermal genes (*T)* (Fig. 11). The expression level of *T* was rapidly upregulated by ActA and BMP4, whereas the expression levels of *OCT4*, *NANOG*, and *SOX2* did not change significantly. Based on this gene expression dynamics, I observed that at least 50 ng/ml of ActA and 5 ng/ml of BMP4 were required for activating the *T* expression level, while maintaining similar *OCT4* and *NANOG* expression levels as PSCs. Notably, the expression level of *BLIMP1* (expressed from 6.5-dpc on in mouse PGCs) was concomitantly upregulated, whereas that of *STELLA* (expressed from 7.5-dpc on in mouse PGCs) was not altered. These findings suggested the presence of an intermediate cell state between the mesoderm and the germ cell lineage, characterised by mesodermal and early PGC gene activation. Taken together, these results indicate that the combinational activity of ActA, BMP4, and bFGF is essential for promoting the differentiation of human PSCs toward mesoderm-committed germ cell precursors mediated by the simultaneous activation of the mesodermal and PGC programs.

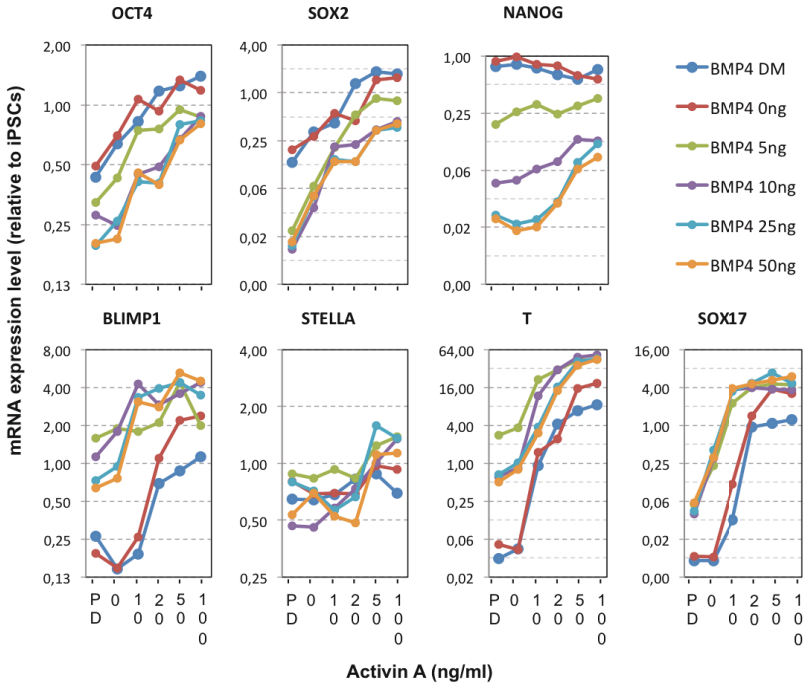

Figure 11 Effects of Activin A and BMP4 on the expression of selected pluripotency, PGC, and mesodermal genes during PGC-precursor induction. All conditions contained bFGF (20 ng/ml). DM: dorsomorphin, SB: SB431542. Samples were calibrated with iPSC values, and iPSC values depict 1. Y-axes are in log2 scale**.**

Next, I sought to determine whether differentiation for 2 days would maximize the induction of mesoderm-committed PGC precursors. To this end, I extended the differentiation period to day 7 and analyzed the gene expression dynamics (Figure 12A). During the entire culture period, expression levels of *OCT4*, *NANOG*, *SOX2* and *STELLA* remained similar to iPSCs levels (we observed 0.5-, 0.5-, 2- and 2-fold changes, respectively). In contrast, *T* and *BLIMP1* expression levels were rapidly upregulated within the first 2 days (512- and 32-fold changes, respectively) and gradually downregulated thereafter. Interestingly, the induction of *T* expression occurred one day earlier than that of *BLIMP1*. *T* expression started on day 1 and *BLIMP1* expression on day 2, results that were confirmed by immunostaining (Fig. 12B). Furthermore, BLIMP1 co-localized with *OCT4*. These results are consistent with observations in mouse studies, suggesting that gene expression dynamics during the induction of PGC precursors are developmentally conserved between the human and mouse species.

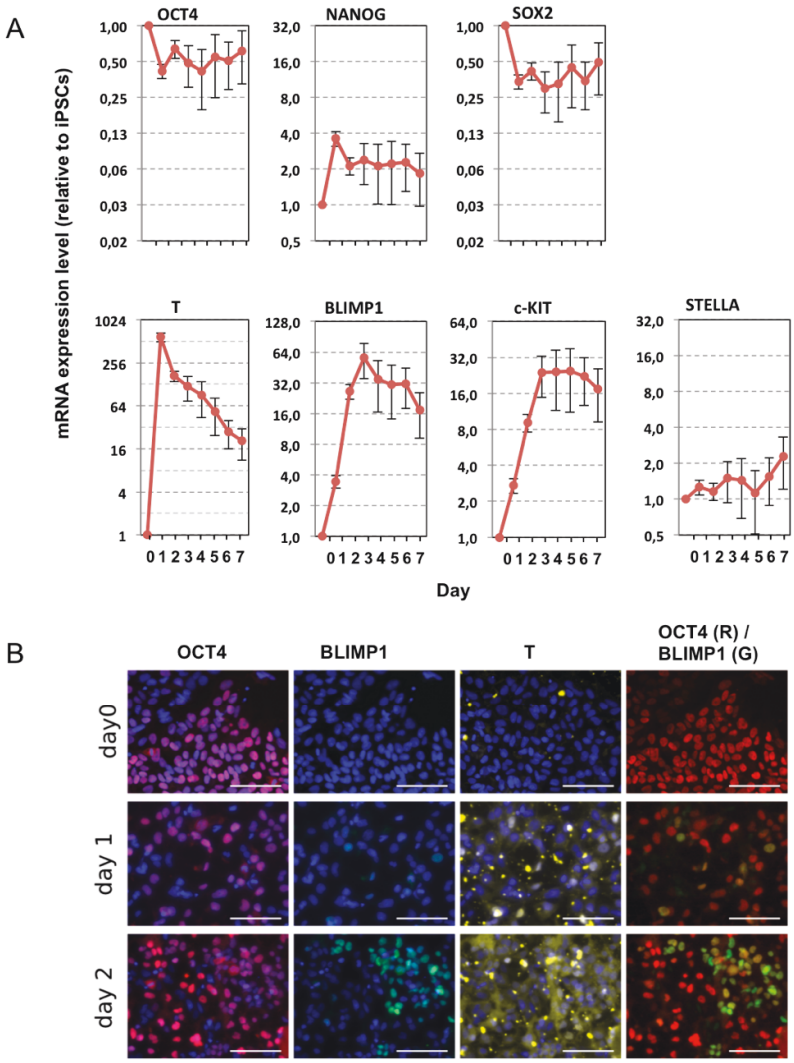

Figure 12 Time course analysis of PGC precursor induction. (**A**) Gene expression dynamics of selected pluripotency, PGC, and mesodermal genes during prolonged PGC-precursor induction up to day 7. Samples were calibrated with iPSC values, and iPSC values depict 1. Y-axes are in log2 scale. (**B**) Immunofluorescence analysis of OCT4, BLIMP1 and T on days 0, 1, and 2. The culture contained BMP4 (5 ng/ml), ActA (50 ng/ml), and bFGF (20 ng/ml) (also in E and F). Scale bar: 100 µm.

Surprisingly, *OCT4* and *BLIMP1* were still expressed at intermediate levels on day 7, implying that mesoderm-committed PGC precursors were still present at later time points of the differentiation. However, immunofluorescence analysis revealed that OCT4 and BLIPM1 no longer co-localized, indicating the loss of mesoderm-committed PGC precursors during prolonged culture *in vitro* (Fig. 13A). Overall, differentiation under defined conditions (N2B27 +ActA +BMP4 +bFGF) for 2 days is sufficient for the generation of mesoderm-committed PGC precursors. However, upon longer culture, the precursors lose their identity, become unstable and undergo further

differentiation into other cell lineages. Of special note is that, I did not detect c-KIT protein levels in OCT4+ cells, although the *c-KIT* transcript level was significantly upregulated until day 7 (Fig. 13B), This result indicates that the PGC precursors do not develop into lineage-restricted PGCs under the given culture conditions, but require another appropriate environment to become PGC-like cells.

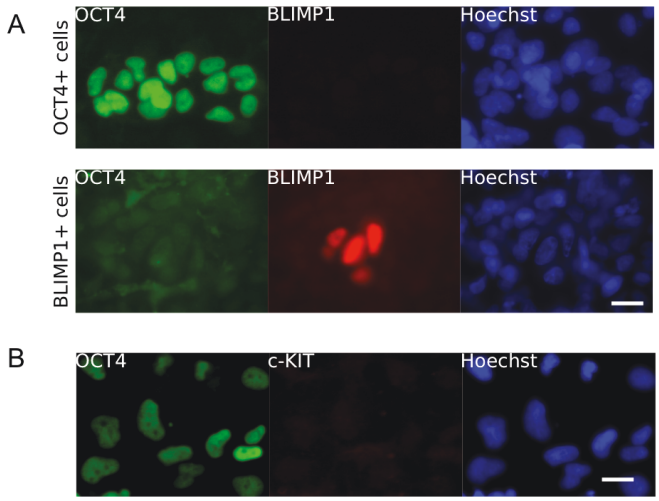

Figure 13 Immunofluorescence analysis of PGC precursor cultures. (**A**) Immunofluorescence analysis of OCT4 and BLIMP1 on day 5 of germ cell precursor induction. Scale bar: 20 µm. (**B**) Immunofluorescence analysis of OCT4 and c-KIT on the day of germ cell precursor induction. Scale bar: 20 µm.

3.1.6. Differentiation of PGC precursors towards PGC-like cells

To obtain PGC-like cells, I cultured the precursors in GK20 containing BMP4 for another 7 days to induce further differentiation (Fig. 14A). I observed an initial population of GFP+ cells on day 6 and found a continuous increase in the number of GFP+ cells until day 9 (14B).

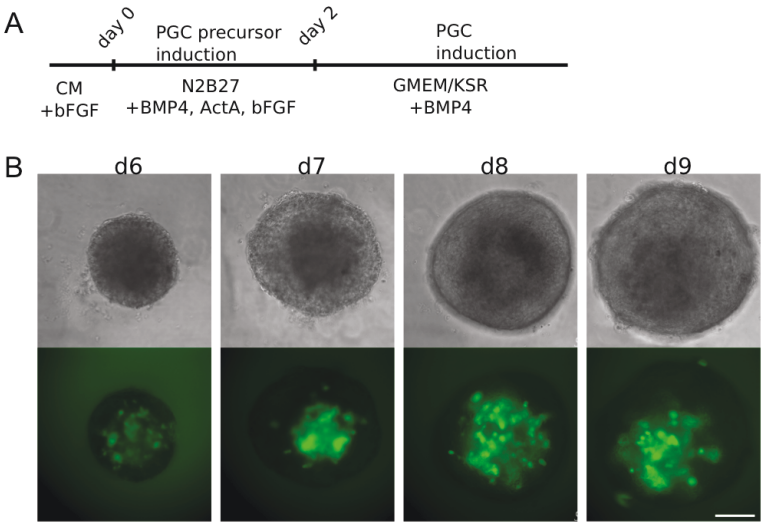

Figure 14 Induction of PGC-like cells from human iPSCs. (**A**) Schematic presentation of PGC-precursor and PGC-like cell induction. (**B**) Time-course images of PGC-like cell induction from days 6 to 9 of differentiation. Phase contrast and GFP fluorescent images are shown. Scale bar: 100 µm.

Then I attempted to isolate theses cells by FACS, but failed to do so due to unknown technical problems. For thi I chose an alternative approach. A previous study demonstrated that TRA-1-81+/c-KIT+ populations represent post-migratory putative germ cells in humans (Gkountela et al, 2013). I utilized this approach and sorted germ cell populations by FACS. Indeed, GFP was highly enriched in both TRA-1-81+/c-KIT+ and TRA-1-81-/c-KIT+ cells, whereas c-KIT- cells, regardless of TRA-1-81 expression, did not express GFP (Fig. 15). Thus, TRA-1-81 and c-KIT are reliable markers for isolating STELLA+ cells and can be used in support of the reporter system.

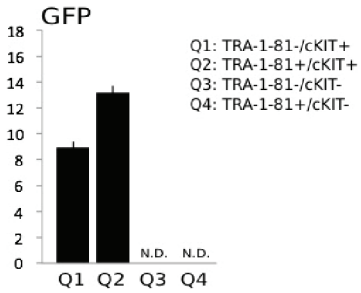

Figure 15 GFP expression of each cell fraction sorted by TRA-1-81 and c-KIT of cells from the aggregate cultures.

Next I titrated for the optimal concentration of BMP4 required for the transition of the precursors toward PGC-like cells. I observed that the number of TRA-1-81+/c-KIT+ cells increased in a dose-dependent manner (from 15.6% to 24%) (Fig. 16A) with an optimal BMP4 concentration of 100 ng/ml. Notably, in the absence of BMP4, we observed that approximately 7% of the cells were TRA-1-81+/c-KIT+, which most probably represented PGC-committed cells, as there was 5 ng/ml of BMP4 in the precursor induction medium. Interestingly, the maximum number of TRA-1-81+/c-KIT+ cells (>20%) was observed on day 4 (Fig. 16B). Thereafter the number of TRA-1-81+/c-KIT+ cells started to decrease, with a significant decrease observed on day 6 and only 2.2% of such cells observed on day 8.

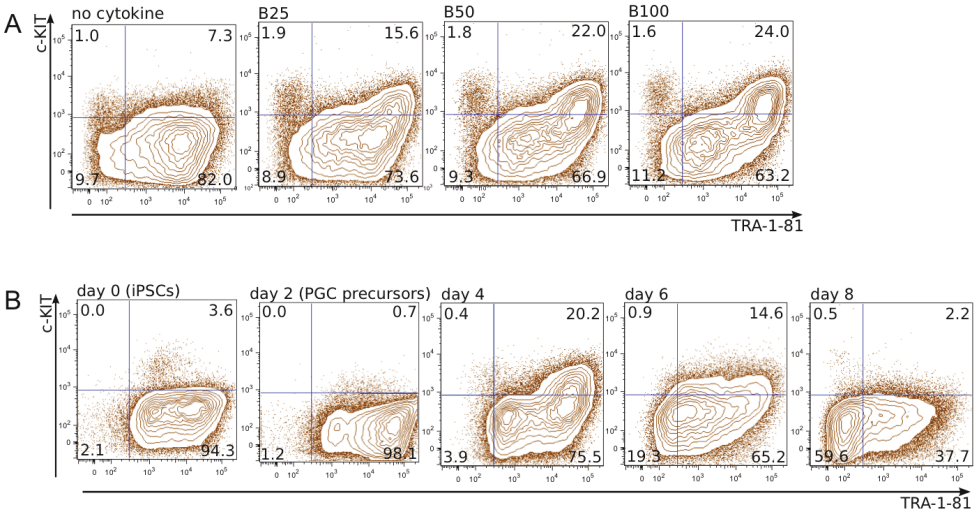

Figure 16 Induction of TRA-1-81+/c-KIT+ PGC-like cells from human iPSCs. (**A**) FACS analysis of the concentration-dependent effect of BMP4 on TRA-1-81+/c-KIT+ PGC-like cells on day 4. B25: 25 ng/ml BMP4; B50: 50 ng/ml BMP4; B100: 100 ng/ml BMP4. All conditions contained human LIF (20 ng/ml). (**B**) FACS analysis of TRA-1-81 and c-KIT during PGC induction up to day 8.

To overcome this loss of PGC-like cells I added SCF to the medium, but this approach was not successful (Fig. 17A). Nonetheless, differentiation of the precursors led to the reproducible induction of a sufficient number of PGC-like cells from independent cell lines (Fig. 17B).

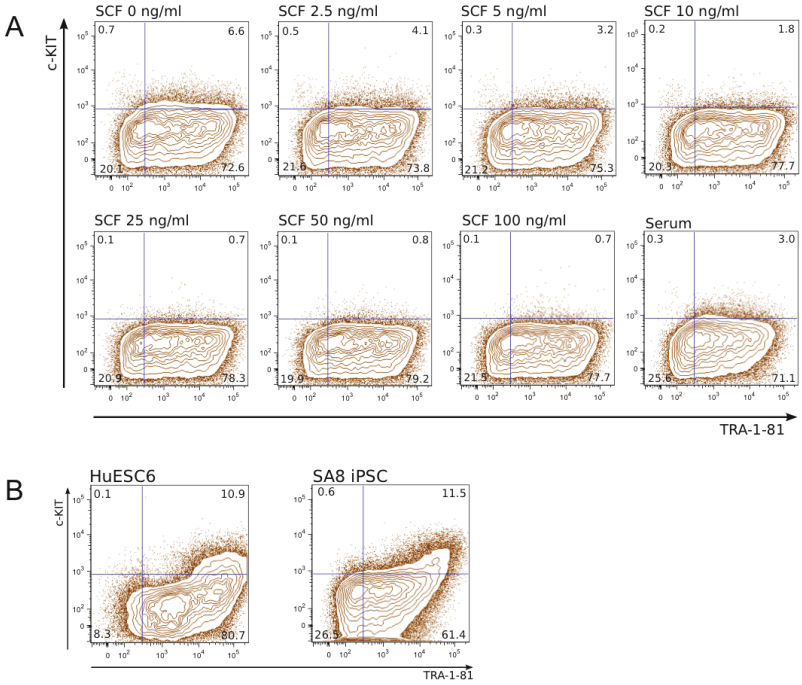

Figure 17 Effect of SCF on the induction of TRA-1-81+/c-KIT+ PGC-like cells. (**A**) Effect of SCF during PGC-like cell induction on PGC- like cell survival of d6 cultures. (**B**) Induction of PGC-like cells from the HuES6 ESCs and SA8 iPSCs on day 4.

3.1.7. Characterization of PCG-like cells

Next, I characterized the isolated PGC-like cells (TRA-1-81+/c-KIT+ cells) in more detail. First, I evaluated the gene expression profiles of key markers (*OCT4*, *NANOG*, *SOX2*, *BLIMP1*, and *STELLA*) (Fig. 18A). In contrast to the c-KIT- populations, *BLIMP1* and *STELLA* expression levels were dramatically upregulated in PGC-like cells, whereas *OCT4* and *NANOG* levels remained similar to iPSC levels. Upregulation of *BLIMP1* expression began on day 4 of differentiation, but that of *STELLA* expression only on day 6. Immunofluorescence analysis confirmed that endogenous *OCT4*, *BLIMP1*, and *STELLA* proteins were enriched in PGC-like cells (Fig. 18B). Interestingly, *SOX2* was downregulated in PGC-like cells, consistent with

the known low *SOX2* expression level in human PGCs. This finding strongly suggested that these cells represent *in vitro* counterparts of natural human PGCs.

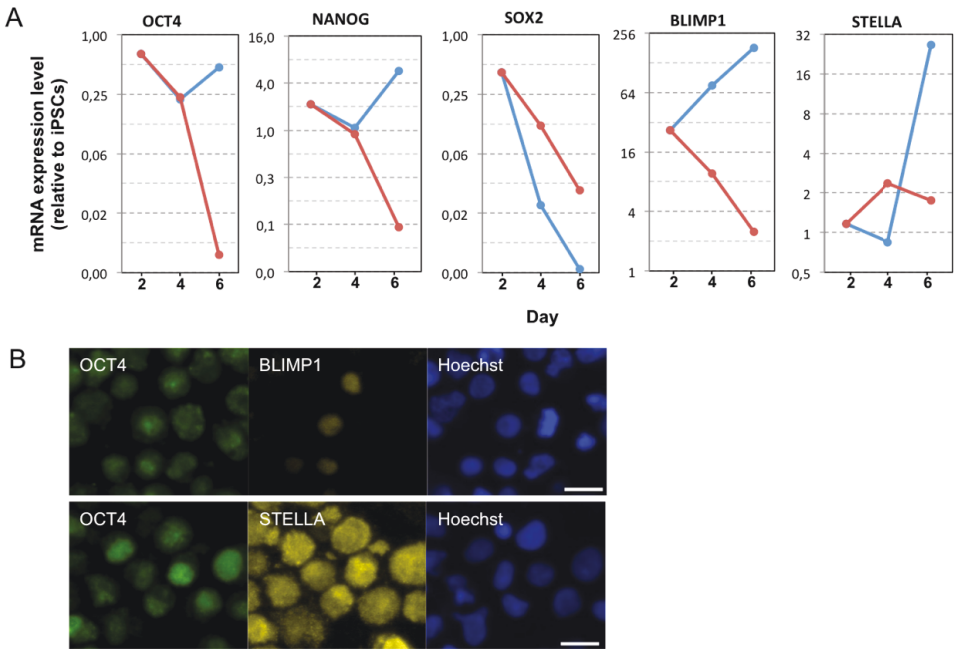

Figure 18 Characterization of PGC-like cells. (**A**) Gene expression dynamics of selected pluripotency and PGC genes in FACS-sorted, specified cells during PGC induction. The value for iPSCs is set as 1, and values are on log2 scale. (**B**) Immunofluorescence staining of TRA-1-81+/c-KIT+ PGC-like cells. Scale bar: 20 µm.

During PGC development, epigenetic reprogramming occurs globally and in a locus-specific manner (Gkountela et al, 2013; Kagiwada *et al*, 2013; Seki et al, 2007). Therefore, I next assessed the erasure of DNA methylation at regulatory regions of imprinted loci and globally in PGC-like cells. PEG1, KvDMR1, PEG10, and NESP55 were differentially methylated in both maternal and paternal alleles of iPSCs, but most became demethylated in PGC-like cells (Fig. 19A). Furthermore, examination of global DNA methylation levels by immunofluorescence against 5mC provided strong evidence that DNA methylation was globally erased in PGC-like cells (Fig. 19B). Taken together, the reduced level of methylation at imprinted loci and the loss of methyl-cytosines in the genome indicate the progress of global epigenetic reprogramming in PGC-like cells similarly to that in PGCs *in vivo*.

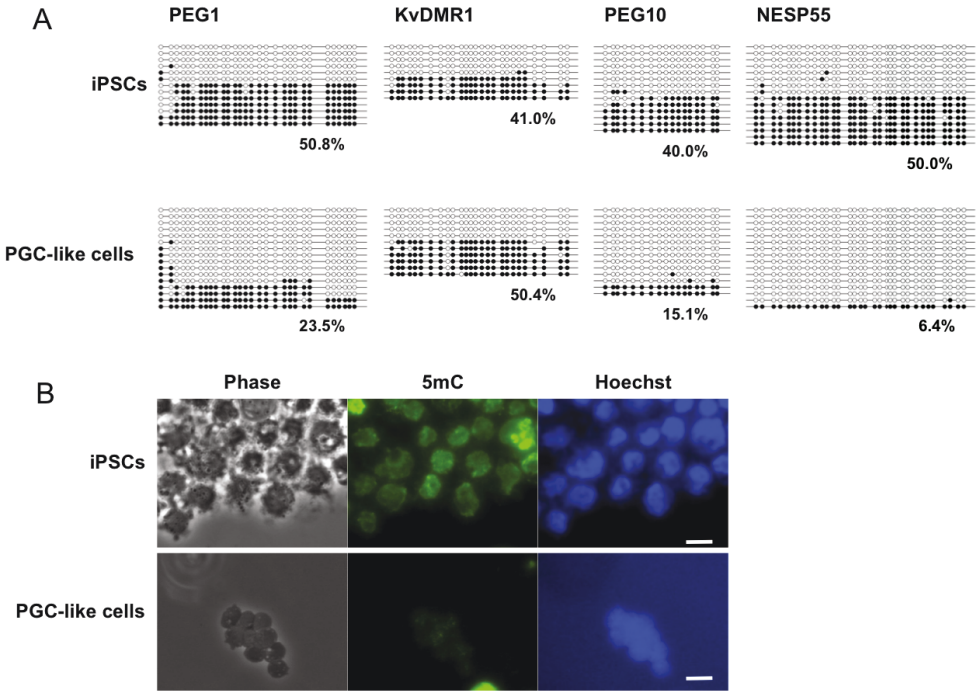

Figure 19 Epigenetic state of PGC-like cells. (**A**) Bisulfite sequence analysis of DMRs of the imprinted genes (PEG1, KvDMR1, PEG10, and NESP55) in iPSCs (top) and TRA-1-81+/c-KIT+ PGC-like cells (bottom). White and black circles represent unmethylated and methylated CpG sequences, respectively. (**B**) Immunofluorescence analysis of 5mC in iPSCs and TRA-1-81+/c-KIT+ PGC-like cells. Scale bar: 20 μm

I then evaluated the developmental potential of the PGC-like cells. PGCs are known to be bipotent, as they develop only into sperm and oocytes *in vivo*. To assess the cells' potential, I performed reconstituted ovary transplantation. PGC-like cells or iPSCs were aggregated with 12.5-dpc mouse embryonic gonadal somatic cells to form reconstituted ovaries *in vitro*, which were then transplanted under the ovarian bursa of female mice. After 3 months teratomas had formed from the reconstituted ovaries generated from iPSCs (n=2) (Fig. 20(i)). Importantly, I did not observe any teratomas from reconstituted ovaries with PGC-like cells, indicating that those cells are not pluripotent (n=10) (Fig. 20(ii)). However, I also did not observe mature PGC-like cells, which can be attributed to a likely non-permissive environmental niche.

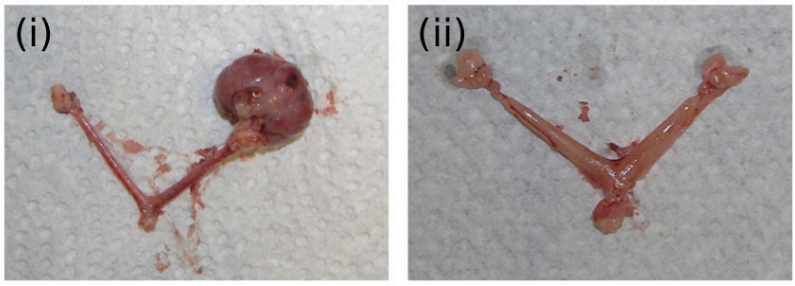

Figure 20 Teratoma formed from iPSCs and PGC-like cells 3 months after transplantation. (i) left ovary: control ovary without transplantation; right ovary: transplanted with iPSC-reconstituted ovary; (ii) ovaries transplanted with PGC-like cell-reconstituted ovaries.

3.1.8. The molecular mechanism of PGC induction *in vitro*

Knockout serum replacement (KSR) is known to enhance differentiation of cells into PGC-like cells in mice by suppressing cell death during the transition of ESCs into epiblast-like cells, which then further differentiate to generate PGCLCs (Hayashi et al, 2011). WNT3A is expressed in the mouse posterior epiblast, plays a crucial role in PGC specification (Aramaki *et al*, 2013; Ohinata et al, 2009) and enhances the differentiation of human ESCs into human PGCs in the presence of serum (Chuang *et al*, 2012). I therefore investigated whether KSR and WNT3A would also similarly affect PGC-like cell induction in our system. To assess the influence of KSR, I added KSR to the PGC precursor medium at a concentration of 0–20% and assessed the expression of *OCT4*, *NANOG, SOX2*, *T, BLIMP1*, and *STELLA* on day 2 (Fig. 21A). *OCT4* and *NANOG* expression levels were similar independent of the KSR concentration, whereas the *SOX2* expression level was strongly upregulated to iPSC level in a concentration-dependent manner. *T* expression levels were similar in KSR concentration between 0% and 4%, but decreased dramatically in 10–20%. *BLIMP1* expression gradually decreased in a concentration-dependent manner. Importantly, *STELLA* expression was not affected by the KSR concentration, indicating that KSR does not enhance the induction of the PGC-like cell state. Taken together, the study showed that KSR suppressed the differentiation of ESCs into mesodermal cells by maintaining their ESC-specific gene expression profile. To assess the PGC induction ability of the cells that had been differentiated with different KSR concentrations, I allowed them to further differentiate in PGC medium. TRA-1-81+/c-KIT+ PGC-like cells were induced under 0–2% KSR conditions, but not under 4%KSR condition (Fig. 21B). Of note, TRA-1-81+/c-KIT+ cells induced under 10 and 20% KSR conditions

lack BLIMP1 expression, which is major PGC determinant, indicating these cells are not PGC-like cells. Based on these data, it seems clear that a high concentration of KSR inhibits the induction of PGC precursors by suppressing mesodermal gene activation.

To address the effect of WNT3A, I added 100 ng/ml of WNT3A to the PGC-precursor medium together with 0–20% KSR and assessed gene expression on day 2 (Fig. 21A). WNT3A did not drastically alter the gene expression patterns, as all genes investigated exhibited relatively similar levels and changes in expression in the presence or absence of WNT3A. Nevertheless, *T* and *BLIMP1* expression seemed slightly enhanced by WNT3A. *T* expression levels were lower in the presence of WNT3A under low KSR conditions (0–4%). However, *T* expression was not sharply downregulated, and levels thus remained intermediate under high KSR conditions (10–20%). *BLIMP1* expression levels were slightly enhanced in the presence of WNT3A and, interestingly, were more slowly reduced by increasing KSR concentrations. Thus, WNT3A does not enhance differentiation toward the mesodermal cell state in our system, but exhibits an antagonistic effect on the repression of mesodermal genes by KSR. I then looked at the efficiency of PGC-like cell induction from each culture. Similarly to the cultures lacking WNT3A, PGC-like cells could be induced from cells grown under low KSR conditions, but not from the cells grown under high KSR conditions (Fig. 21B). These data indicate that WNT3A does not significantly enhance the induction of PGC precursors. I therefore concluded that KSR and WNT3A do not enhance the induction of PGC precursors or PGC-like cells in our system. KSR actually had an inhibitory effect.

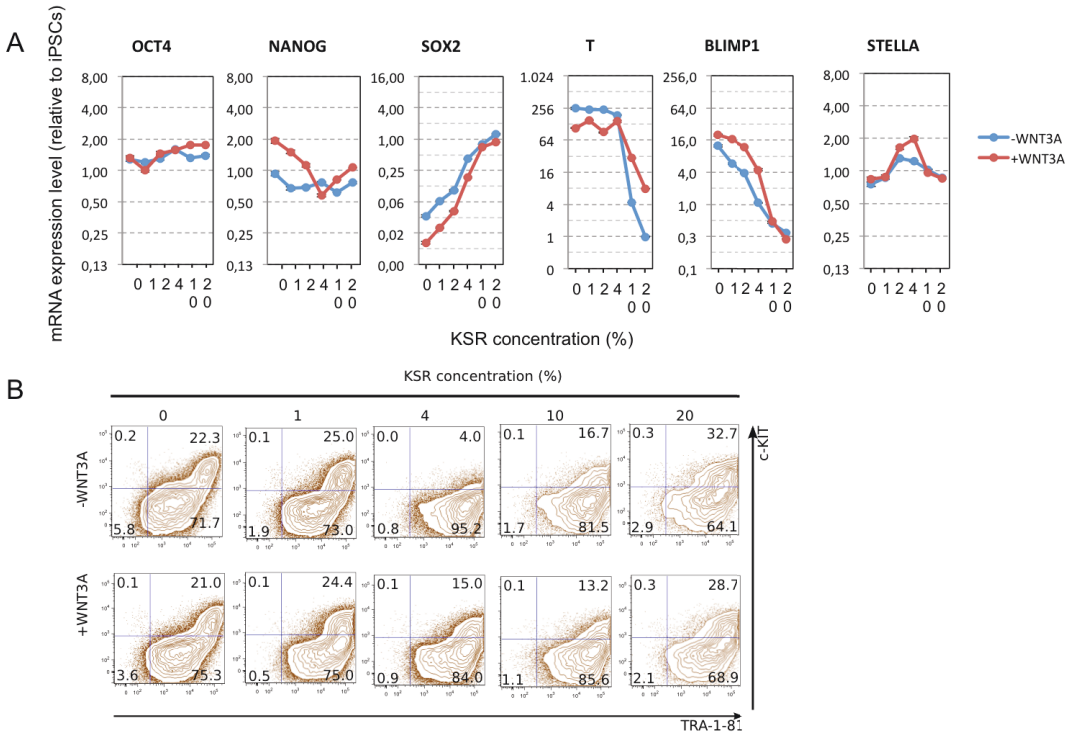

Figure 21 Effects of KSR and WNT3A during PGC-precursor induction. (**A**) Gene expression analysis of selected pluripotency, PGC, and mesodermal genes of d2 cultures. The value for iPSCs is set as 1, and values are on log2 scale. (**B**) The induction of PGC- like cells as analyzed by FACS gated for TRA-1-81 and c-KIT.

Nevertheless, PGC-like cells were still induced in medium containing 4% KSR with WNT3A, which was not seen in medium containing 4% KSR without WNT3A (Fig. 21B). This finding indicated that the two culture conditions possess distinct abilities to induce PGC-like cells. Of all the genes investigated, including ecto-/meso-/endoderm markers, the expression of only *BLIMP1* was significantly different in those cultures (Fig. 21A and 22). Specifically, *BLIMP1* mRNA levels increased in medium containing 0%, 1%, and 2% KSR in the absence or presence of WNT3A, but increased in medium containing 4% KSR only in the presence of WNT3A. We therefore hypothesized that the expression of *BLIMP1* during PGC-precursor induction might be crucial for further PGC induction, similarly to the role of *Blimp1* in mouse PGC specification.

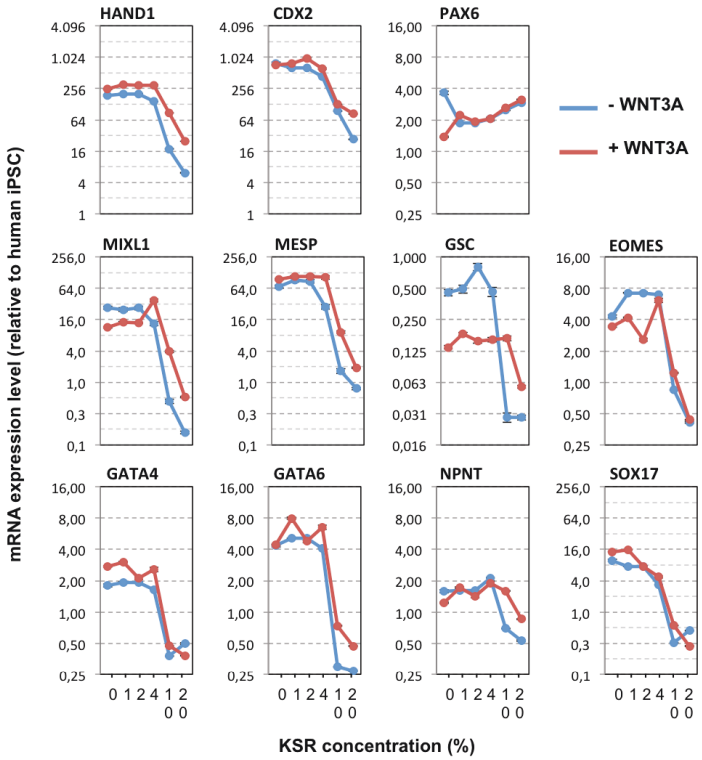

Figure 22 Effects of KSR and WNT3A during PGC-precursor induction on the expression of selected trophecto-, ecto-, endo-, and mesodermal genes of d2 cultures.

To evaluate our hypothesis, I performed immunofluorescence analysis for BLIMP1, together with OCT4 and T (Fig. 23A). In accordance with the qPCR results, I observed that the majority of cells were OCT4+ under all culture conditions, whereas T+ cells were strongly induced only under low KSR conditions. BLIMP1+ cells were significantly induced under both low and high KSR conditions. However, the BLIMP1+ cells under high KSR conditions did not co-express OCT4 and apparently committed to other cell lineages. Statistical cell counts demonstrated that the percentage of OCT4+ cells was the same under all conditions, while that of BLIMP1+ cells modestly decreased in a KSR concentration–dependent manner. Importantly, the number of OCT4+/BLIMP1+ cells within the total BLIMP1+ cell population decreased significantly in a KSR concentration–dependent manner, reaching zero under high KSR conditions (Fig. 23B). These data clearly demonstrate that OCT4+/T+/BLIMP1+ cells indeed represent PGC precursors that subsequently commit to become PGCs, paralleling previously published data on mouse PGC specification (Saitou et al, 2002).

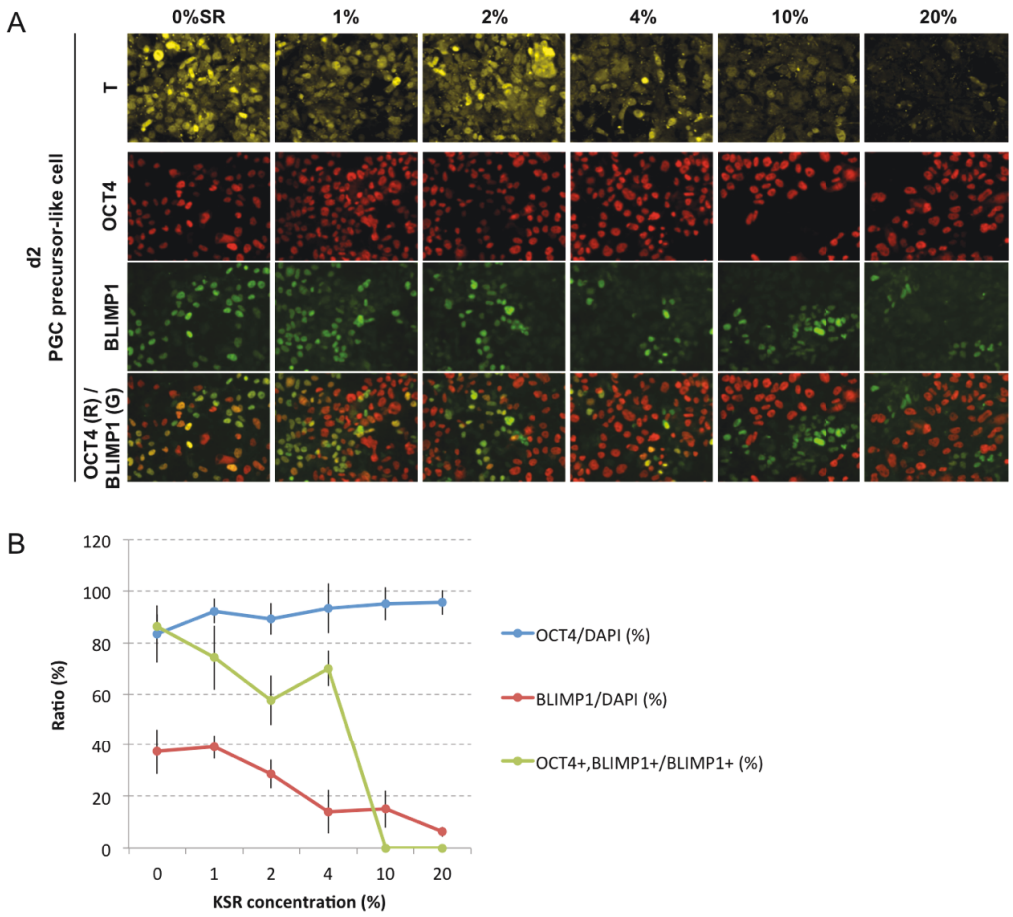

Figure 23 Effects of KSR and WNT3A on PGC-precursor and PGC-like cell induction. (**A**) Immunofluorescence analysis of OCT4, BLIMP1, and T on day 2 and STELLA- GFP on day 8. (**B**) Statistical cell counting of d2 cultures. Pictures were captured at different locations on the cell culture plates and analyzed.

3.1.9. Global gene expression analysis of PGC precursors and PGC-like cells

To further characterize day-2 (d2) PGC-precursor cultures and day-4 (d4) and day-6 (d6) PGC-like cells, I assessed their global transcription profiles (Fig. 24A). Unsupervised hierarchical clustering (UHC) revealed that d2 PGC-precursor cultures clustered together with iPSCs, whereas d4 and d6 PGC-like cells clustered together, but separately from d2 precursors and iPSCs (Fig. 24B). Principal component analysis (PCA) also showed a distinct difference between iPSCs or d2 PGC-precursor cells and d4 or d6 PGC-like cells (Fig. 24C). These data indicate that PGC-like cells acquired a distinct global transcription profile and therefore a different cell identity compared with iPSCs. Scatter plot analysis comparing either d2 PGC-precursor culture, or d4 or d6 PGC-like cells with iPSCs revealed that *OCT4* and *NANOG*

expression levels were similar to those of iPSCs in all differentiated samples and that *SOX2* levels were strongly downregulated in PGC-like cells. These results were validated by qPCR analysis (Fig. 18A). Expression levels of mesodermal genes (such as *CYP26A1*, *GSC*, *MESP*, and *MIXL1*) were upregulated in d2 PGC precursors and thereafter progressively downregulated in d4 and d6 PGC-like cells. Expression levels of PGC genes (such as *STELLA*, *NANOS3*, and *TFAP2C*) did not change in d2 PGC precursors and d4 PGC-like cells, but significantly increased in d6 PGC-like cells, indicating the formation of lineage-restricted PGCs on day 6. The subsequent expression of mesodermal genes and PGC genes in our differentiation system is overall similar to the transcription dynamics observed during mouse PGC specification, with the exception of *SOX2* expression, which is drastically different.

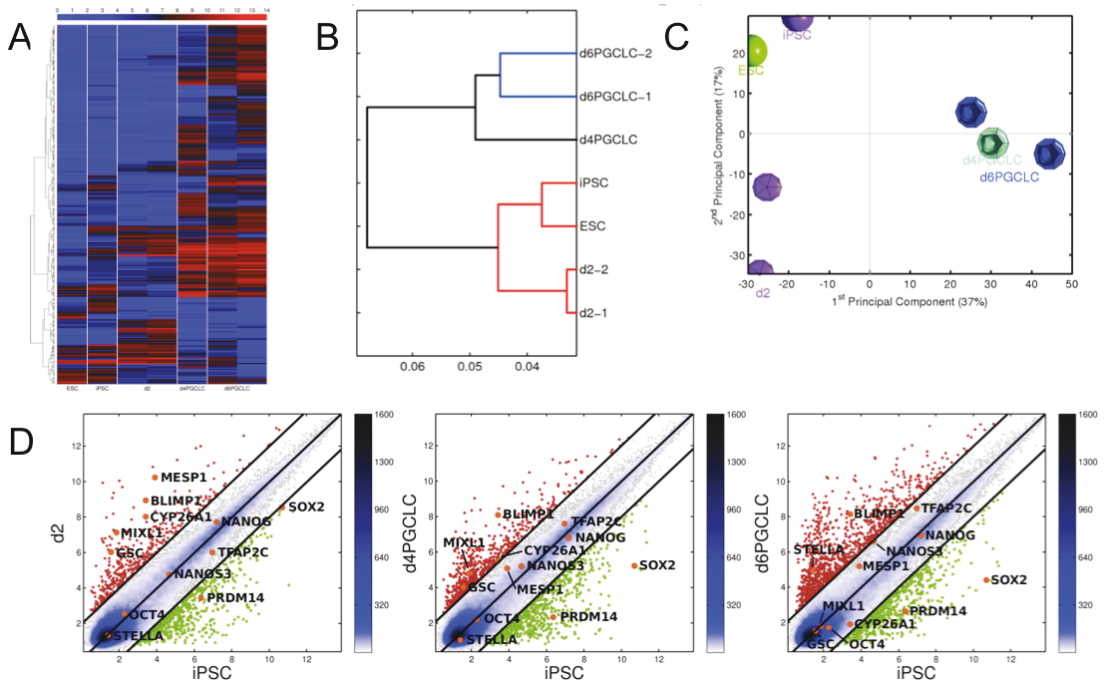

Figure 24 Global transcription profiles during PGC-precursor and PGC-like cell induction. (**A**) Heat map of global gene expression patterns of HuES6 ESCs, 383.2iPSCs, d2 PGC-precursor cultures, and FACS-sorted PGC-like cells. The color bar at top codifies the gene expression in log2 scale. Red and blue colors indicate high and low gene expression, respectively. (**B**) Unsupervised hierarchical clustering (UHC) of HuES6 ESCs, 383.2iPSCs, d2 PGC-precursor cultures, and FACS-sorted PGC-like cells. (**C**) Principal component analysis of HuES6 ESCs, 393.2 iPSCs, d2 PGC-precursor cultures, and FACS-sorted PGC-like cells. (**D**) Scatter plots of global gene expression microarrays comparing d2 PGC-precursor cultures, or d4 or d6 FACS-sorted PGC-like cells with iPSCs.

In addition to the expression of representative key markers, I analyzed the extent of shared gene dynamics between human PGC-like cell induction and mouse PGC specification. A recent mouse study identified two categories of genes that are activated during PGC specification. One category is the "somatic mesodermal genes," which are activated by BMP4 and eventually suppressed upon formation of lineage-restricted PGCs, and the other is the "core PGC genes," which are specifically activated by Blimp1, Prdm14, and Tfap2c (Nakaki et al, 2013). I therefore examined the expression profiles of the genes from each category to assess whether similar transcriptional changes occur during human PGC-like cell induction (Figure 25). Of the 159 somatic mesodermal genes examined, 30 were upregulated (>2 fold) in d2 precursor cells, including *CDX1*, *CDX2*, *HAND1*, *MESP1*, *ID1*, *MSX1*, *MSX2*, *ISL1*, *MIXL1*, *WNT5A*, *FGF8*, and *BMP4*. The number of genes that were upregulated increased to 50 on day 4 and 65 on day 6.

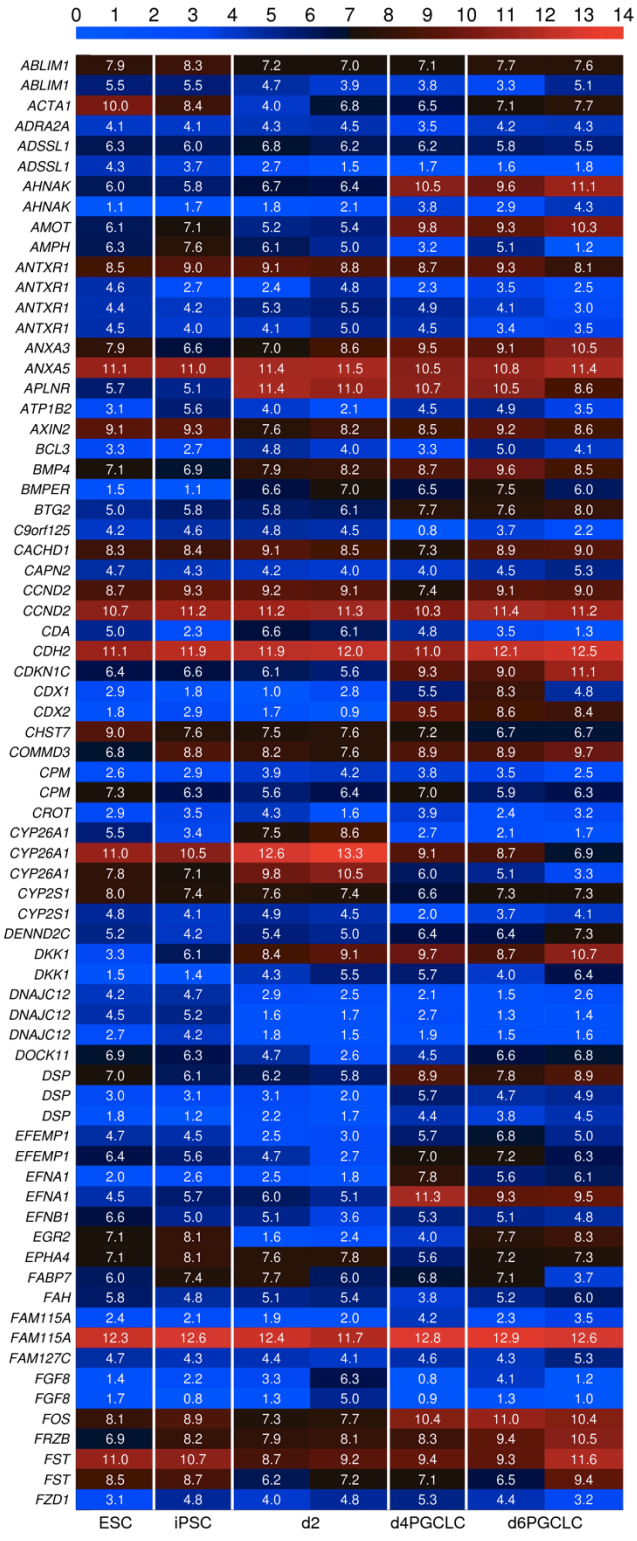

Figure 25 (Continued)

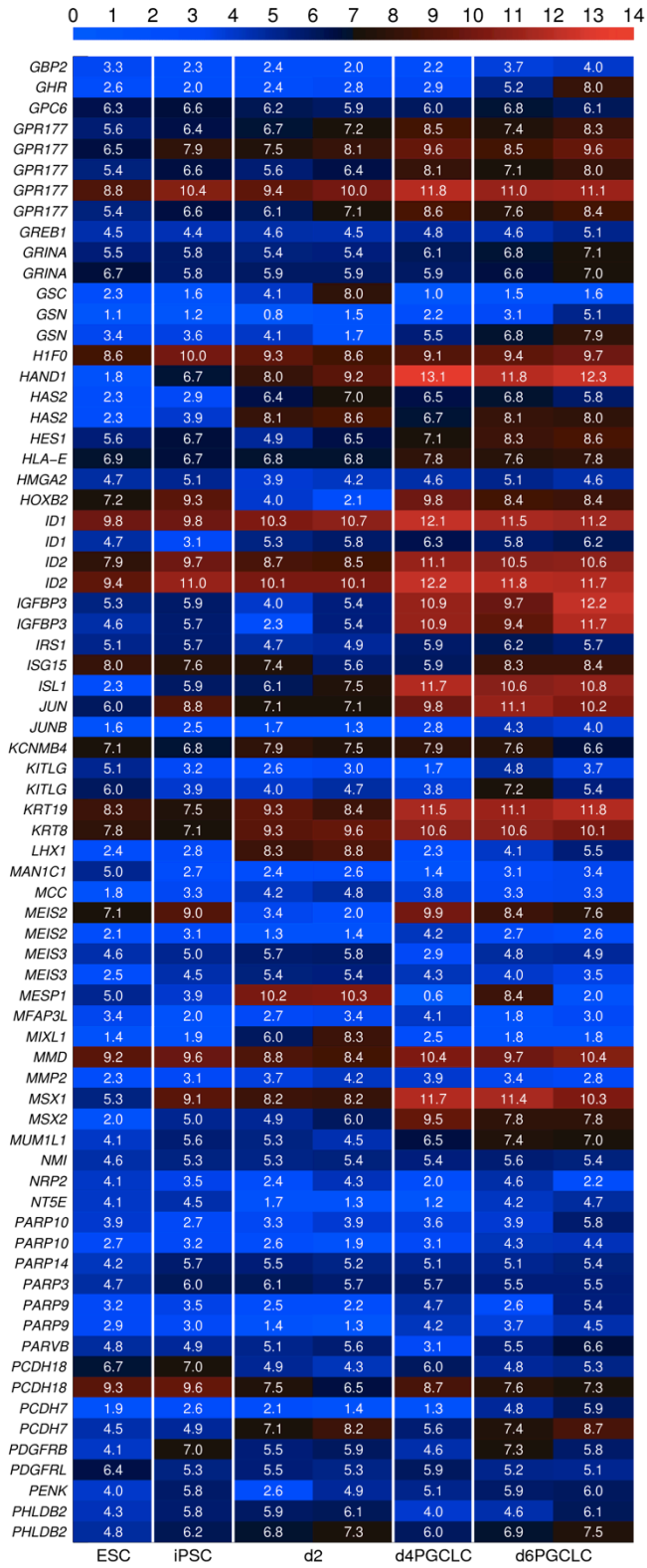

Figure 25 (continued)

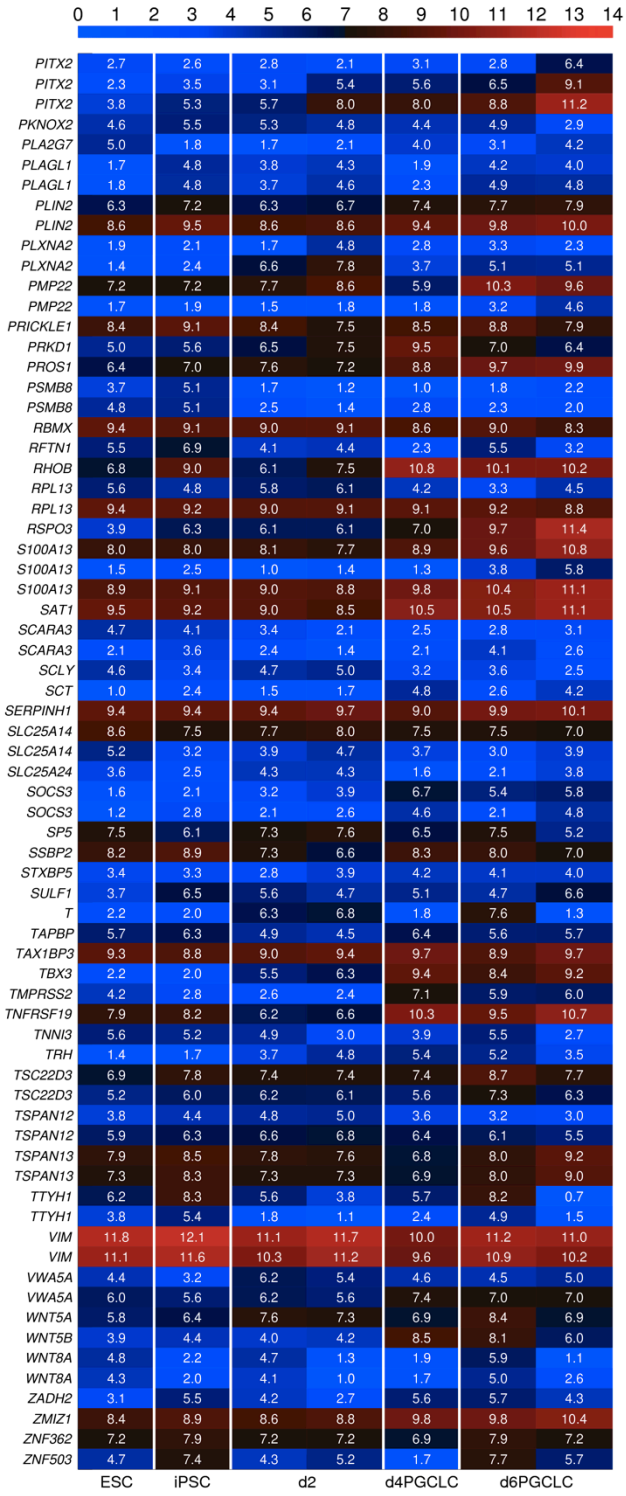

Figure 25 Heat map of somatic mesodermal gene expression patterns of HuES6 ESCs, 383.2iPSCs, d2 PGC-precursor cultures, and FACS-sorted PGC-like cells. The color bar at top codifies the gene expression in log2 scale. Red and blue colors indicate high and low gene expression, respectively.

Of the core PGC genes, I found that 22 of 45 genes were upregulated (>2fold) in d6 PGC-like cells, including *TFAP2C*, *STELLA*, *KLF2*, *ELF3*, *KIT*, and *LIFR* (Figure 26). Thus, the expression of somatic mesodermal genes and core PGC genes during human PGC-like cell induction was similar to that during mouse PGC specification. Taken together, these data reveal that human and mouse PGC-like cell induction share expression patterns of not only a few key markers, but also larger sets of genes within different functional categories.

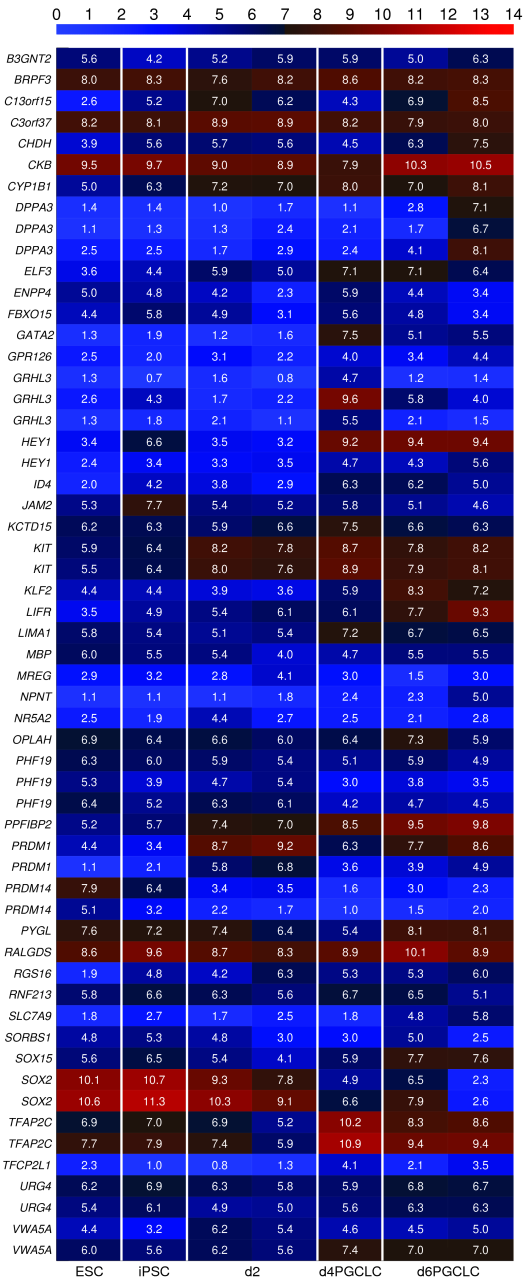

Figure 26 Heat map of core PGC mesodermal gene expression patterns of HuES6 ESCs, 383.2iPSCs, d2 PGC-precursor cultures, and FACS-sorted PGC-like cells. The color bar at top codifies the gene expression in log2 scale. Red and blue colors indicate high and low gene expression, respectively.

Interestingly, I identified some epigenetic modifiers, such as the TET family genes, with similar expression levels in PGC-like cells as in ESCs, but downregulated *DNMT1* and *DNMT3B* levels (Fig. 27). This indicated that the reduction of 5mC levels might involve passive mechanisms by replication-coupled dilution, similarly to mouse PGCs, thus confirming the notion that key epigenetic features are indeed shared between human PGC-like cell induction and mouse PGC specification.

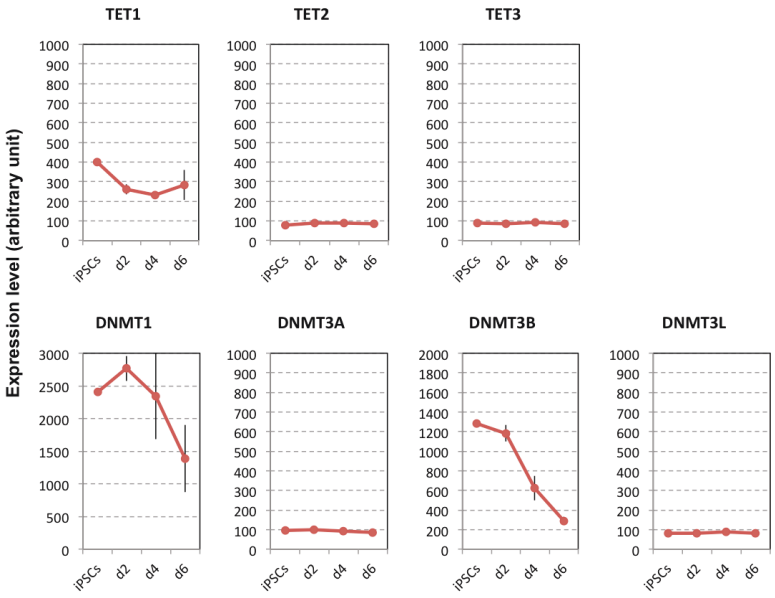

Figure 27 Array expression data for selected epigenetic modifier genes in 383.2 iPSCs, d2 PGC-precursor cultures, and FACS-sorted PGC-like cells.

Surprisingly, I observed that *PRDM14* expression was strongly downregulated in PGC-like cells (Fig. 24D). In mice, Prdm14 is known to function as a key regulator of PGC specification and the lack of Prdm14 leads to loss of PGCs (Yamaji *et al*, 2008). I therefore assessed whether the lack of PRDM14 in our PGC-like cells influences the expression of particular genes activated during mouse PGC specification.

A recent mouse study reported sets of genes that are regulated through the action of Prdm14 (genes upregulated are *Epas1*, *Tcl1*, *Esrrb*, *Klk5*, *Nr5a2*, *ZFfp42*, *Klf4*, *Lifr*, *Dppa2*, *Dppa5a*, and *Nanog*; genes downregulated are Zfp521 [human homolog: *ZNF521]*, *Sox3*, *Nrcam*, and *Hs6st2*) (Nakaki et al, 2013). I first looked at the expression profile of these genes in human PGC-like cells (Figure 28). *EPAS1*, *KLF5*,

KLF4, and *LIFR* expression levels were upregulated (>2 fold) in PGC-like cells, whereas *ZFP42* and *NANOG* levels did not change and were as high as iPSC levels. On the other hand, *TCL1A*, *ESRRB*, *NR5A2*, *DPPA2*, and *DPPA5* levels were low. *ZNF521*, *SOX3*, and *NRCAM* expression levels were downregulated (>2 fold), while the *HS6ST2* level was upregulated in human PGC-like cells. These data clearly demonstrate that a subset of mouse *Prdm14*-regulated genes exhibits a similar expression pattern in human PGC-like cells, even though *PRDM14* is expressed at only very low levels.

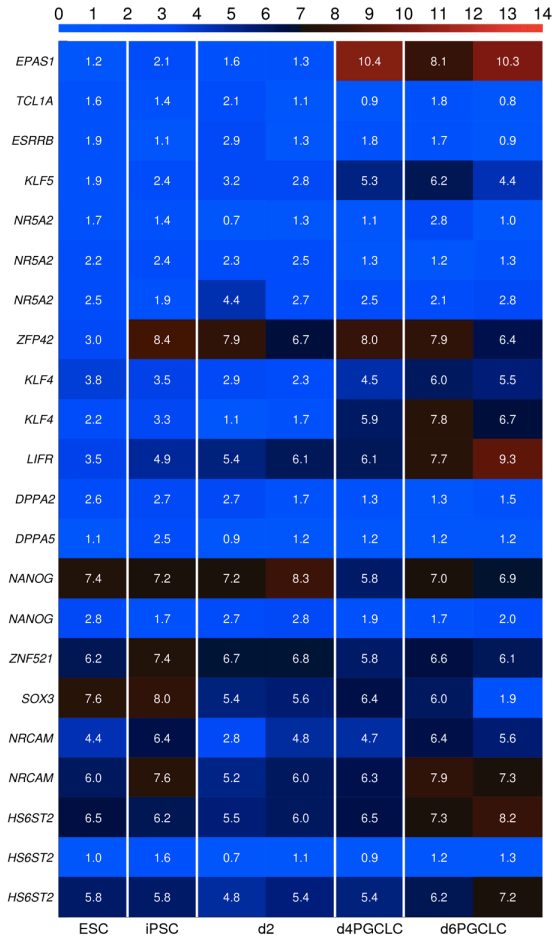

Figure 28 Heat map of mouse Prdm14-regulated genes in HuES6 ESCs, 383.2 iPSCs, d2 PGC-precursor cultures, and d4 and d6 FACS- sorted PGC-like cells. The color bar at top codifies the gene expression in log2 scale. Red and blue colors indicate high and low gene expression, respectively.

In addition, gene set enrichment analysis (GSEA) revealed that genes associated with neural development were significantly downregulated in PGC-like cells (Table 4). The repression of neural differentiation genes is a key characteristic of mouse PGC specification that is mediated by Prdm14. This finding confirms that human PGC-like cell induction exhibits similar transcriptional dynamics to mouse PGC specification, and suggests that mouse Prdm14-regulated genes are actually regulated by other mechanisms in human PGCs.

Table 4 List of significant enriched gene sets between iPSCs and d6 FACS-sorted PGC-like cells from GSEA.

Downregulated gene sets in d6 PGC-like cells

Gene set	P value
Central nervous system development	1,11E-04
Nervous system development	1,45E-04
Multicellular organismal development	2,76E-04
Neurological system process	1,70E-03
Transforming growth factor beta receptor signaling pathway	2,30E-03
Enzyme linked receptor protein signaling pathway	3,14E-03
Anatomical structure development	4,22E-03
Transcription factor activity	6,53E-03
Synaptic transmission	1,85E-02
Sensory reception	2,29E-02
Anatomical structure morphogenesis	3,98E-02

Upregulated gene sets in d6 PGC-like cells

Gene set	P value
Extracellular region	1,15E-08
Extracellular region part	3,34E-08
Extracellular region space	4,55E-08
Lipid transport	1,40E-05
Digestion	1,77E-05
Hormone metabolic process	1,97E-04
Lipid metabolic process	2,24E-04
Steroid metabolic process	2,26E-04
Enzyme activator activity	4,43E-04
Lipid homeostasis	4,86E-04
Steroid binding	6,29E-04

Table 4 (continued)

Negative regulation of secretion	8,56E-04
Chemical homeostasis	1,12E-03
Cell surface receptor linked signal transduction GO 0007166	2,02E-03
Lipid transporter activity	2,06E-03
Cofactor transport	3,02E-03
Receptor activity	3,11E-03
Female pregnancy	3,25E-03
Collagen binding	4,06E-03
Transition metal ion transmembrane transporter activity	4,32E-03
Phospholipase activity	4,26E-03
G protein coupled receptor protein signaling pathway	4,32E-03
Lyase activity	4,88E-03
Metal ion transport	5,29E-03
CDC42 protein signal transduction	5,35E-03
Transmembrane receptor activity	6,41E-03
Reproductive process	6,64E-03
Hormone binding	6,76E-03
Cellular lipid metabolic process	7,00E-03
Ras protein signal transduction	7,82E-03
Myosin complex	8,35E-03
Lipid binding	9,64E-03
Myoblast differentiation	1,01E-02

With the unavailability of human *in vivo* pre-migratory PGC samples and global transcription data of those cells, we compared data from our PGC-like cells and iPSCs with published data sets from Gkountela *et al* and Nakaki *et al* (Gkountela et al, 2013; Nakaki et al, 2013). We performed comparative gene expression analysis and identified 6 and 10 genes that were commonly down- or upregulated, respectively, in PGC-like cells, *in vivo* post-migratory PGCs, and mouse *in vitro*–generated PGCs compared with the corresponding human ESC lines and mouse EpiLCs (Fig. 29-33). Of these, *DNMT3B* was downregulated, indicating suppression of *de novo* DNA methylation, which is a common event at the early stage of PGC development in humans and mice. *BLIMP1*, *STELLA*, and *KLF2* expression was upregulated; however, *SOX2* and *PRDM14* expression was downregulated in human PGCs and PGC-like cells, but not in mouse *in vitro*–generated PGCs. Of note, human PGC-like

cells exhibited similar *LIFR* expression levels as mouse PGCs, indicating that our cells shifted from a FGF-dependent state to an LIF-dependent state to activate pluripotency genes. These observations suggested that the lack of PRDM14 is a characteristic unique to human PGCs, and that human PGCs lack the expression of PRDM14 from their early commitment to the germ lineage until at least the post-migratory stage.

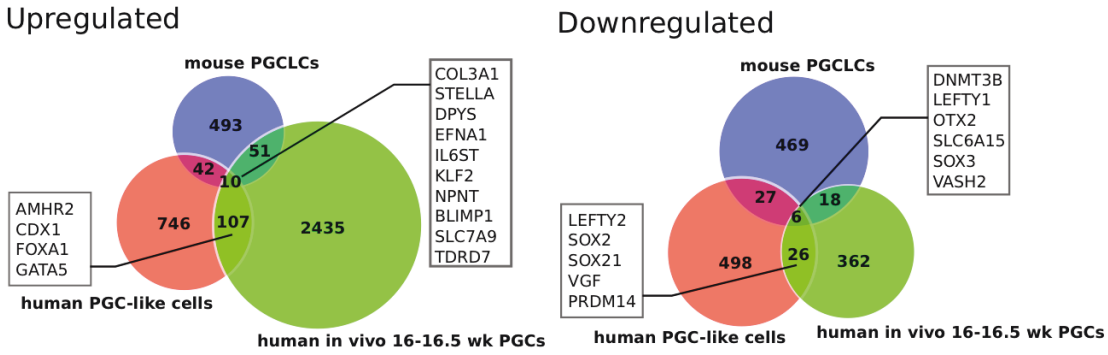

Figure 29 Venn diagrams of intersection between mouse *in vitro* PGCLCs, human *in vivo* PGCs, and human *in vitro* PGC-like cells.

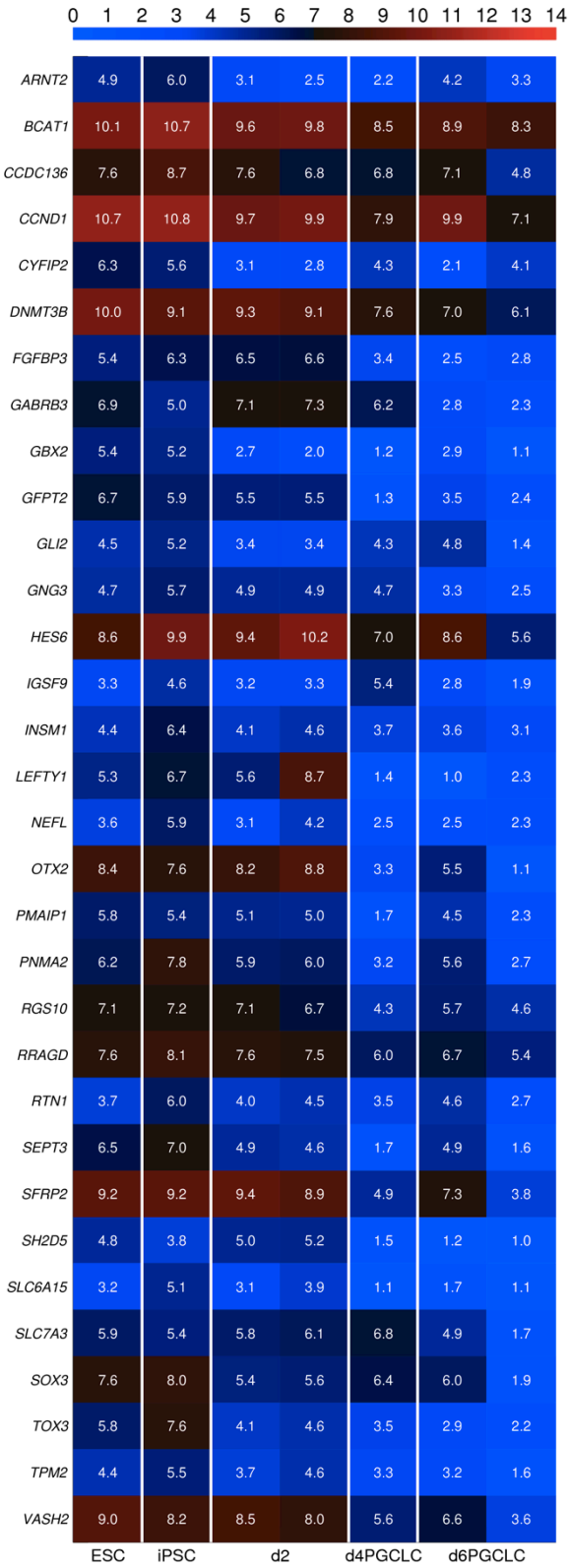

Figure 30 Heat map of genes commonly downregulated in human PGC-like cells and mouse PGC-like cells. The color bar at top codifies the gene expression in log2 scale. Red and blue colors indicate high and low gene expression, respectively.

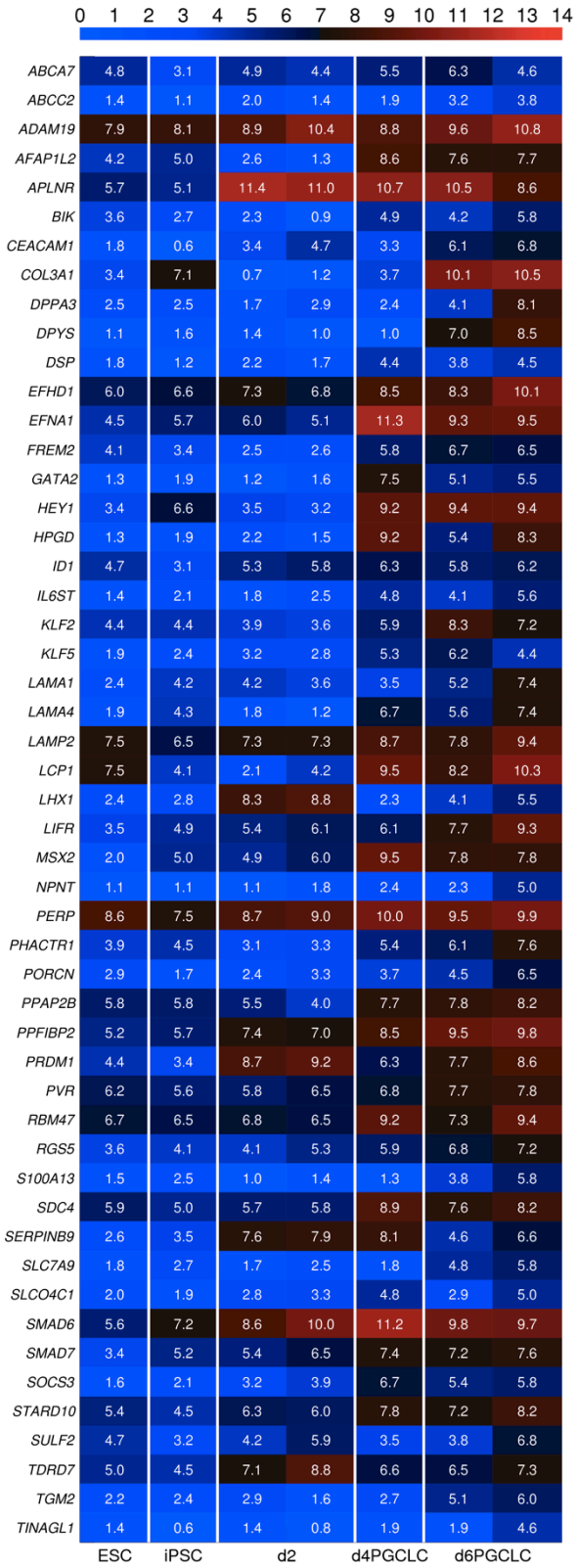

Figure 31 Heat map of genes commonly upregulated in human PGC-like cell and mouse PGC-like. The color bar at top codifies the gene expression in log2 scale. Red and blue colors indicate high and low gene expression, respectively.

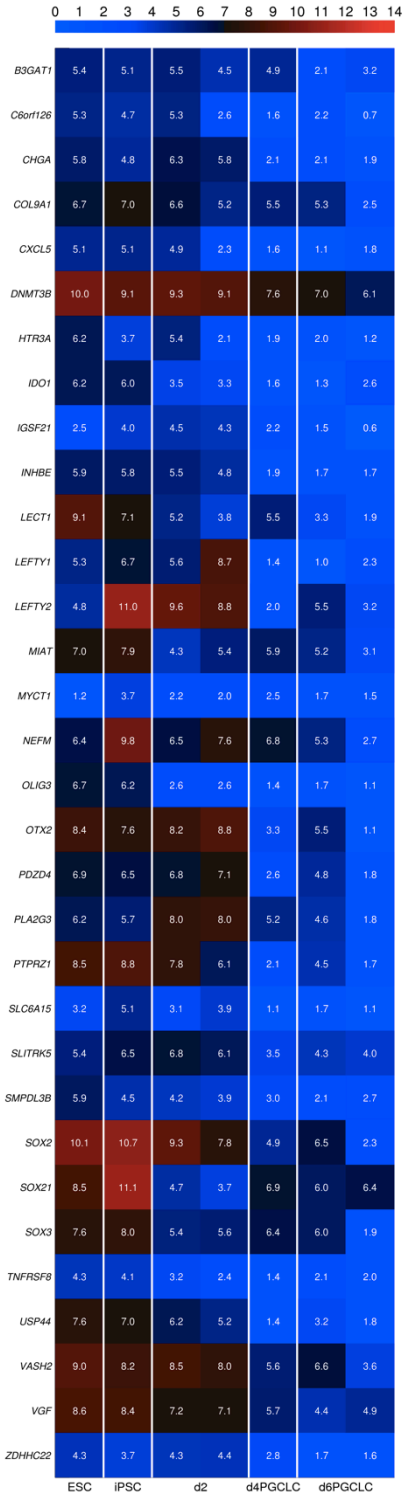

Figure 32 Heat map of genes commonly downregulated in human PGC-like cells and 16-16.5 week PGCs. The color bar at top codifies the gene expression in log2 scale. Red and blue colors indicate high and low gene expression, respectively.

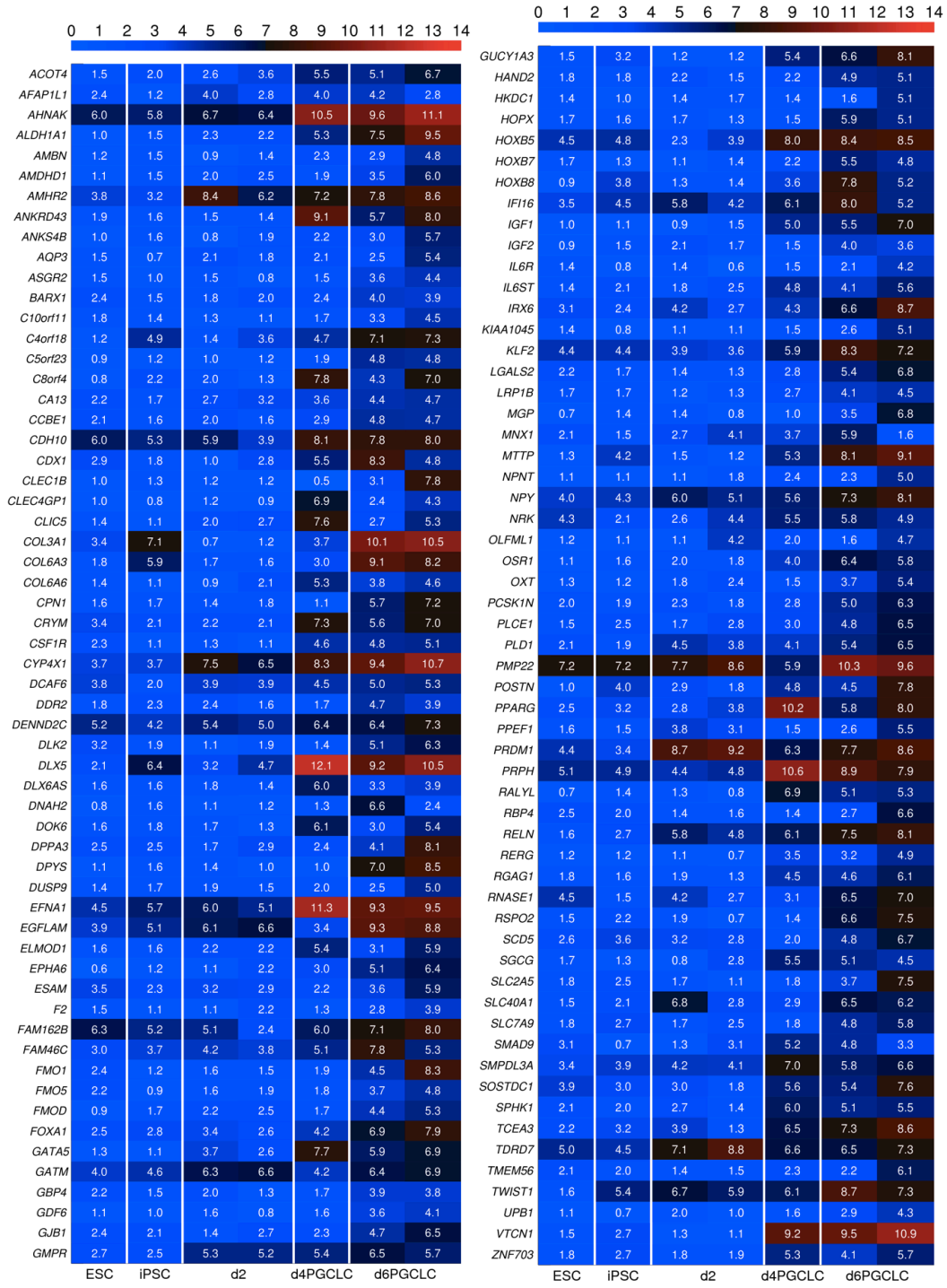

Figure 33 Heat map of genes commonly upregulated in human PGC-like cells and 16-16.5 week PGCs. The color bar at top codifies the gene expression in log2 scale. Red and blue colors indicate high and low gene expression, respectively.

Our data indicated that the expression of BLIMP1 is associated with PGC commitment from human iPSCs, whereas PRDM14 is not. To determine this thought, I transduced iPSCs with lentiviral vectors producing small hairpin RNA (shRNA) against BLIMP1 and PRDM14. The expression level of BLIMP1 or PRDM14 was impaired in BLIMP1- or PRDM14-shRNA-transduced cells, respectively (Fig. 34A). As shown in Figure 34B, the knock-down of BLIMP1 lead to impaired induction of TRA-1-81+/c-KIT+ PGC-like cells on day 4 (ca. 50%). In contrast, the knock-down of PRDM14 did not affect the induction efficiency (ca. 100%). This data clearly indicated that BLIMP1 plays an important role in human PGC commitment, whereas PRDM14 has less or no impact on it.

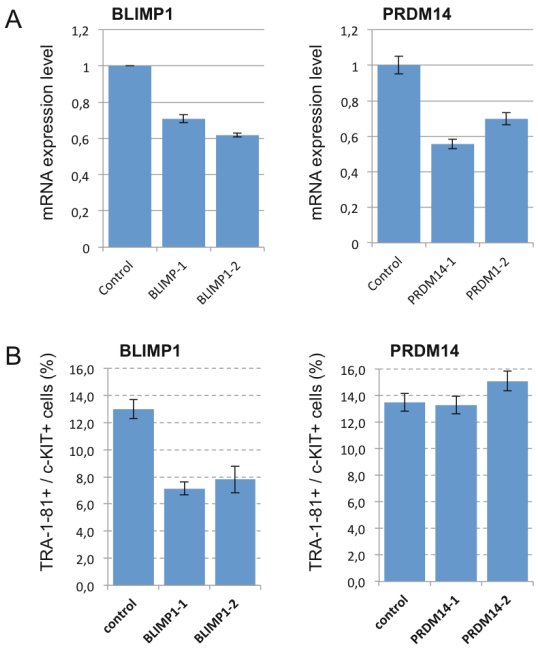

Figure 34 Knock-down of BLIMP1 and PRDM14 (**A**) Knock-down efficiency of shRNAs in human ESCs after 2 days of infection. (**B**) The induction efficiency of TRA-1-81+/c-KIT+ PGC-like cells on day4.

3.2. PGC differentiation from mouse EpiSCs and Δ PE-Oct4-GFP+ EpiSCs

3.2.1. PGC differentiation from mouse EpiSCs

I could demonstrate that our *in vitro* system successfully generated PGC- and oocyte-like cells from mouse ESCs by molecular and ultrastructure analyses (section 4.2). I hypothesized that this differentiation system would also be able to induce PGCs from mouse epiblast stem cells (EpiSCs). EpiSCs are pluripotent stem cells derived from post-implantation embryo (Brons *et al*, 2007; Tesar *et al*, 2007). Although EpiSCs share some common properties with ESCs, such as expression of key pluripotency-associated genes including *Oct4*, *Nanog* and *Sox2*, they are significantly different in their epigenetic state and gene transcription profile (Brons et al, 2007; Guo *et al*, 2009; Hayashi *et al*, 2008; Tesar et al, 2007). In particular, EpiSCs are derived from epiblast cells from which PGCs originate *in vivo*. Therefore, the differentiation of PGCs from EpiSCs could provide a better platform for an investigation on PGC specification. Furthermore, EpiSCs share some properties with human ESCs, such as flattened colony morphology and the culture conditions for maintainance, giving rise to the idea that establishment of a PGC induction protocol from mouse EpiSCs could be instrumental toward the establishment of differentiation systems with human pluripotent stem cells.

Mouse GOF18-EpiSCs that contain a GFP transgene under the control of the entire regulatory region of the Oct4 gene (Yeom *et al*, 1996) were differentiated with a modified protocol to PGCs (Fig. 35A). As shown in Figure 35B, strong GFP signal was observed in differentiated EBs after 7 days of differentiation. FACS analysis revealed that 73.9% of the cells are Oct4-GFP+ and, furthermore, 36.8% of cells exhibit both Oct4-GFP and c-KIT expression, characteristic of *in vivo* PGCs (Fig. 35C). This result indicated that this differentiation protocol efficiently induces OCT4-GFP+/c-KIT+ putative PGCs from mouse EpiSCs. I then analyzed the gene expression level of key genes, *Oct4*, *Sox2*, *Nanog*, *Blimp1*, *Prdm14*, *Stella*, *Dazl* and *Vasa* in Oct4-GFP+/c-KIT+ PGC-like population. As shown in Figure 35D, pluripotency-associated genes, *Oct4*, *Nanog* and *Sox2*, as well as early PGC gene, *Blimp1*, were expressed in the PGC-like population at a similar level to EpiSCs. In contrast, the early PGC genes *Prdm14* and *Stella* were highly upregulated in the PGC-like population (16-fold and 156-fold, respectively). Furthermore, the late PGC genes

Dazl and *Vasa* were also highly upregulated (128-fold and 512-fold, respectively), indicating their progress to the post-migratory stage. In fact, SYCP3 staining by immunofluorescence analysis exhibited a premeiotic staining pattern, indicating that cells prepared to enter meiosis (Fig. 35D). These results suggested that this differentiation protocol induces presumptive PGCs and that the employed protocol apparently worked for EpiSCs.

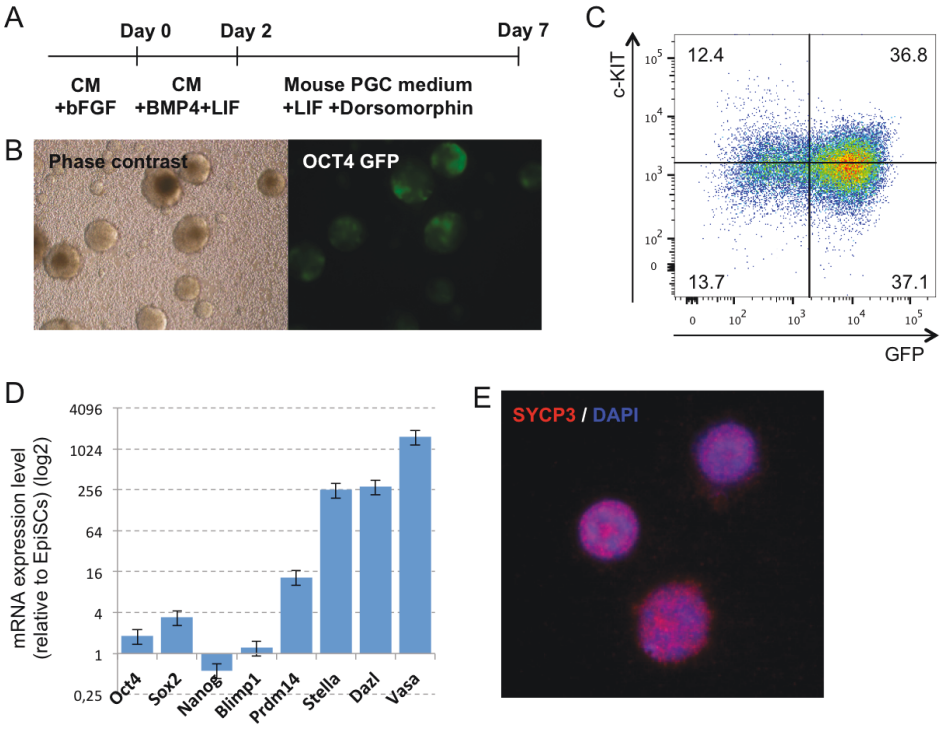

Figure 35 Differentiation of mouse EpiSCs toward PGCs. (**A**) Scheme of PGC differentiation. (**B**) Oct4-GFP expression on day 7 of differentiation. Phase contrast and GFP fluorescence images are shown. (**C**) FACS analysis of the differentiated cells on day 7. (**D**) Gene expression analysis of Oct4-GFP+/c-KIT+ cells. The value for EpiSCs is set as 1, and values are on log2 scale. (**E**) Immunofluorescent analysis of SYCP3 in Oct4-GFP+/c-KIT+ cells.

However, although I obtained this result from my first attempt, I failed to reproduce it later (n=3). Upon differentiation, I regularly obtained similar ratios of Oct4-GFP- and Oct4-GFP+ cells, but I did not observe c-KIT expression anymore (ca. 0.4%) (Fig. 36). This might be attributed to undefined changes of components in MEF-conditioned medium (MEF-CM), which were used for both maintenance and differentiation of EpiSCs. MEF-CM has batch differences depending on the MEF

preparation (see discussion for details). If culturing EpiSCs in defined culture condition resolves this problem has to be elucidated by further investigations.

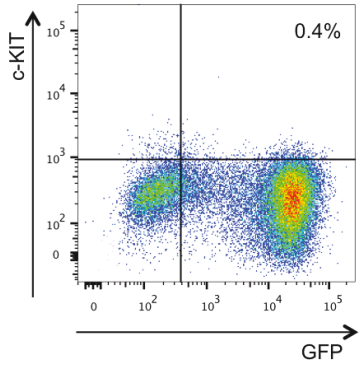

Figure 36 FACS analysis of the day7 differentiated EpiSCs by GFP and c-KIT

3.2.2. PGC differentiation from mouse Δ PE-Oct4-GFP+ EpiSCs

The competence of the epiblast for the germ cell fate is restricted between E5.5 and E6.25, as PGC-like cell are induced only from E5.5-6.25 epiblast, but not from the epiblast later than E6.5 (Ohinata et al, 2009). Interestingly, one of our recent studies demonstrated that EpiSCs have two distinct populations distinguished by Δ PE-Oct4-GFP expression (Han *et al*, 2010). Oct4 contains a proximal (PE) and a distal (DE) enhancer element, which are preferentially used in EpiSCs or ESCs and PGCs, respectively. The study by Han et al. demonstrated that the Δ PE-Oct4-GFP negative population in EpiSCs represents cells of the E6.5 postgastrulation embryo, while the Δ PE-Oct4-GFP positive population represents cells of the E5.5 pregastrulation embryo. Based on this, I hypothesized that the Oct4-GFP+ cells in EpiSCs posess a higher competence for the germ cell fate.

Mouse Δ PE-Oct4-GFP+ EpiSCs (named stabilized EpiSCs, Fig 37A) were differentiated using the modified differentiation protocol to PGCs. As shown in Figure 37B, strong GFP signal was observed in differentiated EBs on day 7 of the differentiation. However, FACS analysis revealed that only a small population of these GFP+ cells expressed c-KIT (1.2%, Fig. 7C), indicating that our differentiation protocol insufficiently induces putative PGCs from stabilized EpiSCs. Interestingly, I

observed the induction of Oct4-GFP+/SSEA-1+ cells (37.1%), which is another marker for PGCs *in vivo* (Fig. 7D). Gene expression analysis was performed for *Oct4*, *Sox2*, *Nanog*, *Prdm14*, *Stella*, *Dazl* and *Vasa* and to our surprise observed that many PGC genes, such as *Bimp1*, *Prdm14*, *Stella*, *Dazl* and *Vasa* were significantly upregulated, independent from SSEA-1 expression, while *Oct4*, *Nanog* and *Sox2* retained similar expression levels to those in EpiSCs (Fig. 7E). Since c-KIT is one of the definitive markers for PGCs, these cells cannot be considered PGCs per se. The detailed character of these Oct4-GFP+/SSEA-1+ cells and how PGC genes are upregulated in these cells at present is unclear. Based on the results, we concluded that our mouse PGC system needs to be optimized to induce PGC-like cells from stabilized EpiSCs.

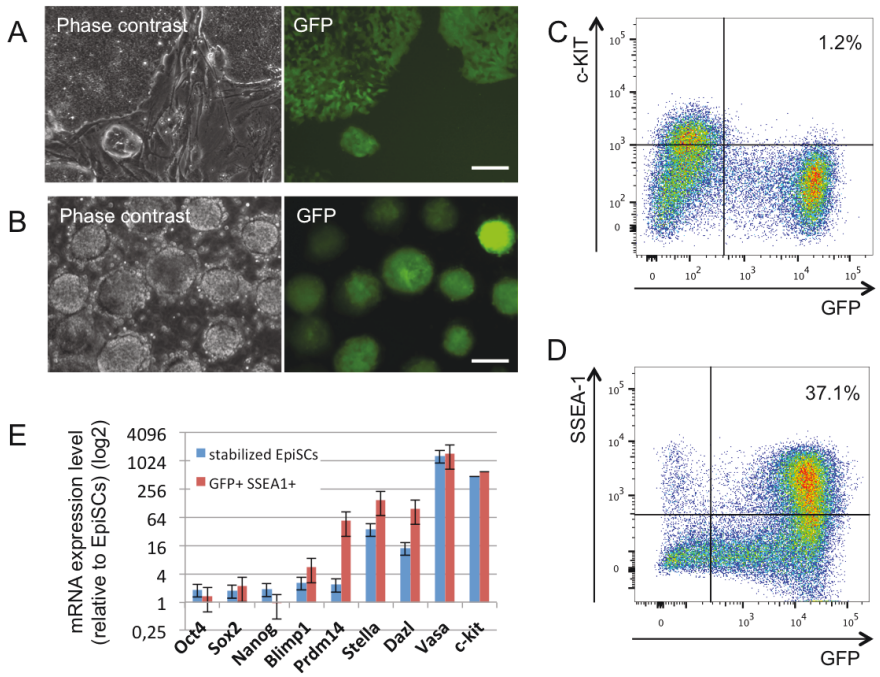

Figure 37 Differentiation of mouse ΔPE-Oct4-GFP+ EpiSCs toward PGCs. (**A**) Oct4-GFP expression in undifferentiated cells. Phase contrast and GFP fluorescence images are shown. Scale bar: 20 µm. (**B**) Oct4-GFP expression on day 7 of differentiation. Phase contrast and GFP fluorescence images are shown. Scale bar: 20 µm. (**C**) FACS analysis of the day 7 differentiated cells by GFP and c-KIT. (**D**) FACS analysis of the day 7 differentiated cells by GFP and SSEA-1. (**E**) Gene expression analysis of Oct4-GFP+/SSEA-1+ cell. The value for EpiSCs is set as 1, and values are on log2 scale.

3.3. Ultrastructural characterization of mouse embryonic stem cell-derived oocytes and granulosa cells

8.3.1. Granulosa cells and the GC–oocyte interface of ESC-derived follicles

The entry of PGCs into meiosis *in vivo* and *in vitro* appears to be a cell autonomous process. Subsequent development of PGCs into competent oocytes and ultimate meiotic arrest during folliculogenesis is dependent on 2-way signaling interactions between the oocyte and surrounding granulosa cells (Adams & McLaren, 2002; Gosden *et al*, 2002). Figure 38A–D shows ESC-derived follicle-like structures. As aggregation of PGCs and granulosa-like cells takes place randomly in this system, we obtained spherical aggregates with centrally located single as well as multiple putative germ cells surrounded by various layers of attached presumptive granulosa cells and ECM. Light microscopy revealed germ cell clusters surrounded by loosely attached somatic granulosa-like cells (Fig. 38A). Scanning electron microscope (SEM) analysis demonstrated follicle-like structures, that is, germ cells surrounded by a dense layer of cuboidal cells (Fig. 38B). Figure 1C shows ESC-derived putative granulosa cells in direct proximity to a zona pellucida-like matrix. The granulosa-like cells exhibit a polygonal shape and a smooth surface with few microvilli (Fig. 38C). SEM and transmission electron microscopy (TEM) analysis revealed a structure specific for granulosa cells, that is, TZPs (Fig. 38C, 38D, arrow) that extend toward the putative oocyte.

Figure 39A shows a light microscopy image of an ESC-derived follicular structure, with presumptive granulosa cells surrounding the GFP-positive oocyte-like cell. To analyze the granulosa cell–oocyte interface by SEM, in vitro-derived follicles were cracked. Figure 39C and D shows both parts of a cracked aggregate, revealing their morphological similarity to natural follicles. Even though the presumptive oocyte was destroyed during the cracking procedure, a round cavity of 50–60 μm in diameter with residual oocyte cell material is evident (Fig. 39C, D). Multiple layers of granulosa cells surround the cavity. The most central ones exhibiting the typical cuboidal-elongated phenotype of natural polarized cumulus cells, that is, those cells in direct contact to the oocyte (Fig. 39C), whose TZPs orientate toward the oocyte (Fig. 39B). TZPs have been well characterized in many mammals by EM (Anderson &

Albertini, 1976; Hertig & Adams, 1967), and their number and form have been demonstrated to change dynamically during follicular development (Albertini et al, 2001).

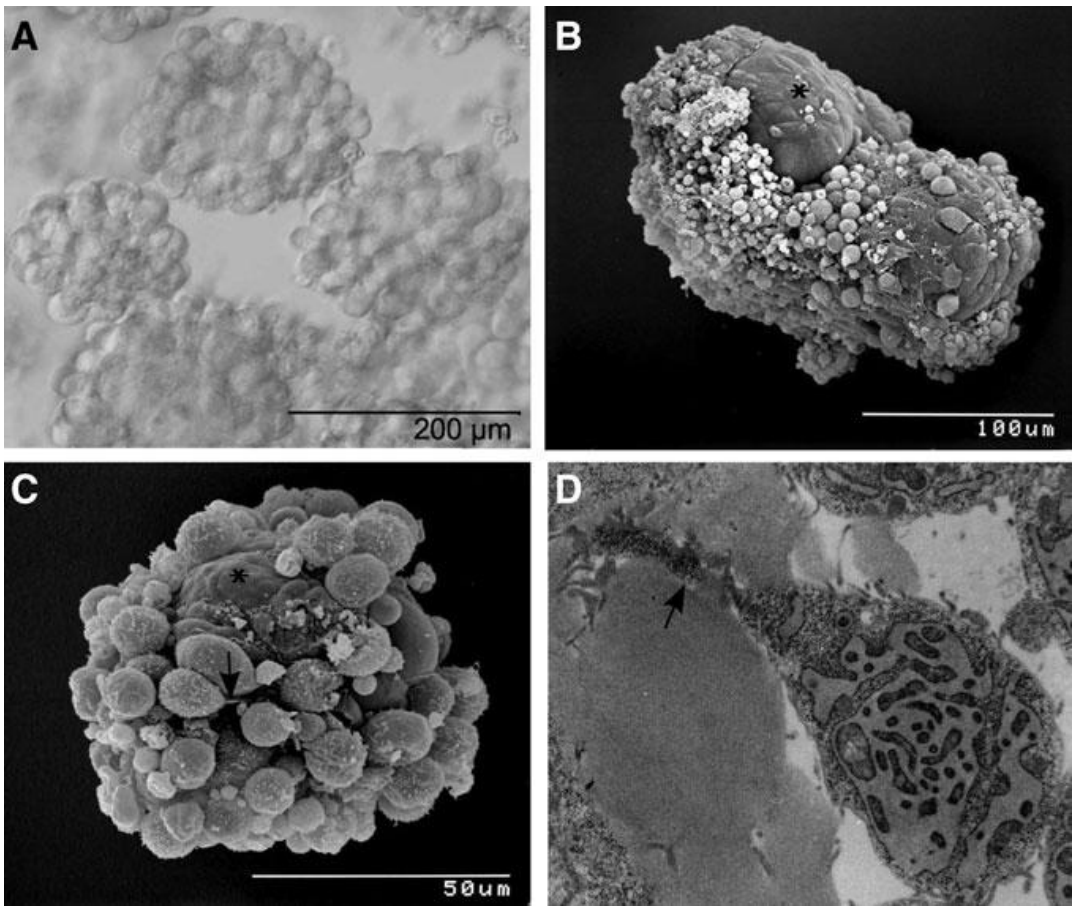

Figure 38 ESC-derived follicle-like structures. (from Psathaki *et al.* 2011) (**A**) Light microscopy image of ESC-derived follicle-like structures with clusters of granulosa cells loosely surrounding the oocyte. (**B**) SEM image of a defined follicle structure. Note the layer of densely attached cuboidal cells (asterisk). (**C**) SEM image of polygonal-shaped granulosa cells around a smooth zona pellucida-like surface (asterisk). The pole of a granulosa cell is facing toward the oocyte (arrow). (**D**) TEM image of a granulosa cell with an extension stretching towards the oocyte (arrow).

To investigate the granulosa cell–oocyte interface in more detail, TEM analyses was performed and compared to granulosa cells of natural follicles to ESC-derived presumptive granulosa cells. The ultrastructure of TZPs of in vitro-derived granulosa cells appeared to be indistinguishable from the TZPs of their natural counterparts, indicating generation of the interface between the oocyte and granulosa cells, the major control structure for healthy follicle development (Albertini et al, 2001). ESC-derived granulosa cells of high electron density exhibited long cellular processes containing the same dark fine granulation as the cytoplasm (Fig. 2E). These processes penetrated the matrix, with some reaching a diameter of ~1 μm, very similar to the branched processes of polarized cumulus cell in natural follicles. The detection of organelles, for example, mitochondria (Albertini et al, 2001; Zamboni, 1970), within the TZPs of in vitro-derived granulosa cells (Fig. 2F, G) is indicative of recapitulation of folliculogenesis in vitro. Further, the ultrastructural texture of the pale amorphous matrix in direct proximity to the granulosa cells *in vitro* (Fig. 2E) resembles the zona pellucida of the granulosa cell–oocyte interface *in vivo* (Fig. 2H).

Figure 39 Granulosa cell–oocyte interface of ESC-derived follicles. (from Psathaki *et al.* 2011) (**A**) Light microscopy image of an ESC-derived follicle structure. Granulosa cells surround the gcOct4-GFP oocyte. (**B**) SEM analysis of an ESC-derived follicle-like structure. A long process originates from a somatic granulosa cell toward the oocyte (arrow). (**C**, **D**) SEM analysis of both halves of a cracked ESC-derived follicle-like structure. The position of the oocyte is clearly apparent by the 50–60-mm-large, round cavity (asterisk in C) and residual oocyte cell material in D (asterisk). The granulosa cells surround the oocyte in multiple layers, with the cell layer in direct contact being cuboidal-elongated in shape (C, arrow). (**E**) TEM analysis of ESC-derived granulosa cells. Cells exert long processes (TZPs) toward the oocyte (arrow). Note the texture of the pale amorphous matrix (asterisk), which is penetrated by the TZPs. (**F**) TZPs contain organelles such as mitochondria (arrow) and have the same ultrastructural texture as the cell cytoplasm. (**G**) TZPs of ESC-derived granulosa cells partly exhibit extreme branching processes (arrow) and reach diameters of almost 1 mm. (**H**) Cellular processes of cumulus cells with branching ends (arrow) of in vivo follicles closely resemble those of in vitro-derived granulosa cells. The ultrastructure of the zona pellucida (asterisk) resembles that of in vitro-derived follicles in E.

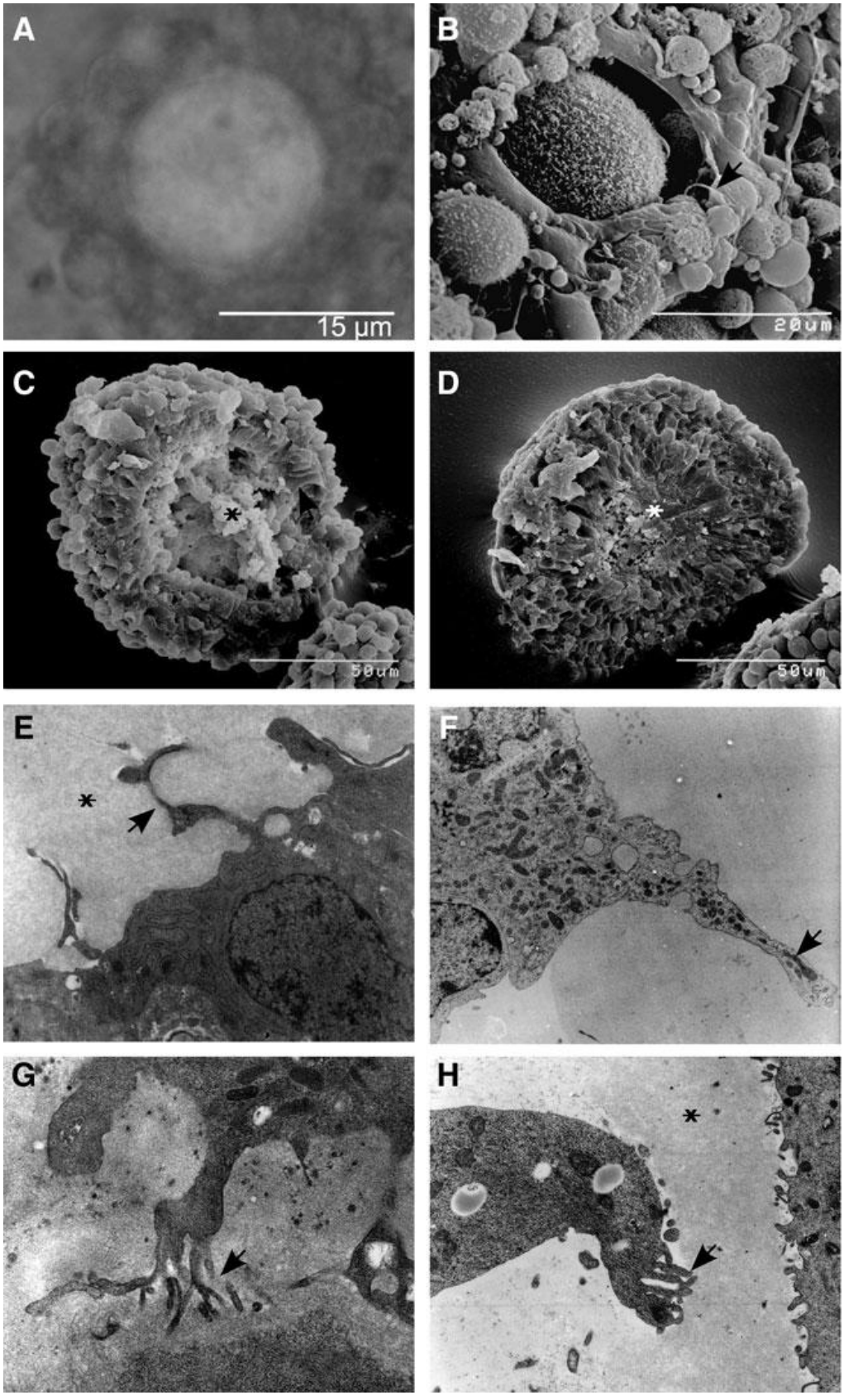
A
15 µm
B
20um
C
50um
D
50um
E
F
G
H

Ultrastructural characterization of in vitro-generated granulosa cell-like cells revealed additional analogies to characteristics of natural granulosa cells described in the literature, for example, the presence of both dark- and light-appearing granulosa cells. Dark granulosa cells possess a dark background nucleoplasm and background cytoplasm (Fig. 40A, C). The electron density is due to the fine granulation of the cytoplasm, which does not correspond to free ribosomes, as free ribosomes would be much larger and stand distinctly out from the granular background (Fig. 40E, F). The cytoplasm of the granulosa cells appears to be partly vacuolated and is populated by mitochondria, ribosomes, and the most prominent organelle of ESC-derived granulosa cells, the rough endoplasmic reticulum. Cisternae of swollen rough endoplasmic reticulum containing granular material wind through the cytoplasm of dark and light in vitro-derived granulosa cells (Fig. 40A, E) as well as pale *in vivo* granulosa cells (Fig. 40F). The ribosomes of natural dark and light granulosa cells and ESC-derived granulosa cells are either free or associated with rough endoplasmic reticulum (Fig. 40A, B, E, F). The presence of free ribosomes is a characteristic feature of protein-secreting cells, such as the granulosa cells of growing follicles. The mitochondria of both dark in vivo and in vitro-derived granulosa cells appear irregular and elongated, containing pale cristae and an electron-dense matrix (Fig. 40A, B). The mitochondria of light granulosa cells exhibit an oval shape and have tubular–vesicular cristae (Fig. 40E, F). Lipid droplets filled with a transparent gray substance and empty vacuoles frequently surrounded by a membrane (Fig. 40B, D) are distributed throughout the cytoplasm of *in vivo* GCs. Vacuolization appears to be a prominent feature of ESC-derived granulosa cells (Fig. 40C), manifested mainly by empty white vacuoles and vacuoles containing a residual gray substance (Fig. 40C). Empty vacuoles appear to be an artifact of sample manipulation, created when the gray substance of lipid droplets is washed out during the dehydration step. The nuclei of both in vitro-derived and in vivo granulosa cells are large and have an irregular contour (Fig. 40A–D). The nucleoplasm of ESC-derived granulosa cells, enclosed by the inner nuclear membrane, contains finely dispersed chromatin and clumps of heterochromatin scattered throughout (Fig. 40A, C, E); the nucleoplasm of *in vivo* granulosa cells is arranged similarly (Fig. 40B, D, F). Taking these data together, the ultrastructural features of in vitro-derived granulosa cells are indistinguishable from natural granulosa cells. Most importantly, to the best of my knowledge, there is no other cell in the body capable of forming unique and typical TZPs. The observed activated rough endoplasmatic

reticulum, indicative for metabolically active and steroid-producing cells, further supports their granulosa cell-like identity.

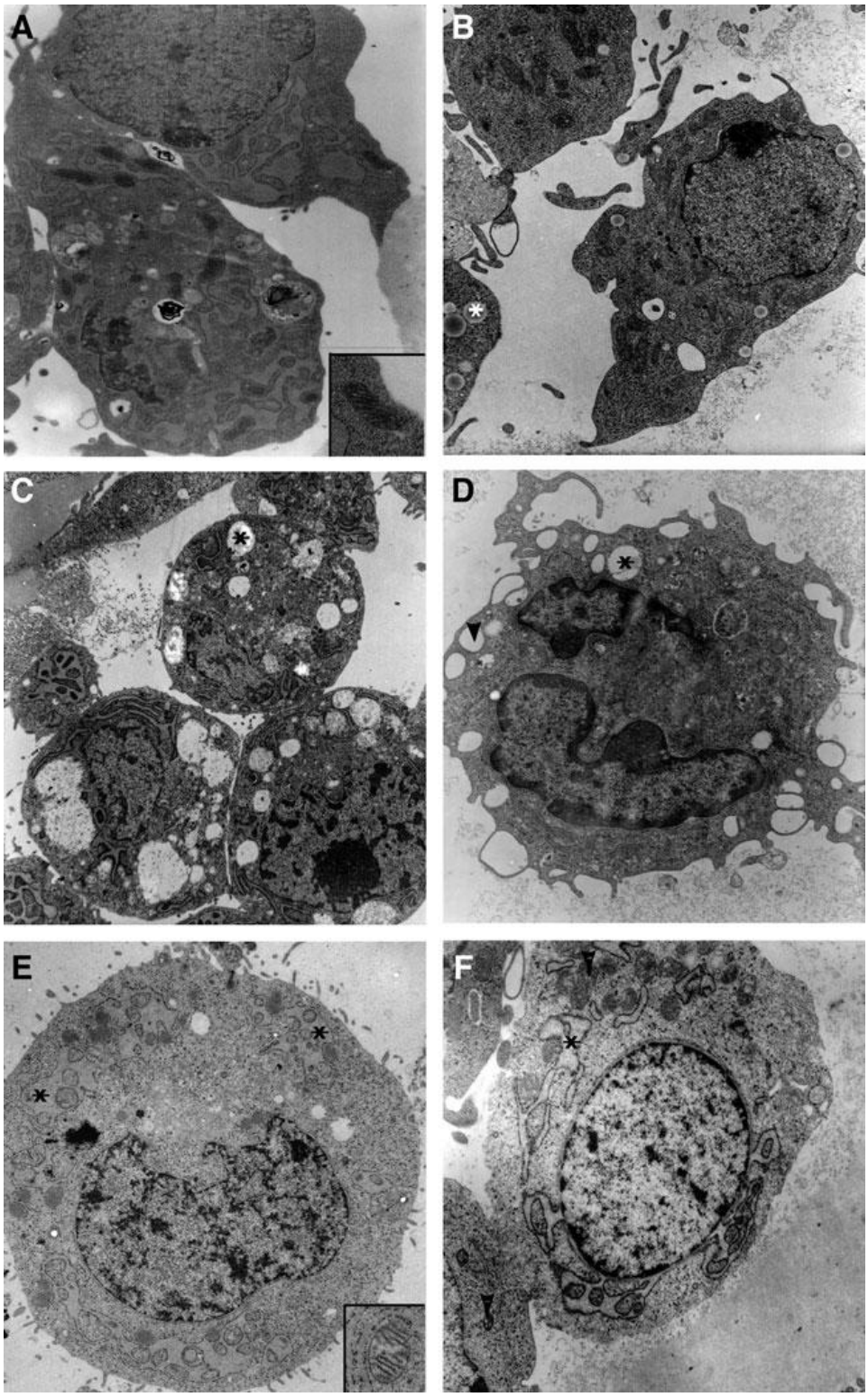

Figure 40 (continued)

Figure 40 TEM analyses of ESC-derived dark- and light-colored granulosa cells. (from Psathaki *et al.* 2011) (**A**) Cuboidal-elongated in vitro-derived granulosa cells with electron dense cytoplasm and swollen rough endoplasmatic reticulum. Mitochondria (insert) exhibit pale tubular cristae. (**B**) In vivo-derived dark granulosa cell. Note lipid droplets (asterisk). (**C**) Dark ESC-derived granulosa cells with numerous vacuoles and droplets containing residual gray translucent substance indicative of lipids (asterisk). Note prominent nucleolus. (**D**) In vivo dark granulosa cell with numerous pseudopodia, branching processes and protrusions of cytoplasmic invaginations, vacuoles (arrowhead), and lipid droplets (asterisk) as detected in in vitro-derived granulosa cell shown in C. (**E**) ESC-derived light granulosa cell with microvilli at the cell surface. The cell exhibits the typical swollen rough endoplasmatic reticulum (asterisk) and oval-shaped tubular mitochondria with dark cristae (insert). (**F**) In vivo-derived light granulosa cell with swollen rough endoplasmatic reticulum (asterisk) and vesicular–tubular mitochondria (arrow).

3.3.2. ESC-derived oocytes

We have developed a suspension culture system that supports the generation of ESC-derived oocytes of different follicular stages. Independent of the differentiation media used to initiate differentiation of ESCs, we obtained putative oocytes of various developmental stages at different yields. Serum-free conditions appeared best to promote germ cell differentiation, and XY-ESCs yielded a higher percentage of oocytes than XX-ESCs. Expression of specific oocyte marker genes was assessed by qPCR in groups of 3 in vitro-derived oocytes and compared with superovulated germinal vesicle-stage oocytes and ESCs. As expected, the generated oocytes (Fig. 41A) exhibited a gene expression pattern very similar to that of control samples (Fig. 41B). Morphologically, *in vitro*-generated oocytes (Figs. 41A and 42A) and *in vitro*-matured oocytes generated from 18.5 days postcoitum (dpc) germ cells under the same culture conditions (Fig. 42C) exhibited a very similar shape, size, and microvillous cell surface (Fig. 42C, D). Interestingly, the surface topography of some in vitro-derived oocytes analyzed by SEM resembled exactly that of unfertilized oocytes *in vivo*, with the typical sparse and relatively uniform microvillous area and a clear mosaic surface containing a polar microvillous-free region (Fig. 42B–D). TEM analyses of generated oocytes revealed large, slightly eccentric nuclei with a characteristic pale background nucleoplasm (paler than the ooplasm) (Fig. 42E). Free ribosomes appeared individually or arranged in clusters of 5–10 (Fig. 42E, insert).

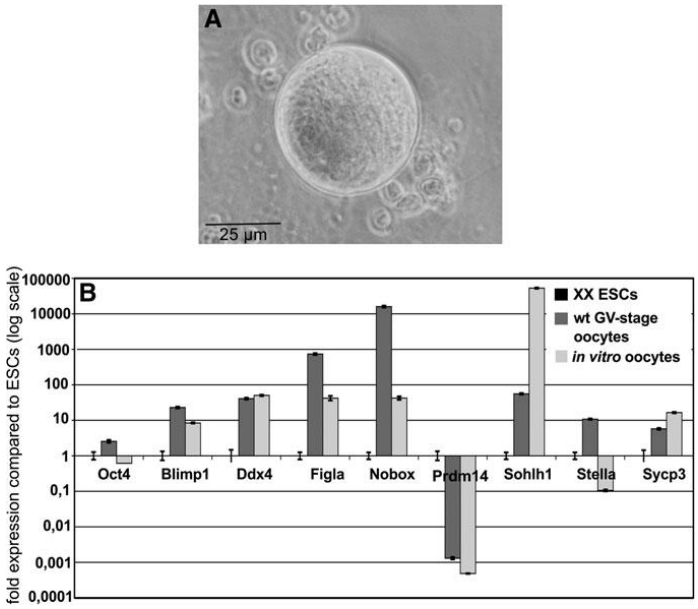

Figure 41 Gene expression of oocyte markers in a pool of 3 *in vitro*-derived oocytes. (from Psathaki *et al.* 2011) (**A**) Light microscopy image of one of the analyzed oocytes. (**B**) Real-time reverse transcription polymerase chain reaction of oocyte markers in a pool of 3 ESC-derived oocytes compared with XX-ESCs.

Elongated staples of fibrils not associated with ribosomes were found throughout the cytoplasm (Fig. 42E, insert, F). Oocyte-specific cortical granules containing a characteristic electron-dense center and a pale outer ring (Fig. 42F, arrow) were mostly distributed throughout the cytoplasm and appeared only sporadically at the cell periphery (Fig. 42F and inserts), a distinct feature of immature oocytes. Further, we detected round as well as elongated mitochondria with a dense matrix and pale, irregularly arranged cristae and intermitochondrial vacuoles, all features of natural oocytes. Noteworthy is that the majority of ESC-derived oocytes showed signs of apoptosis and autophagy, which might be indicative of atresia (Fig. 42E, H). The oocyte shown in Fig. 42E lost its spherical shape. Numerous lysosomes, clear vesicles, and autophagosomes as well as dark cytoplasmic structures were detected. The ESC-derived oocyte shown in Fig. 42H contains numerous apoptotic bodies and secondary lysosomes within the dark condensed cytoplasm. Mitochondria and other organelles cannot be identified. The zona pellucida and most of the microvilli at the oocyte surface appear to have been lost. In comparison, oocytes derived from natural 18.5-dpc PGCs grown for 13 days in the same culture medium as in vitro-derived oocytes (Fig. 42G) also exhibit dark-stained mitochondria without cristae, numerous vacuoles, and secondary lysosomes; other organelles cannot be identified. Microvilli either have

been lost or have retracted from the zona pellucida. These observations indicate that our culture conditions support the maturation of PGCs into oogonia, but further optimization of these conditions is required for the generation of functional oocytes.

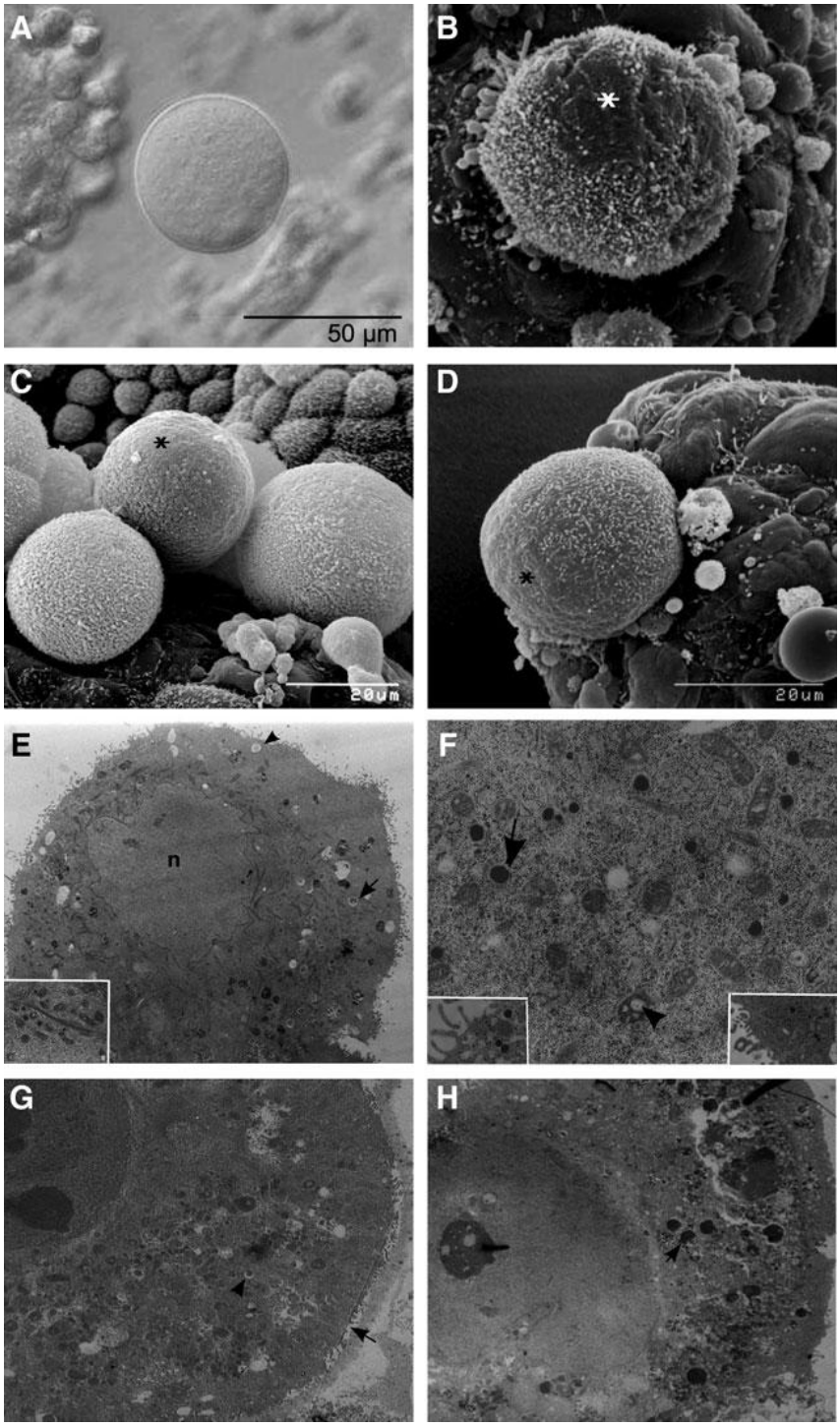

Figure 42 (continued)

Figure 42 Ultrastructural analysis of *in vitro*-derived oocytes. (from Psathaki *et al.* 2011) (**A**) Light microscopy image of an *in vitro*-derived oocyte. (**B**) SEM image of an *in vitro*-derived oocyte with a polar microvillous-free surface (asterisk). (**C**) SEM image of fetal *in vivo* oocytes cultivated under the same culture conditions as the *in vitro*- derived oocytes. Note the polar microvillous-free region (asterisk). (**D**) SEM image of an *in vitro*-derived oocyte with a polar microvillous-free surface (asterisk). Note the similarity of the shape and surface structure to *in vivo* oocytes shown in C. (**E**) TEM image showing an overview of an *in vitro*-derived oocyte. Numerous lysosomes, clear vesicles, lipid droplets (arrow), and autophagosomes (arrowhead) are distributed throughout the cytoplasm. n: nucleus. Insert: Elongated mitochondria with tubular–vesicular cristae and vacuoles are arranged between staples of fibrils. (**F**) TEM image of oocyte-specific cortical granules (arrow) with the typical electron-dense center and pale outer ring of in vitro-derived oocytes. Cortical granules appear only sporadically in the cell periphery (inserts). Note vacuolated mitochondria (arrowhead). (**G**) TEM image of oocytes derived from natural 18.5 dpc primordial germ cells grown for 13 days in the same culture medium as in vitro-derived oocytes. The dark-stained mitochondria contain only few cristae, numerous vacuoles, autophagosomes (arrowhead), and secondary lysosomes. Other organelles are not identifiable. Microvilli are lost or retracted from the zona pellucida (arrow). (**H**) TEM image of *in vitro*-derived oocyte showing numerous apoptotic bodies (arrow) and secondary lysosomes in the dark, condensed cytoplasm. Mitochondria or other organelles are not identifiable. The zona pellucida and most of the microvilli at the oocyte surface are lost.

4. Discussion

4.1. PGC differentiation from human ESCs and iPSCs

Our laboratory had developed the serum-free defined PGC differentiation protocol for mouse ESCs (Psathaki et al, 2011). I initially utilized this protocol to differentiate human ESCs. However, this approach was insufficient to induce a SSEA1+/c-KIT+ PGC population. It is known that mouse and human ESCs possess distinct characteristics, although both cell types are derived from the ICM of blastocysts. For example, mouse ESCs require LIF/STAT3 signaling for self-renewal (Niwa *et al*, 2009). Furthermore, activation of WNT/β-catenin signaling and inhibition of FGF/ERK signaling stabilize their undifferentiated state (Kunath *et al*, 2007; Sato *et al*, 2004). In contrast, hESCs do not respond to LIF (Dahéron *et al*, 2004), but depend on FGF and TGFβ signaling (Amit *et al*, 2004; Frank *et al*, 2012; James *et al*, 2005). In addition, WNT/ β-catenin signaling appeares to induce differentiation under chemically defined conditions (Sumi *et al*, 2008). Those facts strongly indicate a significant difference between cells of both species and highlight the requirement of different approaches to differentiate these cells into germ cells. Interestingly, EpiSCs, which are stem cells derived from mouse post-implantation embryos, share some properties with human ESCs, such as the flat morphology and FGF-dependent maintenance conditions. However, in contrast to mouse EpiSCs, which contain a subpopulation of Blimp1+ and Stella+ cells, our investigations indicate that human ESCs do not contain subpopulations of BLIMP1+ nor STELLA+ cells. Thus, human ESCs possess a distinct character from mouse EpiSCS with respect to the expression of PGC genes. Taken together, these data indicate that human ESCs possess different characteristics from both mouse ESCs and EpiSCs.

The lack of specific markers for early human PGCs hampers the investigation of human PGC commitment processes *in vitro*. Three studies have reported the generation of human GFP reporter ESC and/or iPSCs lines for germ cell investigations (Chuang et al, 2012; Kee et al, 2009; Tilgner *et al*, 2010). Kee et al. and Tilgner et al. utilized a VASA-GFP reporter and successfully isolated PGC-like cells *in vitro* (Kee et al.: 5% and Tilgner et al.: 0.8%). However, *VASA* is expressed in PGCs upon colonization of the gonads and is not expressed in PGCs of earlier stages

of development. Chuang et al. utilized a OCT4-GFP reporter. *OCT4* is known to be expressed in early PGCs in mice (Schöler *et al*, 1990; Yeom et al, 1996) and humans (Gaskell *et al*, 2004; Rajpert-De Meyts *et al*, 2004), but also in mouse and human ESCs (Thomson et al, 1998). Thus, *VASA* and *OCT4* are not really specific markers of early PGCs in humans. One of the known earliest genes expressed in human PGCs is *BLIMP1* (Gkountela et al, 2013; Lin *et al*, 2014), although *BLIMP1* is also known to be expressed in other somatic cell types, such as B cells (Turner et al, 1994), differentiating macrophages (Chang et al, 2000) and a subset of T-cells (Kallies et al, 2006; Martins et al, 2006), which do not express *OCT4*. Therefore, only when *OCT4* and *BLIMP1* are co-expressed, the two genes can be considered specific markers of early PGCs. Through my analysis, I found that *STELLA* and *TEX13B* exhibit concomitant upregulation with *OCT4* and *BLIMP1*. *TEX13B* (mouse homologue: *Tex13*) has been reported to be expressed in testis, but not in ovary, in both mice and humans (Wang *et al*, 2001). However, the expression pattern of *TEX13B*/*Tex13* in early PGCs has not yet been investigated. Therefore, it would be of interest, whether *TEX13B*/*Tex13* is also expressed in pre-migratory PGCs. *Stella* is one of the definitive markers of early PGCs in mice. Stella knockout mice exhibit no gross PGC defects and are fertile (Payer *et al*, 2003), although *Stella* seems to play a role in the protection of maternal imprints in the zygote (Nakamura *et al*, 2007; Nakamura *et al*, 2012). Nevertheless, several studies have utilized Stella to identify PGCs, due to its specific expression in this cell type. In human, the expression pattern of *STELLA* has not been determined. One study reported that undifferentiated human ESCs express STELLA (Clark et al, 2004). In contrast, I did not detect significant levels of STELLA expression in our human ESC lines. Interestingly, one study reported that chromatin around the transcriptional start sites of *STELLA* is not associated with inductive H3K4me3, suggesting that *STELLA* is not actively transcribed in human ESCs (Tesar et al, 2007). The expression level of STELLA in human ESCs has to be further investigated to convincingly characterize this particular similarity or difference between human ESCs and PGCs.

The establishment of a reproducible and efficient differentiation protocol of human PGCs potentially provides the scientific community with an alternative approach to investigate germ cell development. All of the published studies on *in vitro* differentiation of human PGCs utilized serum-based medium. Commercial serum

bears a huge variation between batches, which are uncontrollable and thus, will result in poor reproducibility of available protocols. In fact, my attemps to reproduce the protocol by Kee et al. (Kee et al, 2009) resulted in failure to efficiently induce SSEA1+/c-KIT+ PGCs from human ESCs, although I used serum from the same company. Therefore, in this project, I established a serum-free defined differentiation protocol for the induction of PGCs from human ESCs and iPSCs. This protocol reproducibly induced OCT4+/T+/BLIMP1+ PGC precursors that transitioned into TRA-1-81+/c-KIT+ pre-migratory PGC-like cells. In this system, not all cells were similar to PGCs, likely due to some stochastic/physical parameters or intrinsic differences. However, considering the fact that PGC induction directly from ESCs/iPSCs so far gave rise to only low numbers of PGC-like cells, it becomes apparent, that the two-step induction procedure developed in my thesis strongly induced PGC precursors and subsequently PGC-like cells. To my knowledge, this is the first report of a serum-free defined differentiation protocol for the induction of human PGCs *in vitro*.

My data suggest that Activin A, BMP4, and bFGF are important for the induction of OCT4+/T+/BLIMP1+ PGC precursors from human ESCs and iPSCs, and point to two different possibilities. The first possibility is that human PGC specification, in contrast to mouse PGC specification, requires the activation of TGF β signaling. Mouse *ex vivo* PGC induction from epiblast has been shown to require BMP4 and bFGF, whereas the knock-out of *Smad2*, a transducer of TGFpiblast has been shown to require BMP4 and bFGF, whereas the knock-out of PGC precursors fr(Ohinata et al, 2009). These results indicate that BMP and FGF signaling enhance PGC specification, whereas TGFt of PGC precursors from human ESCs and iPSCs, and point to two different poss disc-like shape that is physically closer to the distal hypoblast in comparison to the cylinder-like shape of the mouse epiblast (Niakan *et al*, 2012). Therefore, it is possible that the human epiblast and PGCs exhibit different reactivity to TGF β signaling than their mouse counterparts. The second possibility is that even though human ESCs and mouse EpiSCs share many features, such as morphology and gene expression profiles, the state of human ESCs might be closer to the naïve cell state than to a primed state with regard to their PGC differentiation ability. In mice, BMP4 treatment of EpiSCs *in vitro* induces *Blimp1*+ cells, but most

of these cells do not progress to become Stella+ PGC-like cells (Hayashi et al, 2011; Hayashi & Surani, 2009). Interestingly, when EpiSCs were reverted to ESC-like cells, they gained the ability to differentiate into *Blimp1*+/*Stella*+ PGC-like cells (Hayashi et al, 2011). These data suggest that EpiSCs exhibit restricted PGC differentiation ability compared with ESCs. Indeed, a previous study showed the divergence of EpiSCs from ESCs as well as epiblast by global transcription analysis (Hayashi et al, 2011). In this context, my data clearly show that human ESCs and iPSCs generate *OCT4*+/*T*+/*BLIMP1*+ PGC precursors that transition under appropriate culture conditions into PGC-like cells with key PGC gene expression, i.e., *BLIMP1*, *STELLA*, *TFAP2C*, and *NANOS3*.

BMP4 played a critical role in the induction of PGC-like cells and enhanced induction in a concentration-dependent manner in our culture system, similar to serum-based differentiation culture systems (Kee et al, 2006). Apart from BMP proteins, SCF, EGF, and bFGF have also been reported to enhance PGC induction in mice (Ohinata et al, 2009). In particular, SCF (also known as KITLG) is considered to be necessary for PGC survival (Pesce *et al*, 1993). As we observed the rapid disappearance of the TRA-1-81+/c-KIT+ PGC-like cell population within 2 days of culture, we attempted to extend the proliferation of PGC-like cells by SCF, but this approach proved to be insufficient. On the other hand, according to the GSEA analysis, genes related to lipid, hormone, and steroid metabolic processes were upregulated in d6 PGC-like cells (Supplementary Table 3). Therefore, the addition of hormones to the culture might be an alternative approach for extending and rescuing the development of human PGC-like cells *in vitro*. For example, retinoic acid (RA) is known to be associated with the initiation of meiosis during PGC development and follicle stimulating hormone (FSH) and luteinizing hormone (LH) are known to play an important role in oogenesis. However, an involvement of hormonesin PGC survival or proliferation has not been reported. Whether hormonal treatment of human PGC-like cells enhances proliferation warrants further investigations.

The human PGC-like cells exhibited expression of *OCT4*, *NANOG*, *BLIMP1*, and *STELLA*, which is characteristic for mouse pre-migratory PGCs. I also confirmed by gene expression array analysis that human *in vivo* post-migratory female PGCs express high levels of *BLIMP1* and *STELLA*, similarly to the human PGC-like cells

and mouse PGCs, suggesting that characteristics of PGCs are conserved between these two species. In addition, global transcription analysis revealed that during differentiation, mesodermal genes, such as *MESP1*, *CYP26A1*, *MIXL1*, and *GSC*, were initially upregulated and subsequently downregulated. Concomitantly, PGC genes, such as *BLIMP1*, *TFAP2C*, *STELLA*, and *NANOS3*, were upregulated. This is similar to the gene expression dynamics observed during mouse PGC specification and indicates that the gene expression dynamics of some gene sets during PGC specification are conserved between humans and mice. In contrast, these cells showed very low expression levels of SOX2 and PRDM14, which seems to be a unique characteristics of human PGCs.

In mice *Blimp1* is one of the earliest genes expressed in mouse PGCs and its expression is first detected in approximately six cells in the posterior epiblast at 6.25 dpc (Ohinata *et al*, 2005). Knock-out of Blimp1 leads to the failure of Hoxa1 or Hoxb1 expressionm and loss of PGCs by 7.5 dpc (Kurimoto et al, 2008; Ohinata et al, 2005). Therefore, it is assumed that Blimp1 plays a key role in repression of the somatic program during PGC specification. Interestingly, a number of specification-associated genes are still induced, although relatively weak, in the absence of Blimp1, suggesting that there are Blimp1-independent mechanisms during specification (Kurimoto et al, 2008). In humans, *BLIMP1* is reported to be expressed in human PGCs/gonocytes at around 12 to 19 week of pregnancy (Eckert et al, 2008). However, the expression pattern of *BLIMP1* in earlier stages has not been reported. Interestingly, I observed that a subset of mesodermal genes, such as *MESP1*, *CYP26A1*, *MIXL1*, and *GSC*, was initially upregulated in PGC-precursor cultures and subsequently downregulated in BLIMP1-expressing PGC-like cells. This gene dynamics might depict the indication that BLIMP1 plays an important role during human PGC specification by suppressing those mesodermal genes. In fact, I showed that the knock-down of BLIMP1 impairs the induction of TRA-1-81+/c-KIT+ PGC-like cells, which has also been reported by another study (Lin et al, 2014). Further investigation need to clarify how BLIMP1 functions during human PGC specification.

The re-acquisition of *Sox2* expression is one of the characteristics of PGC specification in mice (Kurimoto et al, 2008; Yabuta et al, 2006). *Sox2* is repressed at the initiation of specification (6.25 dpc) and re-acquired upon establishment of

committed PGCs (7.25-7.5 dpc), while *Oct4* and *Nanog* are constantly expressed. *Sox3* and *Sox17* also are transiently and specifically upregulated in PGCs at around 7.25 dpc. In contrast, human PGCs appear to lack the expression of *SOX2* (de Jong et al, 2008; Perrett et al, 2008). The expression of *SOX3* and *SOX17* in human PGCs has not been examined yet, but it has been reported that *SOX17* is expressed in carcinoma *in situ* (CIS) and seminoma cells, but not in embryonic carcinoma (EC) cells (de Jong et al, 2008). The PGC-like cells exhibited a low *SOX2* expression level in accordance with the mentioned studies. Interestingly, SOX17 is upregulated in PGC-like cells, whereas SOX3 is not upregulated, but rather downregulated (data not shown). How those SOX genes are regulated during human PGC commitment and how much the expression of SOX genes is conserved between mice will require further investigation.

Surprisingly, only low PRDM14 expression levels could be detected in PGC-like cells. In mice, *Prdm14* plays a key role in ESCs and PGCs. In ESCs, Prdm14 has been reported to repress extraembryonic endoderm (ExEn) differentiation in ESCs (Ma *et al*, 2011). Furthermore, a recent study revealed that Prdm14 antagonizes activation of the fibroblast growth factor receptor (FGFR) signaling and represses expression of de novo DNA methyltransferases (Dnmts) to ensure naïve pluripotency (Yamaji *et al*, 2013). Prdm14 has also been identified as a critical regulator for PGC specification from the epiblast (Yamaji et al, 2008). Prdm14 knock- out mice are sterile and show a progressive loss of PGCs between 7.5 and 12.5 dpc, although a few AP-positive cells do remain even at the latter time point (Yamaji et al., 2008). Somatic genes are appropriately repressed, suggesting that Prdm14 does not function to repress the somatic program but is required for activation of the PGC program. In fact, a recent mouse study showed that ectopic expression of *Prdm14* alone can induce PGC-like cells from Epiblast-like cell (EpiLCs) without activating the somatic program. The authors also suggested that *Prdm14* plays a key role in the repression of neural induction and *de novo* methylation, as well as in the activation of the PGC program during specification (Nakaki et al, 2013). In humans, PRDM14 plays a crucial role in the maintenance of human pluripotency by binding to *OCT4* regulatory elements and thereby regulating OCT4 expression and by suppressing the differentiation of human ESCs (Chia *et al*, 2010). PRDM14 is also thought to repress the expression of PGC-associated genes, such as *NANOS3* and *BMP4*, in human ESCs. On the other hand, the expression pattern of PRDM14 in human PGCs has not been studied. My data, for

the first time, demonstrate low or even absent expression of PRDM14 in PGCs. I confirmed that post-migratory *in vivo* human PGCs also exhibit a very low expression level of *PRDM14*, whereas mouse PGCLCs exhibit a high expression level of this gene. These results suggest that human PGCs do not express *PRDM14* from their early commitment to the germ cell lineage through at least the post-migratory stage. In fact, I demonstrated that the knock-down of *PRDM14* did not affect the induction of TRA-1-81+/c-KIT+ PGC-like cells, whereas that of *BLIMP1* significantly impaired it. My data revealed that human PGC-like cells show some mouse Prdm14-regulated events, such as: 1) the downregulation of genes associated with neural differentiation, 2) similar expression dynamics of a number of mouse Prdm14-regulated genes (such as *KLF5*, *NR5A2*, *KLF4*, *LIFR*, and *NANOG*), 3) the progression of global epigenetic reprogramming by demethylation of differentially methylated regions (DMRs) of selective imprinted genes and a global decrease in 5mC levels, and 4) the expression of *OCT4*, *NANOG*, and other pluripotency genes. The mechanism underlying the regulation of these genes is undetermined at this time. However, my data strongly suggest the presence of yet unknown mechanisms underlying a novel type of transcriptional regulation in humans. PGCs from *Prdm14*-deficient mice have been reported to exhibit abnormal expression of *Sox2*, indicating a putative interaction between *Prdm14* and *Sox2* in mice (Yamaji *et al*, 2008). Considering that *Prdm14* plays a crucial function in the re-acquisition of *Sox2* expression in mouse PGCs, it might be reasonable to postulate that *SOX2* is not expressed in human PGCs due to the absence of *PRDM14*. On the other hand, a recent human study demonstrated that *BLIMP1* binds to a region around the *SOX2* transcriptional start site suppressing *SOX2* expression (Lin et al, 2014). However, the downregulation of *SOX2* is a general phenomenon of BMP4-triggered mesoderm commitment, independent from the expression of *BLIMP1*. In fact, we also observed the downregulation of *SOX2* in FACS-sorted c-KIT- somatic populations from our differentiated EBs. Thus, the suppression of SOX2 by BLIMP1 might be a feedback mechanism to maintain the cell state. Whether human PGCs utilize another mechanisms to actively or passively downregulate SOX2 warrants further investigations.

Taken together, my differentiation protocol facilitates the generation of sufficient amounts of PGC-like cells to investigate gene/protein interactions and epigenetic alterations. Through this study, I provide insight into a novel human transcriptional

regulation during the early stage of human PGC development (3–6 weeks). Continued investigations will provide us with a more comprehensive understanding of human germ cell development and the opportunity to perform research for reproductive medicine, such as drug screening and disease modeling, by utilizing patient-specific iPSCs from reproductively compromised patients.

4.2. PGC differentiation from mouse EpiSCs and Δ PE-Oct4-GFP+ EpiSCs

There have been two reports on the induction of PGCs from mouse EpiSCs (Hayashi et al, 2011; Hayashi & Surani, 2009). Interestingly, both studies demonstrated inefficient or no induction of PGCs from EpiSCs. The first study (Hayashi & Surani, 2009) reported that EpiSCs contain a subpopulation of Blimp1+ cells (10-50 %), some of which were also OCT4+, indicating a spontaneous generation of the PGC precursors and visceral endoderm (VE) cells.. The authors demonstrated that BMP4 treatment slightly induced Stella+ cells, but they did not achieve a significant induction, considering the percentage of Blimp1+ cells within EpiSCs. This indicates that Blimp1+ cells retain their PGC precursor-like state, even after induction with BMP4. The second study (Hayashi et al, 2011) reported the efficient induction of PGC-like cells from ESCs via an epiblast-like state. The differentiation regimen used contained BMP4 and induced PGC-like cells (Blimp1+/Stella+) from the epiblast and from EpiLCs. However, EpiSCs produced only Blimp1+ cell that did not develop into Blimp+/Stella+ PGC-like cells. Interestingly, our differentiation system induced Oct4+GFP+/SSEA1+, but not c-KIT+ cells from EpiSCs. SSEA1 is not expressed in mouse EpiSCs, but is expressed in mouse ESCs and PGCs. Thus, the expression of SSEA1 might indicate the transition of cells from EpiSCs to PGCs, similar to the previous studies. Further optimization of the culture conditions might stimulate these cells to develop into Oct4+GFP+/c-KIT+ putative PGCs.

In this study, we succeeded to induce putative PGCs from mouse EpiSCs only once and failed to reproduce it. Several points can be considered as a potential cause. For example, we used MEF-conditioned medium (MEF-CM) for the maintenance and differentiation of EpiSCs. MEF preparations greatly vary in terms of quality and biological character, such as sensitivity to cytokines. MEF-CM therefore also exhibits batch-dependent differences, like varying concentrations of secreted components like

for instance Activin A. Interestingly, it has been reported that the knock-out of *Smad2*, a transducer of TGF β signaling, leads to an increased number of Blimp1+ PGCs in the epiblast (Ohinata et al, 2009). In addition, it is known that EpiSCs contain a subpopulation of PGC precursors and the number of cells is strongly influenced by the medium composition. Thus, the concentration of Activin A in MEF-CM could significantly affect the differentiation efficiency of PGCs from EpiSCs. Those facts strongly suggest the use of defined medium for PGC differentiation from mouse EpiSCs.

We also attempted PGC differentiation from so called stabilized EpiSCs (Δ so called st). Similar to the induction from normal EpiSCs, we could not induce Oct4-GFP+/c-KIT+ putative PGCs, but obtained Oct4-GFP+/SSEA1+ cells. Interestingly, SSEA1+ as well as SSEA1- cells, i.e. the whole culture upregulated a number of PGC genes, such as Blimp1, Prdm14, Stella and Dazl. Contrary to our expectation that s, such as Blimp1, Prdm14, Stella and Dazl. Activin A in MEF-CM coulsimilar gene expression profile to E5.5 epiblast, we did not observe any difference between normal EpiSCs and ΔPE-Oct4-GFP+ EpiSCs. Again, the utilization of a defined PGC differentiation protocol for mouse EpiSCs is required to investigate the differentiation potential of the two EpiSC lines.

4.3. Ultrastructural characterization of mouse embryonic stem cell-derived oocytes and granulosa cells

The first systematic study of the culture and growth of mouse oocytes in vitro was published by the laboratory of John Eppig (Eppig, 1977). As shown in that study mouse oocytes from primordial follicles could be grown and matured in vitro to produce live offspring after fertilization (Eppig & Schroeder, 1989; O'Brien *et al*, 2003). These data marked a major breakthrough in the field of reproductive biology. Based on this success, various *in vitro* culture systems for female gametes of different mammalian species were established, such as rat (Daniel *et al*, 1989), hamster (Roy & Greenwald, 1989), cat (Jewgenow, 1998), pig (Hirao *et al*, 1994), sheep (Cecconi *et al*, 1999), goat (Huanmin & Yong, 2000), cow (Gutierrez *et al*, 2000; Harada *et al*, 1997), and human (Roy & Treacy, 1993). All these maturation systems, including the

mouse model, are still under investigation in an effort to broaden our understanding of the complex mechanisms involved in germ cell development and maturation. In our study, we performed comparative ultrastructural analyses of follicle-like structures and bona fide oocytes from mouse ESCs with their natural counterparts. With our data, we supplement the genetic and immunological data obtained by standard analyses with a description of the unique ultrastructural properties of oocytes and their supporting granulosa cells during gametogenesis *in vivo*. Specifically, we performed SEM analysis on in vitro-derived follicle-like structures and compared their morphology with that of natural mammalian follicles described by Makabe et al. in 2006 (Makabe *et al*, 2006). Striking morphological similarities indicate that our culture system supports the derivation of germ cells of different developmental follicular stages. We utilized TEM analysis to assess differences in the dynamic structure of TZPs, which form the morphological basis of the oocyte–granulosa cell interface and play a crucial role in the structural integrity of developing follicles and maturing oocytes (Albertini et al, 2001). Many of our *in vitro*-derived granulosa cells developed microvilli, cytoplasmic invaginations, pseudopodia, and cytoplasmic protrusions (not shown here), which have been associated with cell expansion and are considered indirect signs of granulosa cell luteinization both *in vitro* and *in vivo* (Suzuki *et al*, 1981). The presence of numerous lipid droplets within the cytoplasm of *in vitro*-derived granulosa cells, an early sign of luteinization (Crisp *et al*, 1970), correlates with active steroidogenesis (Nottola *et al*, 2006). Taken together, *in vitro*-derived granulosa cells exhibit ultrastructural characteristics typical for metabolically active and steroid-producing cells.

The ovarian follicle represents a morphological and functional unit wherein both somatic and germ cells play a pivotal role in follicle maturation and formation of fully competent, fertilizable oocytes (Canipari, 2000). SEM analysis clearly demonstrated that ESC-derived cuboidal-shaped granulosa cells closely surround the oocyte and extend long TZPs toward the oocyte. In vivo, TZPs are most abundant in preantral follicles. By TEM analysis, we demonstrated that ESC-derived cumulus cells extend typical TZPs, some of which contain mitochondria, an observation consistent with the literature (Albertini et al, 2001; Zamboni, 1970). TZPs are an essential requirement for healthy follicle development (Albertini et al, 2001) and the ultrastructure of TZPs of our *in vitro*-derived granulosa cells demonstrates a profound conformity to that of

natural granulosa cells. This data demonstrate the establishment of an interface, that is, the major control site between the oocyte and granulosa cells *in vitro*. The ultrastructure of the ECM matrix of the in vivo cumulus–oocyte complex closely resembles that of the matrix penetrated by the TZPs of the *in vitro*-derived granulosa cells.

Comparative morphological analysis of ESC-derived oocytes and *in vivo* oocytes revealed remarkable similarities. The oocyte surface varies greatly from one stage of the cell cycle to the other and even within a given stage, suggesting a close association between the surface characteristics and the maturation status of the oocyte (Suzuki *et al*, 2000). A mature, unfertilized mouse oocyte is characterized by small blebs and sparse, relatively uniform microvilli (Eager *et al*, 1976; Suzuki et al, 2000) as well as a clear mosaic surface, that is, a microvillous membrane with a smooth, microvillous-free polar region. This region is relatively free of organelles (Eager et al, 1976) and has fewer granules (Ducibella *et al*, 1988). SEM analysis of *in vitro*-derived oocytes from late cultures revealed a mosaic surface topography typical for mature unfertilized oocytes.

The formation of cortical granules begins during oocyte maturation (Zamboni, 1970) and the distribution of cortical granules in the mouse oocyte cortex changes dynamically during meiotic maturation (Ducibella et al, 1988). Cortical granules are round or elliptical in shape, measure 0.2–0.5 mm in diameter, and consist of a highly dense matrix surrounded by a single smooth membrane (Zamboni, 1970). As described by Ducibella et al. (Ducibella et al, 1988), in immature oocytes, cortical granules are distributed asymmetrically throughout the cortex, whereas in mature oocytes, they are localized mainly to the cortex periphery and are fewer in number. TEM analysis of ESC-derived oocytes showed numerous cortical granules distributed over the entire cortex, with only a few granules at the oocyte periphery, which is indicative for immature oocytes. The distribution of cortical granules and their competence to undergo cortical reaction are important indicators of oocyte cytoplasmic maturation and provide valuable information about the fertilizable lifespan of the oocyte (Ducibella et al, 1988). Overall, these ultrastructural data suggest that the analyzed ESC-derived oocytes resembled immature and growing wild-type oocytes.

Although the derivation and culture of female germ cells from pluripotent stem cells in vitro may lead to ultrastructural alterations in oocytes, this study demonstrates that an *in vitro* culture system can create the essential components required for oocyte development: oocytes, an ECM-based interface, and granulosa-like cells. Future efforts to optimize *in vitro* differentiation conditions should bring us closer to our ultimate goal of generating fully functional oocytes and demonstrate whether all key events of germ cell development in vivo can be truthfully recapitulated *in vitro*.

5. References

Adams I, McLaren A (2002) Sexually dimorphic development of mouse primordial germ cells: switching from oogenesis to spermatogenesis. *Development (Cambridge, England)* **129:** 1155-1164

Albertini D, Combelles C, Benecchi E, Carabatsos M (2001) Cellular basis for paracrine regulation of ovarian follicle development. *Reproduction (Cambridge, England)* **121:** 647-653

Almstrup K, Nielsen J, Mlynarska O, Jansen M, Jørgensen A, Skakkebæk N, Rajpert-De Meyts E (2010) Carcinoma in situ testis displays permissive chromatin modifications similar to immature foetal germ cells. *British journal of cancer* **103:** 1269-1276

Amit M, Shariki C, Margulets V, Itskovitz-Eldor J (2004) Feeder layer- and serum-free culture of human embryonic stem cells. *Biology of reproduction* **70:** 837-845

Ancelin K, Lange U, Hajkova P, Schneider R, Bannister A, Kouzarides T, Surani M (2006) Blimp1 associates with Prmt5 and directs histone arginine methylation in mouse germ cells. *Nature cell biology* **8:** 623-630

Anderson E, Albertini D (1976) Gap junctions between the oocyte and companion follicle cells in the mammalian ovary. *The Journal of cell biology* **71:** 680-686

Anderson R, Fassler R, Georges-Labouesse E, Hynes RO, Bader BL, Kreidberg JA, Schaible K, Heasman J, Wylie C (1999) Mouse primordial germ cells lacking beta1 integrins enter the germline but fail to migrate normally to the gonads. *Development* **126:** 1655-1664

Anderson R, Fulton N, Cowan G, Coutts S, Saunders P (2007) Conserved and divergent patterns of expression of DAZL, VASA and OCT4 in the germ cells of the human fetal ovary and testis. *BMC developmental biology* **7:** 136

Aramaki S, Hayashi K, Kurimoto K, Ohta H, Yabuta Y, Iwanari H, Mochizuki Y, Hamakubo T, Kato Y, Shirahige K, Saitou M (2013) A mesodermal factor, T, specifies mouse germ cell fate by directly activating germline determinants. *Developmental cell* **27:** 516-529

Ashburner M, Ball C, Blake J, Botstein D, Butler H, Cherry J, Davis A, Dolinski K, Dwight S, Eppig J, Harris M, Hill D, Issel-Tarver L, Kasarskis A, Lewis S, Matese J, Richardson J, Ringwald M, Rubin G, Sherlock G (2000) Gene ontology: tool for the unification of biology. The Gene Ontology Consortium. *Nature genetics* **25:** 25-29

Avilion A, Nicolis S, Pevny L, Perez L, Vivian N, Lovell-Badge R (2003) Multipotent cell lineages in early mouse development depend on SOX2 function. *Genes & development* **17:** 126-140

Bayne R, Martins da Silva S, Anderson R (2004) Increased expression of the FIGLA transcription factor is associated with primordial follicle formation in the human fetal ovary. *Molecular human reproduction* **10:** 373-381

Bendel-Stenzel MR, Gomperts M, Anderson R, Heasman J, Wylie C (2000) The role of cadherins during primordial germ cell migration and early gonad formation in the mouse. *Mech Dev* **91:** 143-152

Borgel J, Guibert S, Li Y, Chiba H, Schübeler D, Sasaki H, Forné T, Weber M (2010) Targets and dynamics of promoter DNA methylation during early mouse development. *Nature genetics* **42:** 1093-1100

Boyer L, Lee T, Cole M, Johnstone S, Levine S, Zucker J, Guenther M, Kumar R, Murray H, Jenner R, Gifford D, Melton D, Jaenisch R, Young R (2005) Core transcriptional regulatory circuitry in human embryonic stem cells. *Cell* **122:** 947-956

Brons I, Smithers L, Trotter M, Rugg-Gunn P, Sun B, Chuva de Sousa Lopes S, Howlett S, Clarkson A, Ahrlund-Richter L, Pedersen R, Vallier L (2007) Derivation of pluripotent epiblast stem cells from mammalian embryos. *Nature* **448:** 191-195

Bucay N, Yebra M, Cirulli V, Afrikanova I, Kaido T, Hayek A, Montgomery AM (2009) A novel approach for the derivation of putative primordial germ cells and sertoli cells from human embryonic stem cells. *Stem Cells* **27:** 68-77

Canipari R (2000) Oocyte--granulosa cell interactions. *Hum Reprod Update* **6:** 279-289

Castrillon D, Quade B, Wang T, Quigley C, Crum C (2000) The human VASA gene is specifically expressed in the germ cell lineage. *Proceedings of the National Academy of Sciences of the United States of America* **97:** 9585-9590

Cauffman G, De Rycke M, Sermon K, Liebaers I, Van de Velde H (2009) Markers that define stemness in ESC are unable to identify the totipotent cells in human preimplantation embryos. *Human reproduction (Oxford, England)* **24:** 63-70

Cecconi S, Barboni B, Coccia M, Mattioli M (1999) In vitro development of sheep preantral follicles. *Biol Reprod* **60:** 594-601

Chai N, Phillips A, Fernandez A, Yen P (1997) A putative human male infertility gene DAZLA: genomic structure and methylation status. *Molecular human reproduction* **3:** 705-708

Chang DH, Angelin-Duclos C, Calame K (2000) BLIMP-1: trigger for differentiation of myeloid lineage. *Nature immunology* **1:** 169-176

Chia NY, Chan YS, Feng B, Lu X, Orlov YL, Moreau D, Kumar P, Yang L, Jiang J, Lau MS, Huss M, Soh BS, Kraus P, Li P, Lufkin T, Lim B, Clarke ND, Bard F, Ng HH (2010) A genome-wide RNAi screen reveals determinants of human embryonic stem cell identity. *Nature* **468:** 316-320

Childs A, Cowan G, Kinnell H, Anderson R, Saunders P (2011) Retinoic Acid signalling and the control of meiotic entry in the human fetal gonad. *PLoS One* **6**

Chuang CY, Lin KI, Hsiao M, Stone L, Chen HF, Huang YH, Lin SP, Ho HN, Kuo HC (2012) Meiotic competent human germ cell-like cells derived from human embryonic stem cells induced by BMP4/WNT3A signaling and OCT4/EpCAM selection. *J Biol Chem*

Clark AT, Bodnar MS, Fox M, Rodriquez RT, Abeyta MJ, Firpo MT, Pera RA (2004) Spontaneous differentiation of germ cells from human embryonic stem cells in vitro. *Hum Mol Genet* **13:** 727-739

Cooke H, Lee M, Kerr S, Ruggiu M (1996) A murine homologue of the human DAZ gene is autosomal and expressed only in male and female gonads. *Human molecular genetics* **5:** 513-516

Crisp TM, Dessouky DA, Denys FR (1970) The fine structure of the human corpus luteum of early pregnancy and during the progestational phase of the mestrual cycle. *The American journal of anatomy* **127:** 37-69

Dahéron L, Opitz S, Zaehres H, Lensch M, Lensch W, Andrews P, Itskovitz-Eldor J, Daley G (2004) LIF/STAT3 signaling fails to maintain self-renewal of human embryonic stem cells. *Stem cells (Dayton, Ohio)* **22:** 770-778

Daniel SA, Armstrong DT, Gore-Langton RE (1989) Growth and development of rat oocytes in vitro. *Gamete research* **24:** 109-121

de Jong J, Stoop H, Gillis AJ, van Gurp RJ, van de Geijn GJ, Boer M, Hersmus R, Saunders PT, Anderson RA, Oosterhuis JW, Looijenga LH (2008) Differential expression of SOX17 and SOX2 in germ cells and stem cells has biological and clinical implications. *J Pathol* **215:** 21-30

Ducibella T, Anderson E, Albertini DF, Aalberg J, Rangarajan S (1988) Quantitative studies of changes in cortical granule number and distribution in the mouse oocyte during meiotic maturation. *Dev Biol* **130:** 184-197

Eager DD, Johnson MH, Thurley KW (1976) Ultrastructural studies on the surface membrane of the mouse egg. *Journal of cell science* **22:** 345-353

Eckert D, Biermann K, Nettersheim D, Gillis A, Steger K, Jäck H-M, Müller A, Looijenga L, Schorle H (2008) Expression of BLIMP1/PRMT5 and concurrent histone H2A/H4 arginine 3 dimethylation in fetal germ cells, CIS/IGCNU and germ cell tumors. *BMC developmental biology* **8:** 106

Eguizabal C, Montserrat N, Vassena R, Barragan M, Garreta E, Garcia-Quevedo L, Vidal F, Giorgetti A, Veiga A, Izpisua Belmonte JC (2011) Complete meiosis from human induced pluripotent stem cells. *Stem Cells* **29:** 1186-1195

Eppig JJ (1977) Mouse oocyte development in vitro with various culture systems. *Dev Biol* **60:** 371-388

Eppig JJ (2001) Oocyte control of ovarian follicular development and function in mammals. *Reproduction* **122:** 829-838

Eppig JJ, Schroeder AC (1989) Capacity of mouse oocytes from preantral follicles to undergo embryogenesis and development to live young after growth, maturation, and fertilization in vitro. *Biol Reprod* **41:** 268-276

Eppig JJ, Wigglesworth K, Pendola FL (2002) The mammalian oocyte orchestrates the rate of ovarian follicular development. *Proc Natl Acad Sci U S A* **99:** 2890-2894

Evans MJ, Kaufman MH (1981) Establishment in culture of pluripotential cells from mouse embryos. *Nature* **292:** 154-156

Falin L (1969) The development of genital glands and the origin of germ cells in human embryogenesis. *Acta anatomica* **72:** 195-232

Felix W (1911) Die Entwicklung der Harn- und Geschlechtsorgane. In *Keibel-Mall Handbuch der 1qEntwicklungageschichte des Menshen* Vol. 2, pp 732-955. Leipzig: Hirzel

Fong H, Hohenstein K, Donovan P (2008) Regulation of self-renewal and pluripotency by Sox2 in human embryonic stem cells. *Stem cells (Dayton, Ohio)* **26:** 1931-1938

Frank S, Zhang M, Schöler H, Greber B (2012) Small molecule-assisted, line-independent maintenance of human pluripotent stem cells in defined conditions. *PLoS One* **7**

Freeman B (2003) The active migration of germ cells in the embryos of mice and men is a myth. *Reproduction (Cambridge, England)* **125:** 635-643

Fujimoto T, Miyayama Y, Fuyuta M (1977) The origin, migration and fine morphology of human primordial germ cells. *The Anatomical record* **188:** 315-330

Fujiwara T, Dunn NR, Hogan BL (2001) Bone morphogenetic protein 4 in the extraembryonic mesoderm is required for allantois development and the localization and survival of primordial germ cells in the mouse. *Proc Natl Acad Sci U S A* **98:** 13739-13744

Fuss A (1911) Uber extraregionare Geschlechtszellen bei einem menschlichen Embryo von 4 Wochen. *Anat Am* **39:** 407-409

Fuss A (1912) Uber die Geschlechtszellen des Menschen und der Saugetiere. *Arch Mikrosk Anat Entw Mech* **81:** 1-23

Gardner RL, Rossant J (1979) Investigation of the fate of 4-5 day post-coitum mouse inner cell mass cells by blastocyst injection. *J Embryol Exp Morphol* **52:** 141-152

Gaskell T, Esnal A, Robinson LL, Anderson R, Saunders P (2004) Immunohistochemical profiling of germ cells within the human fetal testis: identification of three subpopulations. *Biology of reproduction* **71:** 2012-2021

Geijsen N, Horoschak M, Kim K, Gribnau J, Eggan K, Daley GQ (2004) Derivation of embryonic germ cells and male gametes from embryonic stem cells. *Nature* **427:** 148-154

Ginsburg M, Snow MH, McLaren A (1990) Primordial germ cells in the mouse embryo during gastrulation. *Development* **110:** 521-528

Gkountela S, Li Z, Vincent J, Zhang K, Chen A, Pellegrini M, Clark A (2013) The ontogeny of cKIT+ human primordial germ cells proves to be a resource for human germ line reprogramming, imprint erasure and in vitro differentiation. *Nature cell biology* **15:** 113-122

Gosden R, Mullan J, Picton H, Yin H, Tan S-L (2002) Current perspective on primordial follicle cryopreservation and culture for reproductive medicine. *Human reproduction update* **8:** 105-110

Guibert S, Forné T, Weber M (2012) Global profiling of DNA methylation erasure in mouse primordial germ cells. *Genome research* **22:** 633-641

Guo G, Yang J, Nichols J, Hall JS, Eyres I, Mansfield W, Smith A (2009) Klf4 reverts developmentally programmed restriction of ground state pluripotency. *Development* **136:** 1063-1069

Gutierrez CG, Ralph JH, Telfer EE, Wilmut I, Webb R (2000) Growth and antrum formation of bovine preantral follicles in long-term culture in vitro. *Biol Reprod* **62:** 1322-1328

Hajkova P, Ancelin K, Waldmann T, Lacoste N, Lange U, Cesari F, Lee C, Almouzni G, Schneider R, Surani M (2008) Chromatin dynamics during epigenetic reprogramming in the mouse germ line. *Nature* **452:** 877-881

Hajkova P, Erhardt S, Lane N, Haaf T, El-Maarri O, Reik W, Walter J, Surani M (2002) Epigenetic reprogramming in mouse primordial germ cells. *Mechanisms of development* **117:** 15-23

Hajkova P, Jeffries S, Lee C, Miller N, Jackson S, Surani M (2010) Genome-wide reprogramming in the mouse germ line entails the base excision repair pathway. *Science (New York, NY)* **329:** 78-82

Han D, Tapia N, Joo J, Greber B, Araúzo-Bravo M, Bernemann C, Ko K, Wu G, Stehling M, Do J, Schöler H (2010) Epiblast stem cell subpopulations represent mouse embryos of distinct pregastrulation stages. *Cell* **143:** 617-627

Harada M, Miyano T, Matsumura K, Osaki S, Miyake M, Kato S (1997) Bovine oocytes from early antral follicles grow to meiotic competence in vitro: effect of FSH and hypoxanthine. *Theriogenology* **48:** 743-755

Hayashi K, Lopes S, Tang F, Surani M (2008) Dynamic equilibrium and heterogeneity of mouse pluripotent stem cells with distinct functional and epigenetic states. *Cell Stem Cell* **3:** 391-401

Hayashi K, Ogushi S, Kurimoto K, Shimamoto S, Ohta H, Saitou M (2012) Offspring from Oocytes Derived from in Vitro Primordial Germ Cell-Like Cells in Mice. *Science*

Hayashi K, Ohta H, Kurimoto K, Aramaki S, Saitou M (2011) Reconstitution of the mouse germ cell specification pathway in culture by pluripotent stem cells. *Cell* **146:** 519-532

Hayashi K, Saitou M (2013) Generation of eggs from mouse embryonic stem cells and induced pluripotent stem cells. *Nature protocols* **8:** 1513-1524

Hayashi K, Surani MA (2009) Self-renewing epiblast stem cells exhibit continual delineation of germ cells with epigenetic reprogramming in vitro. *Development* **136:** 3549-3556

Hertig A, Adams E (1967) Studies on the human oocyte and its follicle. I. Ultrastructural and histochemical observations on the primordial follicle stage. *The Journal of cell biology* **34:** 647-675

Hirao Y, Nagai T, Kubo M, Miyano T, Miyake M, Kato S (1994) In vitro growth and maturation of pig oocytes. *Journal of reproduction and fertility* **100:** 333-339

Houmard B, Small C, Yang L, Naluai-Cecchini T, Cheng E, Hassold T, Griswold M (2009) Global gene expression in the human fetal testis and ovary. *Biology of reproduction* **81:** 438-443

Hoyer PE, Byskov AG, Mollgard K (2005) Stem cell factor and c-Kit in human primordial germ cells and fetal ovaries. *Mol Cell Endocrinol* **234:** 1-10

Huanmin Z, Yong Z (2000) In vitro development of caprine ovarian preantral follicles. *Theriogenology* **54:** 641-650

Hubner K, Fuhrmann G, Christenson LK, Kehler J, Reinbold R, De La Fuente R, Wood J, Strauss JF, 3rd, Boiani M, Scholer HR (2003) Derivation of oocytes from mouse embryonic stem cells. *Science* **300:** 1251-1256

Huntriss J, Hinkins M, Picton H (2006) cDNA cloning and expression of the human NOBOX gene in oocytes and ovarian follicles. *Molecular human reproduction* **12:** 283-289

Hutt KJ, McLaughlin EA, Holland MK (2006) Kit ligand and c-Kit have diverse roles during mammalian oogenesis and folliculogenesis. *Mol Hum Reprod* **12:** 61-69

Irizarry R, Bolstad B, Collin F, Cope L, Hobbs B, Speed T (2003) Summaries of Affymetrix GeneChip probe level data. *Nucleic acids research* **31**

Jagarlamudi K, Reddy P, Adhikari D, Liu K (2010) Genetically modified mouse models for premature ovarian failure (POF). *Mol Cell Endocrinol* **315:** 1-10

James D, Levine A, Besser D, Hemmati-Brivanlou A (2005) TGFbeta/activin/nodal signaling is necessary for the maintenance of pluripotency in human embryonic stem cells. *Development (Cambridge, England)* **132:** 1273-1282

Jewgenow K (1998) Role of media, protein and energy supplements on maintenance of morphology and DNA-synthesis of small preantral domestic cat follicles during short-term culture. *Theriogenology* **49:** 1567-1577

Kagiwada S, Kurimoto K, Hirota T, Yamaji M, Saitou M (2013) Replication-coupled passive DNA demethylation for the erasure of genome imprints in mice. *The EMBO journal* **32:** 340-353

Kallies A, Hawkins ED, Belz GT, Metcalf D, Hommel M, Corcoran LM, Hodgkin PD, Nutt SL (2006) Transcriptional repressor Blimp-1 is essential for T cell homeostasis and self-tolerance. *Nature immunology* **7:** 466-474

Kang L, Wang J, Zhang Y, Kou Z, Gao S (2009) iPS cells can support full-term development of tetraploid blastocyst-complemented embryos. *Cell Stem Cell* **5:** 135-138

Kee K, Angeles VT, Flores M, Nguyen HN, Reijo Pera RA (2009) Human DAZL, DAZ and BOULE genes modulate primordial germ-cell and haploid gamete formation. *Nature* **462:** 222-225

Kee K, Gonsalves JM, Clark AT, Pera RA (2006) Bone morphogenetic proteins induce germ cell differentiation from human embryonic stem cells. *Stem Cells Dev* **15:** 831-837

Kerr CL, Hill CM, Blumenthal PD, Gearhart JD (2008a) Expression of pluripotent stem cell markers in the human fetal ovary. *Hum Reprod* **23:** 589-599

Kerr CL, Hill CM, Blumenthal PD, Gearhart JD (2008b) Expression of pluripotent stem cell markers in the human fetal testis. *Stem Cells* **26:** 412-421

Kim K-P, Thurston A, Mummery C, Ward-van Oostwaard D, Priddle H, Allegrucci C, Denning C, Young L (2007) Gene-specific vulnerability to imprinting variability in human embryonic stem cell lines. *Genome research* **17:** 1731-1742

Koubova J, Menke DB, Zhou Q, Capel B, Griswold MD, Page DC (2006) Retinoic acid regulates sex-specific timing of meiotic initiation in mice. *Proc Natl Acad Sci U S A* **103:** 2474-2479

Kunath T, Saba-El-Leil M, Almousailleakh M, Wray J, Meloche S, Smith A (2007) FGF stimulation of the Erk1/2 signalling cascade triggers transition of pluripotent embryonic stem cells from self-renewal to lineage commitment. *Development (Cambridge, England)* **134:** 2895-2902

Kurimoto K, Yabuta Y, Ohinata Y, Shigeta M, Yamanaka K, Saitou M (2008) Complex genome-wide transcription dynamics orchestrated by Blimp1 for the specification of the germ cell lineage in mice. *Genes Dev* **22:** 1617-1635

Kuwana T, Fujimoto T (1983) Active locomotion of human primordial germ cells in vitro. *The Anatomical record* **205:** 21-26

Lacham-Kaplan O, Chy H, Trounson A (2006) Testicular cell conditioned medium supports differentiation of embryonic stem cells into ovarian structures containing oocytes. *Stem Cells* **24:** 266-273

Lawson KA, Dunn NR, Roelen BA, Zeinstra LM, Davis AM, Wright CV, Korving JP, Hogan BL (1999) Bmp4 is required for the generation of primordial germ cells in the mouse embryo. *Genes Dev* **13:** 424-436

Le Bouffant R, Guerquin M, Duquenne C, Frydman N, Coffigny H, Rouiller-Fabre V, Frydman R, Habert R, Livera G (2010) Meiosis initiation in the human ovary requires intrinsic retinoic acid synthesis. *Human reproduction (Oxford, England)* **25:** 2579-2590

Ledda S, Bogliolo L, Bebbere D, Ariu F, Pirino S (2010) Characterization, isolation and culture of primordial germ cells in domestic animals: recent progress and insights from the ovine species. *Theriogenology* **74:** 534-543

Lin IY, Chiu F-L, Yeang C-H, Chen H-F, Chuang C-Y, Yang S-Y, Hou P-S, Sintupisut N, Ho H-N, Kuo H-C, Lin K-I (2014) Suppression of the SOX2 Neural Effector Gene by PRDM1 Promotes Human Germ Cell Fate in Embryonic Stem Cells. *Stem cell reports* **2:** 189-204

Liu Y, Wu C, Lyu Q, Yang D, Albertini D, Keefe D, Liu L (2007) Germline stem cells and neo-oogenesis in the adult human ovary. *Developmental biology* **306:** 112-120

Ma Z, Swigut T, Valouev A, Rada-Iglesias A, Wysocka J (2011) Sequence-specific regulator Prdm14 safeguards mouse ESCs from entering extraembryonic endoderm fates. *Nat Struct Mol Biol* **18:** 120-127

Maatouk D, Kellam L, Mann M, Lei H, Li E, Bartolomei M, Resnick J (2006) DNA methylation is a primary mechanism for silencing postmigratory primordial germ cell genes in both germ cell and somatic cell lineages. *Development (Cambridge, England)* **133:** 3411-3418

Makabe S, Naguro T, Stallone T (2006) Oocyte-follicle cell interactions during ovarian follicle development, as seen by high resolution scanning and transmission electron microscopy in humans. *Microscopy research and technique* **69:** 436-449

Martin GR (1981) Isolation of a pluripotent cell line from early mouse embryos cultured in medium conditioned by teratocarcinoma stem cells. *Proc Natl Acad Sci U S A* **78:** 7634-7638

Martins GA, Cimmino L, Shapiro-Shelef M, Szabolcs M, Herron A, Magnusdottir E, Calame K (2006) Transcriptional repressor Blimp-1 regulates T cell homeostasis and function. *Nature immunology* **7:** 457-465

Mc KD, Hertig AT, Adams EC, Danziger S (1953) Histochemical observations on the germ cells of human embryos. *The Anatomical record* **117:** 201-219

Medrano JV, Ramathal C, Nguyen HN, Simon C, Reijo-Pera RA (2011) Divergent RNA-Binding Proteins, DAZL and VASA, Induce Meiotic Progression in Human Germ Cells Derived In vitro. *Stem Cells*

Mollgard K, Jespersen A, Lutterodt MC, Yding Andersen C, Hoyer PE, Byskov AG (2010) Human primordial germ cells migrate along nerve fibers and Schwann cells from the dorsal hind gut mesentery to the gonadal ridge. *Mol Hum Reprod* **16:** 621-631

Molyneaux KA, Zinszner H, Kunwar PS, Schaible K, Stebler J, Sunshine MJ, O'Brien W, Raz E, Littman D, Wylie C, Lehmann R (2003) The chemokine SDF1/CXCL12 and its receptor CXCR4 regulate mouse germ cell migration and survival. *Development* **130:** 4279-4286

Moriguchi H, Zhang Y, Mihara M, Sato C (2012) Successful cryopreservation of human ovarian cortex tissues using supercooling. *Scientific reports* **2:** 537

Nakaki F, Hayashi K, Ohta H, Kurimoto K, Yabuta Y, Saitou M (2013) Induction of mouse germ-cell fate by transcription factors in vitro. *Nature* **501:** 222-226

Nakamura T, Arai Y, Umehara H, Masuhara M, Kimura T, Taniguchi H, Sekimoto T, Ikawa M, Yoneda Y, Okabe M, Tanaka S, Shiota K, Nakano T (2007) PGC7/Stella protects against DNA demethylation in early embryogenesis. *Nature cell biology* **9:** 64-71

Nakamura T, Liu Y-J, Nakashima H, Umehara H, Inoue K, Matoba S, Tachibana M, Ogura A, Shinkai Y, Nakano T (2012) PGC7 binds histone H3K9me2 to protect against conversion of 5mC to 5hmC in early embryos. *Nature* **486:** 415-419

Nayernia K, Nolte J, Michelmann HW, Lee JH, Rathsack K, Drusenheimer N, Dev A, Wulf G, Ehrmann IE, Elliott DJ, Okpanyi V, Zechner U, Haaf T, Meinhardt A, Engel W (2006) In vitro-differentiated embryonic stem cells give rise to male gametes that can generate offspring mice. *Dev Cell* **11:** 125-132

Niakan K, Han J, Pedersen R, Simon C, Pera R (2012) Human pre-implantation embryo development. *Development (Cambridge, England)* **139:** 829-841

Nicholas CR, Haston KM, Grewall AK, Longacre TA, Reijo Pera RA (2009) Transplantation directs oocyte maturation from embryonic stem cells and provides a therapeutic strategy for female infertility. *Hum Mol Genet* **18:** 4376-4389

Niwa H, Ogawa K, Shimosato D, Adachi K (2009) A parallel circuit of LIF signalling pathways maintains pluripotency of mouse ES cells. *Nature* **460:** 118-122

Noce T, Okamoto-Ito S, Tsunekawa N (2001) Vasa homolog genes in mammalian germ cell development. *Cell Struct Funct* **26:** 131-136

Nottola SA, Heyn R, Camboni A, Correr S, Macchiarelli G (2006) Ultrastructural characteristics of human granulosa cells in a coculture system for in vitro fertilization. *Microscopy research and technique* **69:** 508-516

Novak I, Lightfoot DA, Wang H, Eriksson A, Mahdy E, Hoog C (2006) Mouse embryonic stem cells form follicle-like ovarian structures but do not progress through meiosis. *Stem Cells* **24:** 1931-1936

O'Brien MJ, Pendola JK, Eppig JJ (2003) A revised protocol for in vitro development of mouse oocytes from primordial follicles dramatically improves their developmental competence. *Biol Reprod* **68:** 1682-1686

Ohinata Y, Ohta H, Shigeta M, Yamanaka K, Wakayama T, Saitou M (2009) A signaling principle for the specification of the germ cell lineage in mice. *Cell* **137:** 571-584

Ohinata Y, Payer B, O'Carroll D, Ancelin K, Ono Y, Sano M, Barton SC, Obukhanych T, Nussenzweig M, Tarakhovsky A, Saitou M, Surani MA (2005) Blimp1 is a critical determinant of the germ cell lineage in mice. *Nature* **436:** 207-213

Ohta H, Wakayama T, Nishimune Y (2004) Commitment of fetal male germ cells to spermatogonial stem cells during mouse embryonic development. *Biol Reprod* **70:** 1286-1291

Okita K, Ichisaka T, Yamanaka S (2007) Generation of germline-competent induced pluripotent stem cells. *Nature* **448:** 313-317

Panula S, Medrano JV, Kee K, Bergstrom R, Nguyen HN, Byers B, Wilson KD, Wu JC, Simon C, Hovatta O, Reijo Pera RA (2011) Human germ cell differentiation from fetal- and adult-derived induced pluripotent stem cells. *Hum Mol Genet* **20:** 752-762

Paredes A, Garcia-Rudaz C, Kerr B, Tapia V, Dissen GA, Costa ME, Cornea A, Ojeda SR (2005) Loss of synaptonemal complex protein-1, a synaptonemal complex protein, contributes to the initiation of follicular assembly in the developing rat ovary. *Endocrinology* **146:** 5267-5277

Park TS, Galic Z, Conway AE, Lindgren A, van Handel BJ, Magnusson M, Richter L, Teitell MA, Mikkola HK, Lowry WE, Plath K, Clark AT (2009) Derivation of primordial germ cells from human embryonic and induced pluripotent stem cells is significantly improved by coculture with human fetal gonadal cells. *Stem Cells* **27:** 783-795

Payer B, Saitou M, Barton SC, Thresher R, Dixon JP, Zahn D, Colledge WH, Carlton MB, Nakano T, Surani MA (2003) Stella is a maternal effect gene required for normal early development in mice. *Curr Biol* **13:** 2110-2117

Pepling ME, Spradling AC (2001) Mouse ovarian germ cell cysts undergo programmed breakdown to form primordial follicles. *Dev Biol* **234:** 339-351

Perrett RM, Turnpenny L, Eckert JJ, O'Shea M, Sonne SB, Cameron IT, Wilson DI, Rajpert-De Meyts E, Hanley NA (2008) The early human germ cell lineage does not express SOX2 during in vivo development or upon in vitro culture. *Biol Reprod* **78:** 852-858

Pesce M, Farrace MG, Piacentini M, Dolci S, De Felici M (1993) Stem cell factor and leukemia inhibitory factor promote primordial germ cell survival by suppressing programmed cell death (apoptosis). *Development* **118:** 1089-1094

Psathaki OE, Hubner K, Sabour D, Sebastiano V, Wu G, Sugawa F, Wieacker P, Pennekamp P, Scholer HR (2011) Ultrastructural characterization of mouse embryonic stem cell-derived oocytes and granulosa cells. *Stem Cells Dev* **20:** 2205-2215

Qing T, Shi Y, Qin H, Ye X, Wei W, Liu H, Ding M, Deng H (2007) Induction of oocyte-like cells from mouse embryonic stem cells by co-culture with ovarian granulosa cells. *Differentiation* **75:** 902-911

Rajpert-De Meyts E, Hanstein R, Jorgensen N, Graem N, Vogt PH, Skakkebaek NE (2004) Developmental expression of POU5F1 (OCT-3/4) in normal and dysgenetic human gonads. *Hum Reprod* **19:** 1338-1344

Rossant J, Gardner RL, Alexandre HL (1978) Investigation of the potency of cells from the postimplantation mouse embryo by blastocyst injection: a preliminary report. *J Embryol Exp Morphol* **48:** 239-247

Roy SK, Greenwald GS (1989) Hormonal requirements for the growth and differentiation of hamster preantral follicles in long-term culture. *Journal of reproduction and fertility* **87:** 103-114

Roy SK, Treacy BJ (1993) Isolation and long-term culture of human preantral follicles. *Fertility and sterility* **59:** 783-790

Sabour D, Arauzo-Bravo MJ, Hubner K, Ko K, Greber B, Gentile L, Stehling M, Scholer HR (2011) Identification of genes specific to mouse primordial germ cells through dynamic global gene expression. *Hum Mol Genet* **20:** 115-125

Saitou M, Barton SC, Surani MA (2002) A molecular programme for the specification of germ cell fate in mice. *Nature* **418:** 293-300

Sato N, Meijer L, Skaltsounis L, Greengard P, Brivanlou A (2004) Maintenance of pluripotency in human and mouse embryonic stem cells through activation of Wnt signaling by a pharmacological GSK-3-specific inhibitor. *Nature medicine* **10:** 55-63

Schöler H, Dressler G, Balling R, Rohdewohld H, Gruss P (1990) Oct-4: a germline-specific transcription factor mapping to the mouse t-complex. *The EMBO journal* **9:** 2185-2195

Seki Y, Hayashi K, Itoh K, Mizugaki M, Saitou M, Matsui Y (2005) Extensive and orderly reprogramming of genome-wide chromatin modifications associated with specification and early development of germ cells in mice. *Developmental biology* **278:** 440-458

Seki Y, Yamaji M, Yabuta Y, Sano M, Shigeta M, Matsui Y, Saga Y, Tachibana M, Shinkai Y, Saitou M (2007) Cellular dynamics associated with the genome-wide epigenetic reprogramming in migrating primordial germ cells in mice. *Development* **134:** 2627-2638

Sugawa F, Hübner K, Schöler H (2013) In vitro differentiation of germ cells from stem cells. In *Biology and Pathology of the oocye, 2nd edn.*, 20, pp 236-249. Cambridge University Press

Sugimoto K, Koh E, Sin H-S, Maeda Y, Narimoto K, Izumi K, Kobori Y, Kitamura E, Nagase H, Yoshida A, Namiki M (2009) Tissue-specific differentially methylated regions of the human VASA gene are potentially associated with maturation arrest phenotype in the testis. *Journal of human genetics* **54:** 450-456

Sumi T, Tsuneyoshi N, Nakatsuji N, Suemori H (2008) Defining early lineage specification of human embryonic stem cells by the orchestrated balance of canonical Wnt/beta-catenin, Activin/Nodal and BMP signaling. *Development (Cambridge, England)* **135:** 2969-2979

Suzuki H, Jeong BS, Yang X (2000) Dynamic changes of cumulus-oocyte cell communication during in vitro maturation of porcine oocytes. *Biol Reprod* **63:** 723-729

Suzuki S, Kitai H, Tojo R, Seki K, Oba M, Fujiwara T, Iizuka R (1981) Ultrastructure and some biologic properties of human oocytes and granulosa cells cultured in vitro. *Fertility and sterility* **35:** 142-148

Suzumori N, Pangas S, Rajkovic A (2007) Candidate genes for premature ovarian failure. *Current medicinal chemistry* **14:** 353-357

Takahashi K, Tanabe K, Ohnuki M, Narita M, Ichisaka T, Tomoda K, Yamanaka S (2007) Induction of pluripotent stem cells from adult human fibroblasts by defined factors. *Cell* **131:** 861-872

Takahashi K, Yamanaka S (2006) Induction of pluripotent stem cells from mouse embryonic and adult fibroblast cultures by defined factors. *Cell* **126:** 663-676

Tam PP, Zhou SX (1996) The allocation of epiblast cells to ectodermal and germ-line lineages is influenced by the position of the cells in the gastrulating mouse embryo. *Dev Biol* **178:** 124-132

Tesar P, Chenoweth J, Brook F, Davies T, Evans E, Mack D, Gardner R, McKay R (2007) New cell lines from mouse epiblast share defining features with human embryonic stem cells. *Nature* **448:** 196-199

Thomson JA, Itskovitz-Eldor J, Shapiro SS, Waknitz MA, Swiergiel JJ, Marshall VS, Jones JM (1998) Embryonic stem cell lines derived from human blastocysts. *Science* **282:** 1145-1147

Tilgner K, Atkinson SP, Yung S, Golebiewska A, Stojkovic M, Moreno R, Lako M, Armstrong L (2010) Expression of GFP under the control of the RNA helicase VASA permits fluorescence-activated cell sorting isolation of human primordial germ cells. *Stem Cells* **28:** 84-92

Toyooka Y, Tsunekawa N, Akasu R, Noce T (2003) Embryonic stem cells can form germ cells in vitro. *Proc Natl Acad Sci U S A* **100:** 11457-11462

Toyooka Y, Tsunekawa N, Takahashi Y, Matsui Y, Satoh M, Noce T (2000) Expression and intracellular localization of mouse Vasa-homologue protein during germ cell development. *Mechanisms of development* **93:** 139-149

Turner CA, Jr., Mack DH, Davis MM (1994) Blimp-1, a novel zinc finger-containing protein that can drive the maturation of B lymphocytes into immunoglobulin-secreting cells. *Cell* **77:** 297-306

Vincent J, Huang Y, Chen P-Y, Feng S, Calvopiña J, Nee K, Lee S, Le T, Yoon A, Faull K, Fan G, Rao A, Jacobsen S, Pellegrini M, Clark A (2013) Stage-specific roles for tet1 and tet2 in DNA demethylation in primordial germ cells. *Cell Stem Cell* **12:** 470-478

Wang J, Rao S, Chu J, Shen X, Levasseur D, Theunissen T, Orkin S (2006) A protein interaction network for pluripotency of embryonic stem cells. *Nature* **444:** 364-368

Wang PJ, McCarrey JR, Yang F, Page DC (2001) An abundance of X-linked genes expressed in spermatogonia. *Nat Genet* **27:** 422-426

Weismann A (1893) The Germ-plasm; A Theory of Heredity. *Charles Scribner's Sons, New York, NY*

Wermann H, Stoop H, Gillis A, Honecker F, van Gurp R, Ammerpohl O, Richter J, Oosterhuis J, Bokemeyer C, Looijenga L (2010) Global DNA methylation in fetal human germ cells and germ cell tumours: association with differentiation and cisplatin resistance. *The Journal of pathology* **221:** 433-442

Wernig M, Meissner A, Foreman R, Brambrink T, Ku M, Hochedlinger K, Bernstein B, Jaenisch R (2007) In vitro reprogramming of fibroblasts into a pluripotent ES-cell-like state. *Nature* **448:** 318-324

West FD, Machacek DW, Boyd NL, Pandiyan K, Robbins KR, Stice SL (2008) Enrichment and differentiation of human germ-like cells mediated by feeder cells and basic fibroblast growth factor signaling. *Stem Cells* **26:** 2768-2776

West FD, Mumaw JL, Gallegos-Cardenas A, Young A, Stice SL (2011) Human haploid cells differentiated from meiotic competent clonal germ cell lines that originated from embryonic stem cells. *Stem Cells Dev* **20:** 1079-1088

Yabuta Y, Kurimoto K, Ohinata Y, Seki Y, Saitou M (2006) Gene expression dynamics during germline specification in mice identified by quantitative single-cell gene expression profiling. *Biol Reprod* **75:** 705-716

Yamaji M, Seki Y, Kurimoto K, Yabuta Y, Yuasa M, Shigeta M, Yamanaka K, Ohinata Y, Saitou M (2008) Critical function of Prdm14 for the establishment of the germ cell lineage in mice. *Nat Genet* **40:** 1016-1022

Yamaji M, Ueda J, Hayashi K, Ohta H, Yabuta Y, Kurimoto K, Nakato R, Yamada Y, Shirahige K, Saitou M (2013) PRDM14 Ensures Naive Pluripotency through Dual Regulation of Signaling and Epigenetic Pathways in Mouse Embryonic Stem Cells. *Cell Stem Cell*

Yeom Y, Fuhrmann G, Ovitt C, Brehm A, Ohbo K, Gross M, Hübner K, Schöler H (1996) Germline regulatory element of Oct-4 specific for the totipotent cycle of embryonal cells. *Development (Cambridge, England)* **122:** 881-894

Ying Y, Liu XM, Marble A, Lawson KA, Zhao GQ (2000) Requirement of Bmp8b for the generation of primordial germ cells in the mouse. *Mol Endocrinol* **14:** 1053-1063

Ying Y, Zhao GQ (2001) Cooperation of endoderm-derived BMP2 and extraembryonic ectoderm-derived BMP4 in primordial germ cell generation in the mouse. *Dev Biol* **232:** 484-492

Yoshimizu T, Obinata M, Matsui Y (2001) Stage-specific tissue and cell interactions play key roles in mouse germ cell specification. *Development* **128:** 481-490

Yu J, Vodyanik M, Smuga-Otto K, Antosiewicz-Bourget J, Frane J, Tian S, Nie J, Jonsdottir G, Ruotti V, Stewart R, Slukvin I, Thomson J (2007) Induced pluripotent stem cell lines derived from human somatic cells. *Science (New York, NY)* **318:** 1917-1920

Zamboni L (1970) Ultrastructure of mammalian oocytes and ova. *Biology of reproduction Supplement* **2:** 44-63

Zhao X-y, Li W, Lv Z, Liu L, Tong M, Hai T, Hao J, Guo C-l, Ma Q-w, Wang L, Zeng F, Zhou Q (2009) iPS cells produce viable mice through tetraploid complementation. *Nature* **461:** 86-90